NASA/TM—2001-210575

Overview of Propulsion Systems for a Mars Aircraft

Anthony J. Colozza
Dynacs Engineering Company, Inc., Brook Park, Ohio

Christopher J. Miller, Brian D. Reed, Lisa L. Kohout, and Patricia L. Loyselle
Glenn Research Center, Cleveland, Ohio

August 2001

The NASA STI Program Office . . . in Profile

Since its founding, NASA has been dedicated to the advancement of aeronautics and space science. The NASA Scientific and Technical Information (STI) Program Office plays a key part in helping NASA maintain this important role.

The NASA STI Program Office is operated by Langley Research Center, the Lead Center for NASA's scientific and technical information. The NASA STI Program Office provides access to the NASA STI Database, the largest collection of aeronautical and space science STI in the world. The Program Office is also NASA's institutional mechanism for disseminating the results of its research and development activities. These results are published by NASA in the NASA STI Report Series, which includes the following report types:

- TECHNICAL PUBLICATION. Reports of completed research or a major significant phase of research that present the results of NASA programs and include extensive data or theoretical analysis. Includes compilations of significant scientific and technical data and information deemed to be of continuing reference value. NASA's counterpart of peer-reviewed formal professional papers but has less stringent limitations on manuscript length and extent of graphic presentations.

- TECHNICAL MEMORANDUM. Scientific and technical findings that are preliminary or of specialized interest, e.g., quick release reports, working papers, and bibliographies that contain minimal annotation. Does not contain extensive analysis.

- CONTRACTOR REPORT. Scientific and technical findings by NASA-sponsored contractors and grantees.

- CONFERENCE PUBLICATION. Collected papers from scientific and technical conferences, symposia, seminars, or other meetings sponsored or cosponsored by NASA.

- SPECIAL PUBLICATION. Scientific, technical, or historical information from NASA programs, projects, and missions, often concerned with subjects having substantial public interest.

- TECHNICAL TRANSLATION. English-language translations of foreign scientific and technical material pertinent to NASA's mission.

Specialized services that complement the STI Program Office's diverse offerings include creating custom thesauri, building customized data bases, organizing and publishing research results . . . even providing videos.

For more information about the NASA STI Program Office, see the following:

- Access the NASA STI Program Home Page at *http://www.sti.nasa.gov*

- E-mail your question via the Internet to help@sti.nasa.gov

- Fax your question to the NASA Access Help Desk at 301–621–0134

- Telephone the NASA Access Help Desk at 301–621–0390

- Write to:
  NASA Access Help Desk
  NASA Center for AeroSpace Information
  7121 Standard Drive
  Hanover, MD 21076

NASA/TM—2001-210575

Overview of Propulsion Systems for a Mars Aircraft

Anthony J. Colozza
Dynacs Engineering Company, Inc., Brook Park, Ohio

Christopher J. Miller, Brian D. Reed, Lisa L. Kohout, and Patricia L. Loyselle
Glenn Research Center, Cleveland, Ohio

National Aeronautics and
Space Administration

Glenn Research Center

August 2001

Acknowledgments

The authors would like to acknowledge the contributions made by the following individuals to the information contained within this report. Dr. Thomas Maloney of Dynacs Engineering Company, Inc. supplied the fuel cell information used in the comparative analysis. Jim Biaglow of NASA Glenn Research Center managed the MON–25 rocket propulsion testing contracts. Steve Schneider of NASA Glenn Research Center provided the information on the proposed rocket system pyrovalve testing. Leonard Dudzinski and Leon Gefert of NASA Glenn Research Center provided an analysis for the future concept Mars solar aircraft. Steve Smith of NASA Ames Research Center provided the information on the 2–D propeller airfoil testing. Finally, Fred Oswald of NASA Glenn Research Center provided information on the proposed gearbox testing.

Available from

NASA Center for Aerospace Information
7121 Standard Drive
Hanover, MD 21076

National Technical Information Service
5285 Port Royal Road
Springfield, VA 22100

Available electronically at http://gltrs.grc.nasa.gov/GLTRS

OVERVIEW OF PROPULSION SYSTEMS FOR A MARS AIRCRAFT

Anthony J. Colozza
Dynacs Engineering Company, Inc.
Brook Park, Ohio 44142

Christopher J. Miller, Brian D. Reed, Lisa L. Kohout, and Patricia L. Loyselle
National Aeronautics and Space Administration
Glenn Research Center
Cleveland, Ohio 44135

INTRODUCTION

The capabilities and performance of an aircraft depends greatly on the ability of the propulsion system to provide thrust. Since the beginning of powered flight, performance has increased in step with advancements in aircraft propulsion systems. These advances in technology from combustion engines to jets and rockets have enabled aircraft to exploit our atmospheric environment and fly at altitudes near the Earth's surface to near orbit at speeds ranging from hovering to several times the speed of sound. One of the main advantages of our atmosphere for these propulsion systems is the availability of oxygen. Getting oxygen basically "free" from the atmosphere dramatically increases the performance and capabilities of an aircraft. This is one of the reasons our present-day aircraft can perform such a wide range of tasks. But this advantage is limited to Earth; if we want to fly an aircraft on another planetary body, such as Mars, we will either have to carry our own source of oxygen or use a propulsion system that does not require it.

The Mars atmosphere, composed mainly of carbon dioxide, is very thin. Because of this low atmospheric density, an aircraft flying on Mars will most likely be operating, in aerodynamical terms, within a very low Reynolds number regime. Also, the speed of sound within the Martian environment is approximately 20 percent less than it is on Earth. The reduction in the speed of sound plays an important role in the aerodynamic performance of both the aircraft itself and the components of the propulsion system, such as the propeller. This low Reynolds number-high Mach number flight regime is a unique flight environment that is very rarely encountered here on Earth.

BACKGROUND AND HISTORY

The concept of flying an aircraft on Mars has been around since the 1970's. However, the environment on Mars imposes several constraints on the ability to produce thrust and fly because of the planet's thin atmosphere. Figure 1 compares the atmospheric densities on Earth and on Mars; the atmospheric density on the surface of Mars is comparable to that at an Earth altitude of approximately 30 km (~100 kft).

The first significant work on Mars flight was based on the Mini-Sniffer project (ref. 1) run by NASA Dryden Flight Research Center. Taking advantage of the Mini-Sniffer technology, the Jet Propulsion Laboratory (JPL) tried to adapt this aircraft to a Mars atmospheric flight vehicle. The Mini-Sniffer was a small, remotely piloted aircraft designed to fly at an altitude of up to 30 km (100 000 ft) on Earth. It used a propeller with a hydrazine-burning engine. The engine was designed by James Akkerman from NASA Johnson Space Center. A prototype engine was constructed, and some testing was performed. However, by the end of the 1970's, the program was put on hold, and all development of the hydrazine engine was stopped. A picture of the Mini-Sniffer aircraft is shown in figure 2.

Since this initial work with the hydrazine-powered aircraft, all subsequent work on a Mars aircraft has been mostly analysis and design, with little actual hardware development. The series of studies that followed examined several types of aircraft, both powered and unpowered. Figure 3 shows a glider concept for a Mars aircraft. The propulsion systems examined for the powered aircraft basically fell into one of two categories: electrically powered systems, an example of which, a solar-electric Mars aircraft, is shown in figure 4 (ref. 2); and fueled systems using either a monopropellant or a bipropellant. In the mid-1990's, NASA Ames Research Center began a series of studies looking into the design of a Mars aircraft. The aircraft that Ames researchers proposed, which advanced to the preliminary design phase, was powered by a hydrazine engine similar to the Akkerman-designed engine. An artist's conception of this aircraft is shown in figure 5.

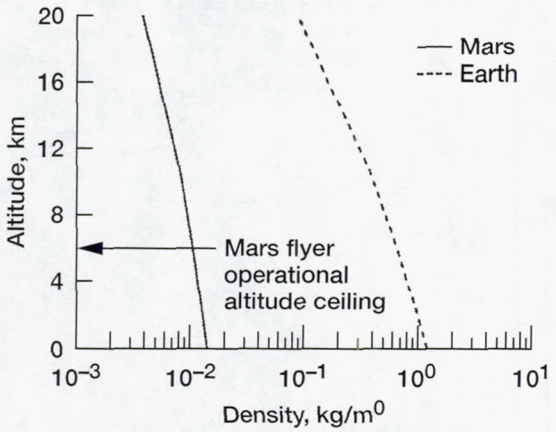

Figure 1.—Comparison of atmospheric densities on Earth and on Mars.

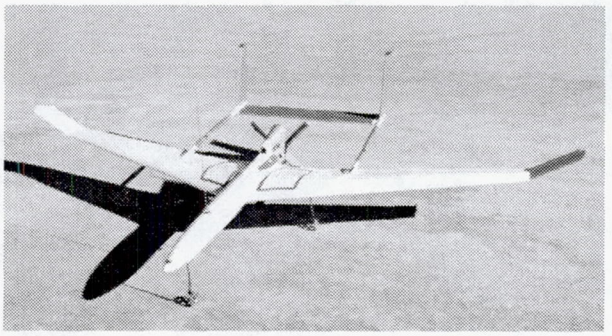

Figure 2.—Mini-Sniffer aircraft.

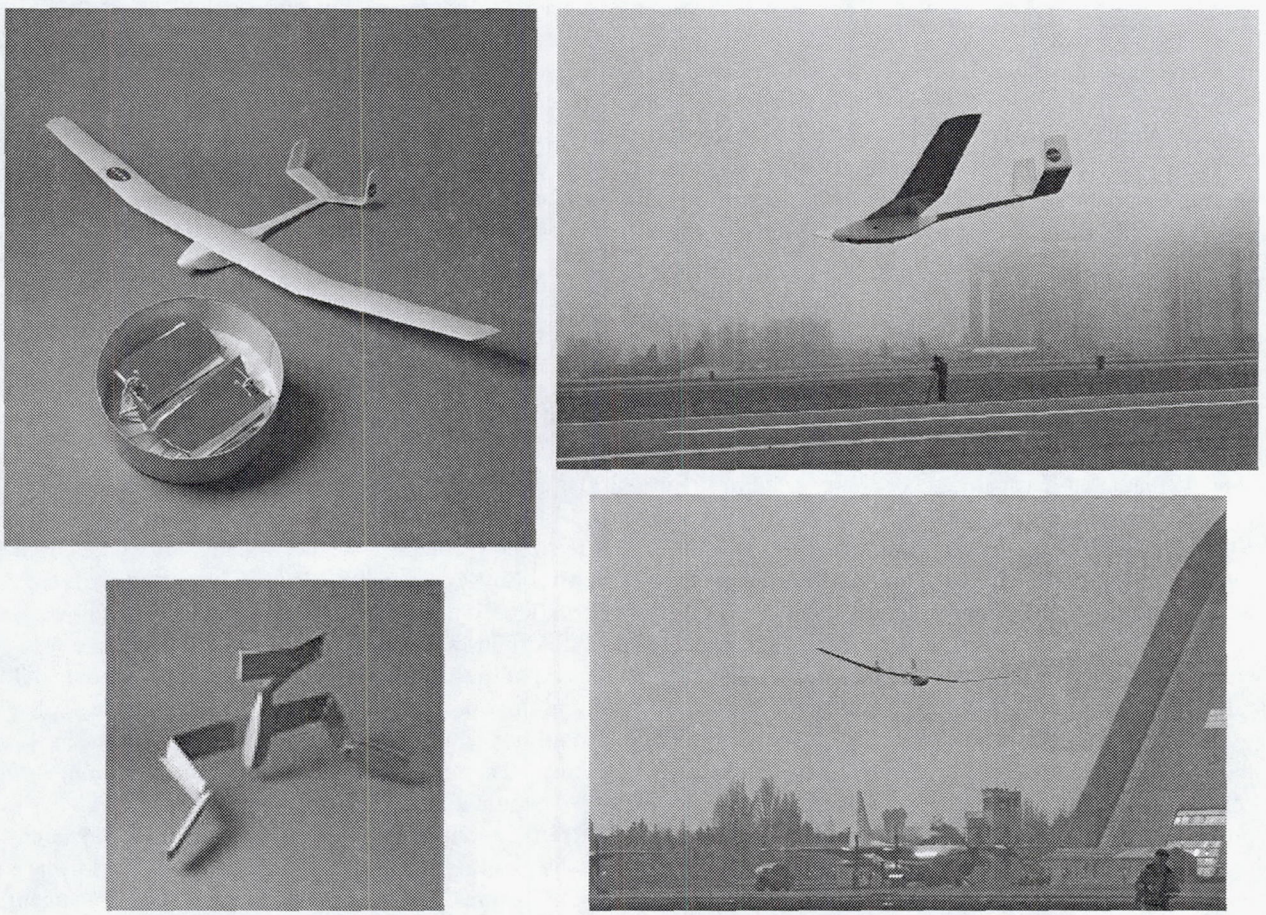

Figure 3.—Mars aircraft glider concept.

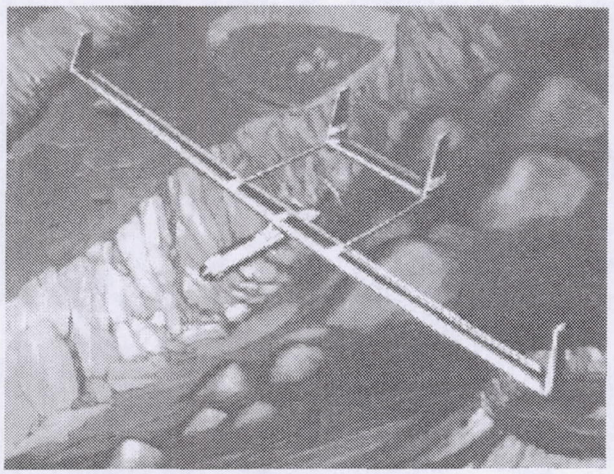

Figure 4.—Solar-electric Mars aircraft concept.

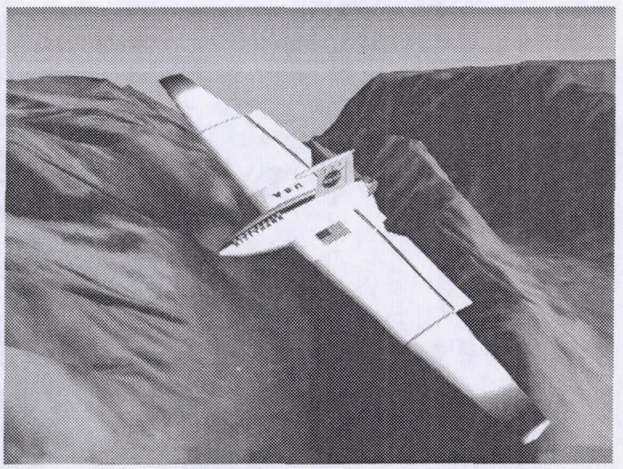

Figure 5.—Ames concept for a hydrazine-powered Mars aircraft.

Flying an aircraft on Mars was presented in early 1999 as the potential first mission for the newly created Mars Micromission Program. The program was based on a cooperative agreement between NASA and the French space agency CNES to deliver several small (50 kg) payloads to low Earth orbit as a stow-away package on an Ariane 5 launch vehicle. The payload, along with its Mars transfer vehicle, would occupy one quarter of the outer ring shroud of the Ariane 5 (a diagram of the proposed transfer spacecraft and its positioning on the Ariane 5 is shown in fig. 6). The Mars aircraft was proposed for launch during the first launch opportunity in late 2002. If this launch timeframe were met, the aircraft would fly on Mars by mid-December 2003, almost exactly 100 years after the first Wright Brothers flight at Kitty Hawk.

The goal to have an operational, flight-ready aircraft available for the 2002 launch date meant that very little development work could be done. The majority of the components for the aircraft, including the propulsion system, needed to be off-the-shelf and require as little development time as possible. This limitation on development time, as much as any other constraint, defined what could be considered a candidate propulsion system.

The issues of flying an aircraft on Mars and the constraints of the micromission spacecraft bus and proposed launch date introduced challenges for the design and operation of the aircraft and its propulsion system. An aeroshell small enough to be carried by the Mars micromission spacecraft would be much smaller than that used for previous Mars missions. Several potential micromission aeroshells and the Mars Pathfinder aeroshell are compared in figure 7. The overall aircraft size was limited by what could be packaged into the aeroshell. Even with the most optimistic packaging scheme, the small aircraft would have an approximate wingspan of 1.5 m, on the order of present-day model aircraft.

With this small aircraft size and the very low atmospheric density on Mars, the aircraft would be operating at a Reynolds number of approximately 40 000 and at a Mach number between 0.5 and 0.8. If a propeller were used as part of the propulsion system, the aircraft would operate at a Reynolds number of approximately 15 000 at a tip Mach number of about 0.85. This very low Reynolds number-high Mach number flight regime is unique. There are no present-day aircraft that fly in this regime, and very little work has been done on aerodynamic performance in this area. Figure 8 shows the Reynolds and Mach numbers for some typical present-day aircraft and some of the proposed Mars aircraft micromission concepts. Because of the very limited data on airfoils within this flight regime, designing an airfoil and predicting its performance is difficult.

The environmental conditions on Mars and the launch vehicle size and weight play a significant role in selecting the aircraft propulsion system to be used. The systems that were considered as potentially viable for a Mars micromission aircraft are listed below, and each is described in greater detail in the following sections of this report. Some propulsion systems for future Mars aircraft after the proposed 2003 flight were also examined. Because of the required degree of development, these systems would not be applicable to the proposed 2003 Mars micromission, but they did hold promise for future missions.

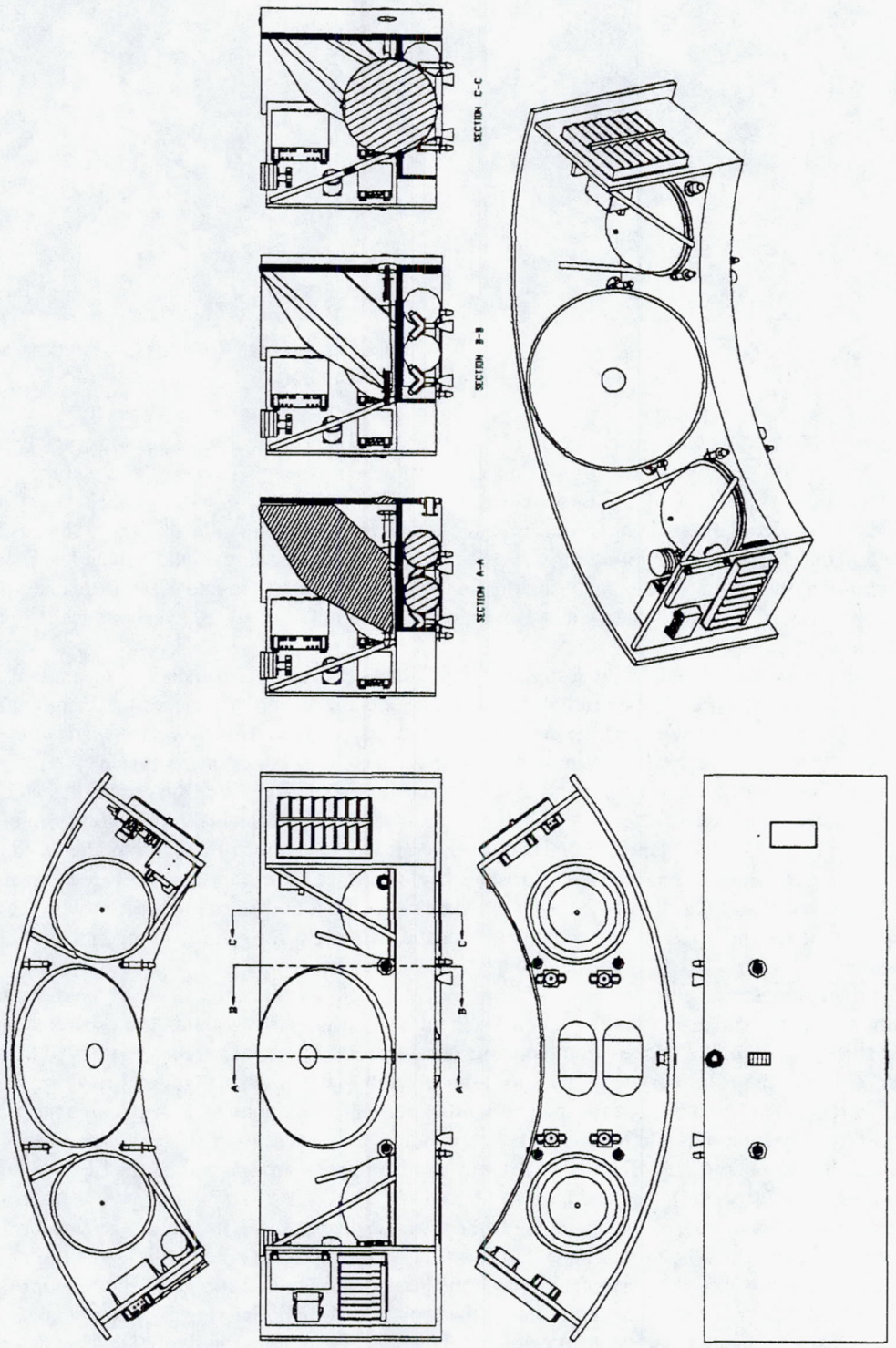

Figure 6.—Positioning of proposed transfer spacecraft on the Ariane 4 launch vehicle.

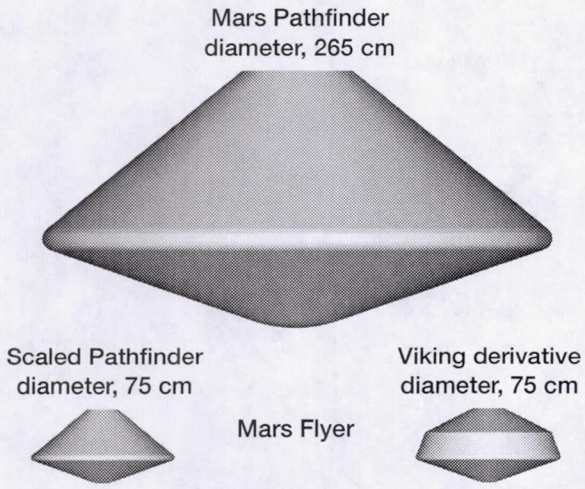

Figure 7.—Mars Pathfinder aeroshell and candidate aeroshells for Mars micromission.

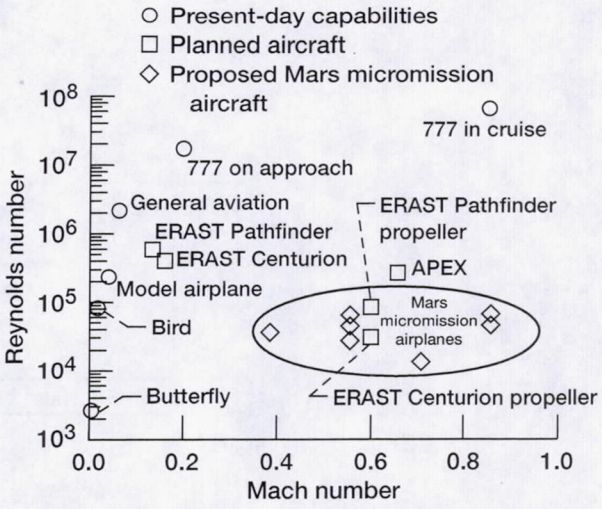

Figure 8.—Combinations of Reynolds and Mach numbers of present-day aircraft and some proposed Mars micromission airplanes. The oval indicates projected range for the Mars micromission aircraft.

1. Electric system: batteries, propeller, gearbox, electric motor
2. Combustion system: hydrazine engine, piston expander, jet
3. Rocket: solid, monopropellant, bipropellant
4. Future concepts: solar and/or inflatable vehicles, entomopter

For the propulsion system operation, certain system requirements were established by the preliminary aircraft design. Constraints also were set by the micromission requirements, as well as the environmental conditions present both on Mars and in transit. These base requirements are summarized in table I.

The component selection and designated testing for the various candidate propulsion systems was done largely to meet the operational and environmental requirements. These requirements and the proposed mission time line dictated the kinds of systems to be considered. The objective was to use off-the-shelf components as much as possible. However, due to the unique environmental and operational constraints, each of the components that made up the propulsion system had to be evaluated or designed to ensure their survival and operation for the duration of the mission. Although only state-of-the-art components were considered, modifications could have been necessary to ensure that they would meet the mission goals. All propulsion systems that were considered and any evaluation that was performed on the components is presented in this report.

TABLE I.—SYSTEM REQUIREMENTS
FOR MARS AIRCRAFT MICROMISSION

Operational thrust level	~10 N
Flight speed	150 to 220 m/sec (depending on type of propulsion system)
Flight altitude	Within 1- to 5-km range (depending on mission)
Flight duration	20 min (flight duration set by communication window time)
Total aircraft weight	<25 kg
Estimated temperature in transit	−30 to 0 °C
Other considerations	Space radiation environment little to no outgassing allowed Launch and Mars entry vibration g-loads

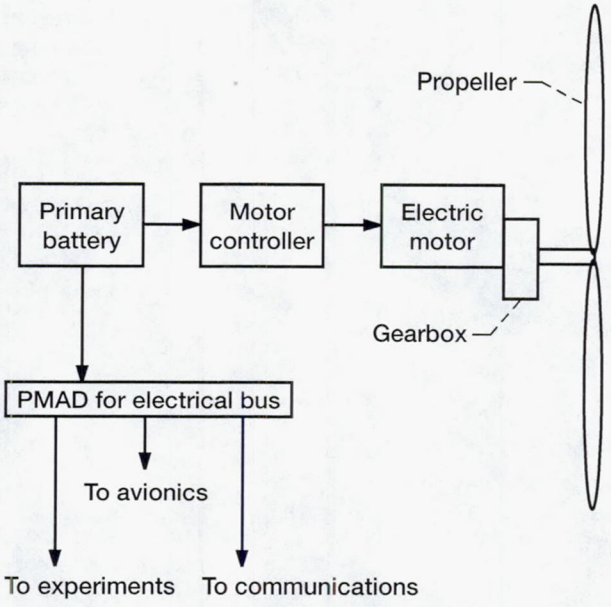

Figure 9.—Electric-powered propulsion system.

ELECTRIC SYSTEM

Of the preliminary designs developed for a 2003 Mars mission, two used electric-based propulsion systems. The NASA Dryden design required a power level of 1.1 kW for 5 min, while the NASA Ames design required a 1.5-kW power level for 15 min. A key component of the electric propulsion system is the power source to the motor. Throughout the conceptual design phase, mass and volume were the prime constraints on all of the airplane subsystems. Since the total airplane mass was limited to 24 kg and the interior volume of the plane had to accommodate not only the batteries and motor but also the avionics, science instruments, and communications equipment, the power system mass and volume had to be minimized. Also, since the mission was to fly in 2003, the technology chosen had to require little or no development.

During the conceptual design phase, it was assumed that the carrier spacecraft would provide enough power to the batteries while in transit to maintain the battery temperature and state-of-charge and avoid capacity loss and performance degradation. After the conclusion of the conceptual design phase, it became apparent that only a limited, but negotiable, amount of power would be available to the payload from the carrier spacecraft. The numbers presented in this report reflect best-case scenarios in which the batteries are maintained within an acceptable temperature range and trickle charged in transit to avoid any performance degradation.

The electric propulsion system configuration for the Mars aircraft consists of an energy source, an electric motor, a gearbox, and a propeller. A diagram of this propulsion system is shown in figure 9. The majority of the components for this type of propulsion system can be obtained without much development, except for the propeller. Even though the technologies for most of these components are mature, they would still need to be evaluated and/or modified to ensure that they would operate under the environmental conditions encountered during this mission.

Battery

Many potential power sources for the airplane were considered. For extended duration missions, hydrogen-oxygen fuel cells exhibit much higher energy densities than batteries. However, for the given mission times and power levels, fuel cells could not compare with the energy density of advanced batteries. Batteries have the additional advantage that they are generally passive systems with no moving parts. Both primary (nonrechargeable) and secondary (rechargeable) batteries were considered. Primary batteries have the advantage that their state of charge does not have to be maintained during the mission, thus reducing the load on the carrier spacecraft power system. Nickel-based secondary batteries are widely used for satellite applications and are to be used in the International

Space Station, their main advantage over other types of batteries being their relatively long cycle life. Both primary and secondary silver-zinc cells generally provide a higher energy density and a higher discharge rate than nickel-based systems, but have a lower cycle life. Primary silver-zinc cells exhibit a rapid self-discharge rate when launched wet (i.e., with electrolyte in the cells). One way to overcome this problem would be to launch them dry and have an external electrolyte reservoir connected to the cells via a common manifold. This would require additional mass, volume, and complexity to accommodate the reservoir and manifolds. Secondary silver-zinc cells also exhibit a high self-discharge rate, although not as high as the primary silver-zinc cells. Conversations with personnel at Yardney Technical Products indicate that the high-rate and low-rate secondary cells have a wet life of 9 to 12 and 12 to 18 months, respectively. Also, below –10 °C, silver-zinc cells show significant performance degradation, which means that they would require some type of heating to maintain a nominal operating temperature of 20 °C.

Primary lithium chemistries exhibit higher energy densities and operate over a larger temperature range than silver-zinc cells. Two predominant lithium chemistries are lithium thionyl chloride ($LiSOCl_2$) and lithium sulfur dioxide ($LiSO_2$). $LiSOCl_2$ cells exhibit better low-temperature performance than $LiSO_2$ cells do (the typical operating range for $LiSOCl_2$ cells is –55 to +85 °C, compared to –60 to +70 °C for $LiSO_2$). Nominal operating temperatures for both of these chemistries is 20 °C, with their performance becoming significantly degraded as the temperature is lowered. However, the percentage of performance degradation with temperature is cell specific and not adequately quantified for all cells. Consequently, there is very little data available either in the literature or from the battery manufacturers on temperature effects for primary lithium cells. Since JPL has had a considerable amount of experience with primary lithium batteries in space missions, the NASA Glenn Research Center team visited them to discuss lithium batteries for the Mars airplane. Unfortunately, the JPL battery group was unable to locate any low-temperature data from their previous missions.

While primary lithium cells do exhibit very high energy densities, their main drawback is that they cannot achieve high discharge rates (typically much less than C/2, where 1C is equivalent to fully discharging the battery in 1 hr) for an extended period of time. When sizing a system, there is a temptation to use the manufacturer's cell-level energy density to extrapolate to the battery level. For systems with a limited discharge rate such as the lithium cell, the energy density will be substantially lower at the battery level than at the cell level because of the limit on current draw, which means that more cells connected in parallel are needed to boost the current to the required level. Consequently, there is an excess of capacity in the battery that is never used (i.e., the cells are never fully discharged). This effect can be seen in figure 10, which is a plot of the mass of a lithium battery as a function of the discharge time for a range of power levels. These numbers are based on the SAFT LO39SHX cell, which is a high-rate $LiSO_2$ cell. The characteristics of this cell are shown in table II. As can be seen from this plot, for discharge times of less than 1 hr, the excess capacity being carried will not change the mass of the battery because of the limited discharge rate. Although the cell energy density is 250 Whr/kg, the battery energy density delivered for the Mars airplane requirements is in the range of 20 to 60 Whr/kg.

There is some question whether these cells can be pushed beyond the manufacturer's recommended maximum rate. Typically, for safety reasons, lithium manufacturers tend to be conservative when stating the maximum discharge rate. Therefore, none of the manufacturers contacted would commit to anything higher than their published rates. The Naval Research Laboratory has done some abuse testing of lithium cells. After contacting researchers at the Laboratory early in the program, the Glenn team received initial information that they had pushed SAFT $LiSO_2$ high-rate cells to the 1C rate with active cooling.

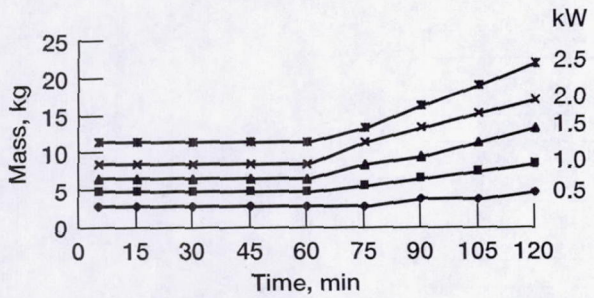

Figure 10.—Effect of discharge time on SAFT $LiSO_2$ lithium battery mass.

TABLE II.—CHARACTERISTICS OF SAFT LO39SHX LITHIUM CELL

Size	F
Nominal capacity at 20 °C (68 °F), 2 V cutoff	11.5 Ahr C/5
Open circuit voltage at 20 °C	3.0 V
Nominal voltage at 20 °C	2.8 V C/5
Maximum recommended constant current	8.0 A
Operating temperature range	–60 to +71 °C
Storage temperature range	–60 to +71 °C
Diameter (max.)	31.4 mm
Height (max.)	100 mm
Weight	125 g

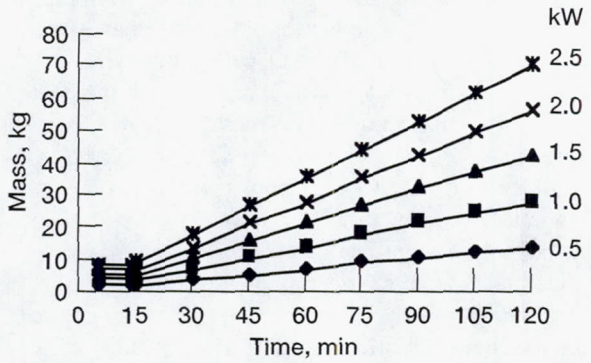

Figure 11.—Effect of discharge time on Yardney Ag-Zn silver-zinc battery mass.

TABLE III.—CHARACTERISTICS OF YARDNEY HR 1.5 SILVER-ZINC CELL

Nominal capacity	1.5 Ahr
Maximum continuous current at 20 °C	8.0 A
Output at maximum current	1.9 Ahr
Average voltage	1.35 V
Storage temperature range	wet: −40 to +49 °C dry: −54 to +74 °C
Operational temperature range	−23 to +74 °C optimal: 10 to 50 °C
Overall height	58.9 mm
Width	27.4 mm
Depth	13.7 mm
Weight	36.9 g

Although the silver-zinc cell energy density is lower than that of the primary lithium systems, it does offer high discharge rate capability. Yet, for mission times of 15 min or less, the maximum current draw is reached, requiring the battery to carry some excess capacity (as seen in fig. 11), although not nearly as much as for the lithium battery. The graph in figure 11 is based on the Yardney HR 1.5 cell, a high-rate silver-zinc cell whose characteristics are shown in table III. Overall, for this type of high-power, short-duration mission, silver-zinc cells offer a lower system mass than do lithium cells.

Preliminary sizings using high-rate silver-zinc cells were completed based on the given requirements. For the purposes of the conceptual designs, which were focused on meeting mass and volume constraints, issues such as integration into the airplane and thermal control were not addressed. Since the batteries were to be dedicated to the propulsion system (a separate battery would power the avionics, communications, and science payloads), it was assumed that the motor would be designed to accommodate any battery output voltage and current. This allowed choosing a battery output voltage and current that would minimize the battery mass and volume.

Consider first the requirement for1500 W for 15 min (375 Whr), which was based on the design presented by NASA Ames. Along with the power requirements, there was an additional requirement to allow for packaging in the wings, which limited the cell size. The total wing volume available for batteries was 2900 cm^3, assuming a battery cross section of 0.018 by 0.05 m. Additional volume in the fuselage, comparable to the wing volume, was also available for batteries, with a desired cell dimension of 0.018 by 0.05 by 0.27 m.

The limits imposed on the cell dimensions dictated the use of the Yardney HR 1.5 cell. Minimum mass and volume was achieved for a battery output of 40.5 V and 37.1 A. The 40.5 V output voltage translates to a battery capacity of 9.3 Ahr. This would require 5 battery packs connected in parallel with each pack containing 30 series-connected cells. The battery mass and volume were 6.08 kg and 3658 cm^3, both of which include a 10-percent build-up factor to go from the cell to the battery level.

For the requirement presented by NASA Dryden for 1100 W for 5 min, the minimum battery mass was achieved using the Yardney HR 5 cell (ref. 2), whose characteristics are shown in table IV. No volume requirements

TABLE IV.—CHARACTERISTICS OF YARDNEY HR 5 SILVER-ZINC CELL

Nominal capacity	5.0 Ahr
Maximum continuous current at 20 °C	60.0 A
Average voltage	1.31 V
Storage temperature range	wet: −40 to +49 °C dry: −54 to +74 °C
Operational temperature range	−23 to +74 °C optimal: 10 to 50 °C
Overall height	73.7 mm
Width	52.8 mm
Depth	20.3 mm
Weight	127.6 g

or cell dimensions were specified for this case. This cell is considerably larger than the HR 1.5, which allows for better energy density. The battery consisted of 1 pack of 14 series-connected cells. The battery mass and volume were 2.0 kg and 1218 cm, including the 10-percent build-up factor (Hutchison, R.A., and Turner, L., Propulsion System Final MDS Report, L-1613-GWNL90-024. Internal Boeing Report, March 30, 1990). The battery output was 60 A and 18.3 V.

To refine the estimates presented here, a complete set of mission requirements must be established and a thermal analysis performed to determine the environment in which the batteries will operate. To achieve optimal performance from the silver-zinc batteries, sufficient power must be supplied in transit to maintain temperature and state-of-charge. If temperature and/or state-of-charge cannot be maintained, the mass and volume estimates reported here will increase, reflecting the increase in capacity required to offset the performance degradation.

Propeller

For an electric-powered aircraft, the key element to generate thrust in the very thin atmosphere of Mars is the performance of the propeller. In general, a propeller is an efficient and effective way to generate thrust. The use of a propeller is characteristic of conventional aircraft flight on Earth, and for a given amount of stored energy, propellers provide the greatest range. However, the performance of a propeller on Mars will be different than it is on Earth.

Attempting to operate a propeller within the Mars environment entails a substantial amount of risk. Most of this risk stems from the fact that no history exists for a propeller operating under atmospheric conditions like those on Mars. Generating thrust within the low-density atmosphere of Mars is a substantial undertaking, similar to operating a propeller at an altitude of approximately 33 km (110 000 ft) on Earth. The main issue in a low-density environment is the low Reynolds number the propeller (or airfoil) must operate under. Reynolds number (Re) is a nondimensional quantity that represents the ratio of the inertial forces (pressure) to the viscous forces (shearing stress) of a fluid as it passes over the airfoil.

Re = [(velocity fluid density) characteristic length]/ coefficient of viscosity

For a conventional airfoil, the higher the Reynolds number, the more stable the operation. As the operational Reynolds number decreases, the performance of the airfoil becomes more chaotic and less predictable and its overall performance decreases. This can be seen in figure 12.

Some of the most important aerodynamic issues that must be understood when dealing with low Reynolds number flow are as follows:

1. Understanding the formation of the boundary-layer separation bubble
2. Being able to predict and enhance boundary-layer transition from laminar to turbulent
3. Being able to induce reattachment of the boundary layer upon separation
4. Understanding the aeroelastic behavior of the propeller (This is important because large changes in pressure can occur from small changes in angle of attack. With a thin lightweight blade, the main goal would be to prevent flutter.)

The main objective of the propeller development is to produce an efficient design. However, no data exists on the aerodynamic performance of an airfoil under the

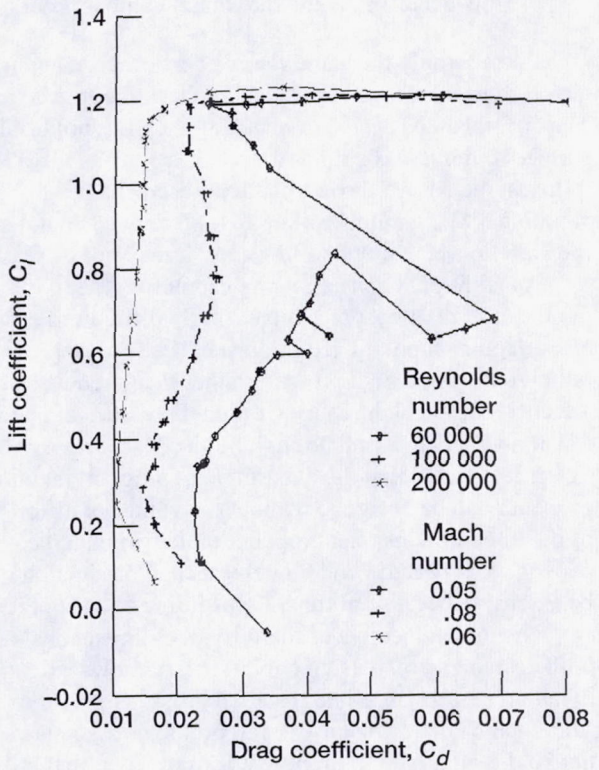

Figure 12.—Airfoil lift and drag coefficients with decreasing Reynolds number (airfoil data from Langley Research Center Low-Turbulence Pressure Tunnel).

low Reynolds number (15 000)-high Mach number (~0.8 to 0.95) conditions that would be encountered on Mars. Because of this lack of data, an experimental program is needed to obtain data to validate airfoil analysis codes. If validated, these codes could then be used with confidence to design a propeller. The code validation could be accomplished by a series of two-dimensional airfoil tests under the correct combination of Reynolds and Mach numbers. The main objective of the two-dimensional airfoil testing is to obtain the airfoil aerodynamic performance over a range of operating conditions. Use of wind tunnels with low turbulence levels is mandatory for this testing because of the strong tendency of the flow to remain laminar and the potential to relaminarize after forced transition. Wind tunnels with high turbulence levels will optimistically predict good airfoil performance that is not attainable by flight through the atmos-phere. The length scales of turbulence in wind tunnels that interact with the boundary layer are fundamentally different from those found in the convectively active atmosphere, which are not likely to interact substantially with the boundary layer. To attain good airfoil performance, it is likely that forced boundary-layer transition will be needed, and it is vital to demonstrate that these boundary-layer trips will actually work during flight on Mars. The performance of the airfoil can be determined by measuring the following quantities and properties:

- The measurement of the lift and drag of the airfoil can be determined by pressure measurements. Surface pressure orifices are integrated to determine lift, while wake momentum can be measured with a pressure rake to determine drag. Approximately 20 pressure orifices are required on both the upper and lower surface for accurate lift integration. In addition, approximately 50 wake pressure measurements should be made to determine the airfoil's drag force.

- The boundary-layer state can be inferred from the pressure distribution and measured lift and drag of the airfoils. Changes in pressure distribution and performance due to installation of various boundary-layer trips will need to be investigated.

- The location of transonic flow and any associated shocks can be easily detected in the surface pressure orifice measurements. Transonic performance should be investigated because of the potential for transonic flow occurring at the maximum camber point on the propeller tip airfoil sections.

Because only the aerodynamic performance and not structural integrity is at issue in a two-dimensional test, the airfoil shapes must be similar but the airfoil construction does not have to be identical to the airfoil actually used. The airfoil can be scaled to match a given Reynolds number and constructed of any suitable material (as long as the surface roughness is similar to that of the actual airfoil) without affecting the desired results. This allows some flexibility in the size of the test chamber used. To be applicable to this test, the experimental facility must be capable of attaining a Mach number of up to 0.85 with a Reynolds number down to 15 000 for the propeller airfoil. Because of the high tip Mach number, however, it may not be feasible to test the propeller airfoils in a two-dimensional facility.

An additional concern is the geometric fidelity of the models. If a low Reynolds number is obtained by scaling the model size, it becomes increasingly difficult to ensure that the manufactured shape matches the airfoil design. It also becomes more difficult to install the surface pressure orifices. It is desirable to achieve the low Reynolds number by reducing tunnel pressure rather than model scale. A practical lower limit on the airfoil chord is approximately 7.5 cm (3 in.), which requires a tunnel pressure of about 50 mbar (0.75 psia) to achieve the desired Reynolds and Mach numbers to simulate flight in the Mars atmosphere.

If it is found that the experimental program mentioned above is not practical or possible to perform, then the propeller can be designed without the validated airfoil design codes. This approach would require iterative testing of the three-dimensional propeller under simulated environmental conditions. The drawback of this approach is the expense of repeated wind tunnel tests and production of several prototype propellers. The time required could also be extensive because of tunnel scheduling and propeller construction.

The main objective of the full three-dimensional testing would be to obtain data on propeller performance for both design and off-design conditions. It allows extensive proof-of-concept demonstration, including of basic aerodynamic performance and installed propeller performance. Full three-dimensional tests can also be invaluable in finding and correcting any design problems associated with the propeller's operation. As stated above, this would not be the preferred environment for propeller airfoil development or design issues of overall geometry such as blade twist, etc.

The measurement of the other aspects of the propeller such as operation over a range of flight conditions can be accomplished in a number of ways depending on the experimental facilities. The easiest and most accurate is a direct measurement of forces and moments using a strain-gauge hub balance. Wake surveys can be performed to infer the

propeller's performance by measuring the change in the free-stream airflow. This was the method Boeing used to estimate the performance of the propeller for the Condor, an unmanned high-altitude aircraft (Hutchison, R.A., and Turner, L., Propulsion System Final MDS Report, L–1613–GWNL90–024. Internal Boeing Report, March 30, 1990). Ideally, thrust measurements would be taken over a range of operating conditions to get a complete picture of the propeller's performance capabilities. It is probably not practical to install pressure instrumentation on the propeller blades, but propeller airfoil behavior can be inferred from thrust measurements.

Strain or structural loading information can also be collected. This can be done by mounting strain gauges at various locations along the propeller blade. This provides information on the aeroelastic deflections as well. Knowing the structural loading of the propeller under operation can also help diagnose any performance problems.

Test facilities.—For either the two-dimensional airfoil or three-dimensional propeller testing, a suitable facility must be found that can meet the conditions described above. A summary of some of the available pressurized wind tunnels that could potentially be used for this type of testing is given below.

To date, six potential facilities have been identified for Mars aircraft wind tunnel testing. Additional facilities that might be candidates for testing may be found and added to this evaluation:

- The Mars Wind Tunnel at NASA Ames Research Center
- The 12-Foot Subsonic Pressure Wind Tunnel at NASA Ames Research Center
- The Low-Turbulence Pressure Tunnel at NASA Langley Research Center
- The Transonic Dynamics Tunnel at NASA Langley Research Center
- The 10- by 10-Foot Supersonic Wind Tunnel at NASA Glenn Research Center
- The Space Power Facility at NASA Glenn Research Center's Plum Brook Station

The Mars Wind Tunnel is an open-circuit ejector-driven tunnel located in a large pressure chamber that can simulate Mars' atmospheric conditions. It is capable of 160 m/sec velocity with a test section appropriate for two-dimensional airfoil sections. Accurate Mach number and Reynolds number simulation is therefore attainable. However, the turbulence levels of the ejector-driven circuit are unknown at this time. It may be possible to fabricate a turbulence reduction system to allow high-quality testing in this facility.

The 12-Foot Subsonic Pressure Wind Tunnel is a closed-circuit pressurized wind tunnel with a nominally 12-foot octagonal test section. This tunnel would be used for full three-dimensional testing and isolated propeller testing. Under normal conditions, the tunnel can achieve a Reynolds number of 0.1 to 12 million/ft of the test article by changing the pressure within the tunnel. The tunnel's normal operating pressure ranges from 2 to 90 psia. The main advantage of this tunnel for low Reynolds number experimentation is that it has a very low turbulence level of $u'/U < 0.05$ percent and $v'/U < 0.2$ percent. An alternative pumping system was investigated to determine the possibility of pumping the tunnel to lower pressures, but that does not appear feasible at this time. One other possibility is to obtain the required low Reynolds numbers by using a lighter gas. The wind tunnel circuit could be evacuated to 2 psia, filled with helium, and then evacuated to the appropriate pressure to obtain the desired Mach and Reynolds numbers while retaining reasonable model scale for geometric fidelity.

The Low-Turbulence Pressure Tunnel is a closed-circuit pressurized wind tunnel designed for testing of two-dimensional airfoils. It features extremely low turbulence levels. The tunnel is capable of Mach numbers up to about 0.5, but normally cannot be evacuated to the required pressure. An auxiliary pumping system was assembled in the 1970's that allowed the tunnel to be evacuated to low pressures. This system would presumably need to be reactivated. The Transonic Dynamics Tunnel may be suitable for both two-dimensional and three-dimensional testing. This tunnel can be pumped down to an air density of 0.05 atm (0.70 psia), or perhaps even lower. The low pressure enables achieving the desired Reynolds number while utilizing a near full-scale airfoil section. The tunnel test section is square and measures 4.9 m (16 ft) per side. To date, the turbulence measurements in this tunnel have been limited to 1-atm testing conditions. The current state of the tunnel is being investigated to see whether it could be brought online to perform the desired testing. The possible use of the tunnel will depend on the results of planned calibration tests. The time scale in which this may occur is uncertain. To use this tunnel for two-dimensional testing, a set of splitter plates would need to be developed to create a narrow two-dimensional channel in the test section appropriate for two-dimensional testing. Some large tunnels such as the NASA Ames 11- by 11-Foot Transonic Wind Tunnel have these, so similar designs exist that could be copied. This does add additional delay and cost before two-dimensional testing could begin.

The NASA Glenn Research Center 10- by 10-Foot Supersonic Wind Tunnel has a number of characteristics that make it a candidate for the proposed low Reynolds number-high Mach number testing. It can be pumped down to low pressures (0.5 psia) and can achieve high Mach number flow (3.5). However, to be used for the airfoil testing,

a separate flow passage would have to be added onto the tunnel to meet the required pressure and low-turbulence conditions. The modifications would provide a 0.5-m (20-in.)-sq test section, as well as a continuous-flow capability. The estimated cost of this modification is around $700 000.

The Space Power Facility at NASA Glenn Research Center's Plum Brook Station consists of a vacuum chamber 30.5 m (100 ft) in diameter and 36.6 m (120 ft) high. The facility can be pumped down to high-vacuum conditions (10^{-6} torr). For this type of testing, it would need to be modified by placing an atmospheric wind tunnel section inside the chamber and connecting it to the atmosphere through an outside vent. The chamber would be pumped down and evacuated; a control valve would then be opened to regulate the flow of outside air into the chamber. This airflow would provide the necessary test conditions. The cost to modify the tunnel and produce the wind tunnel section is estimated at $800 000.

Other test facilities.—In addition to the proposed two-dimensional and three-dimensional wind tunnel testing, the APEX High-Altitude Flight Experiment or an operational balloon drop from about 120 000 ft could demonstrate complete aircraft systems proof-of-concept. This would include demonstrations of complete propeller and/or airfoil performance and of the propeller deployment scheme. Propeller performance may also be tested on a static or rotating test rig in a large low-pressure test cell (vacuum tank).

APEX flight experiment.—The APEX flight project was established at NASA Dryden as a platform for testing components related to high-altitude subsonic aircraft (ref. 3). The main goal of the APEX project aerodynamics testing is to gather data to validate computational fluid dynamics (CFD) codes used in the analysis of ultrahigh-altitude airfoils. The objective of the testing will be to obtain boundary-layer flight test data at ultrahigh altitudes. The data collected will include the airfoil pressure distribution, and drag and boundary-layer data indicating the state of the boundary layer.

The APEX vehicle is an unmanned glider containing testing equipment, data acquisition systems, power supplies, and control systems to conduct various experiments. The APEX glider is carried to an altitude of 33.5 km (110 000 ft) by a high-altitude balloon. At this altitude the glider is released and begins a controlled descent, during which experiments are performed. The airfoil aerodynamic testing will be accomplished by a pod-mounted instrumented airfoil section. The initial targeted flight conditions for the airfoil testing include a Mach number of 0.65, a coefficient of lift C_l of 0.96, a Reynolds number of 200 000, and an angle of attack of 4°. Data can be taken over a range of altitudes. It is estimated that 4 to 6 flights will be necessary to collect the desired amount of data and to factor out any experimental error. A diagram of the test section that could be mounted on the APEX flight vehicle is shown in figure 13.

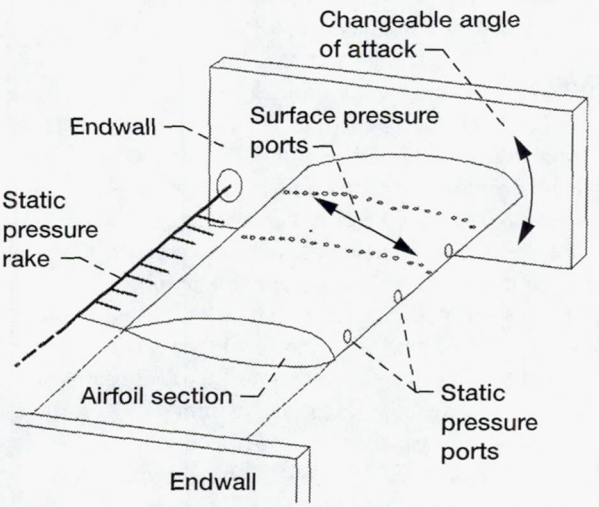

Figure 13.—Two-dimensional airfoil test section for APEX High-Altitude Flight Experiment.

In June 1999, the APEX High-Altitude Flight Experiment was still under development. The original schedule was to fly by the end of 1997. However, because of design and construction problems and funding issues, the schedule has slipped. It is not clear when the APEX vehicle will be operational. If and when it does become operational, it should provide enough information to be able to successfully validate the computer codes for two-dimensional low Reynolds number-high subsonic Mach number applications.

Atmospheric drop test.—An alternate approach to performing a wind tunnel test on the propeller airfoil is to test it at altitude under the same operational conditions that it would experience during flight. A balloon drop can be made to validate the complete propeller system, including aerodynamics, deployment mechanism operation, and integration to the airframe. This concept was examined as a means of accomplishing full three-dimensional system testing if a suitable wind tunnel could not be found. The concept would entail using a balloon to lift a platform to high altitudes, around 39.6 km (130 000 ft). The balloon would raise the platform to its starting altitude and release it. Once the desired capsule speed and altitude were attained, which would be similar to that of the proposed flight aircraft, the propeller and/or aircraft would deploy and begin flight. A balloon lifting system capable of raising the platform to the required altitude can be supplied by the National Center for Atmospheric Research. The balloon and its support facilities cost approximately $30 000 per flight.

Propeller static test rig.—Some three-dimensional propeller testing can be done on a static test stand in a simulated Mars atmosphere. A different propeller design could be developed for static testing to validate airfoil performance and propeller characteristics, and this data base used to confirm the performance of the cruise-point propeller design. A test rig that moves the propeller on the end of a rotating arm on a rotary test rig is a possibility. The Mars Atmosphere facility at NASA Ames or the Space Power Facility at NASA Glenn's Plum Brook Station are large enough to accommodate a large rotary test rig.

Other aspects of the propeller operation aside from performance are packaging and deployment. To achieve a sufficient diameter for the propeller during operation, it must be packaged within the aeroshell in a stowed configuration. From this stowed configuration, the propeller must deploy by either unfolding its blades or sliding them down a shaft (or both) to achieve its operational configuration. A propeller concept showing a potential deployment scheme is shown in figure 14. This propeller deployment entails a risk to the aircraft's operation. Significant testing will need to be performed to ensure that the propeller will deploy as desired under flight conditions.

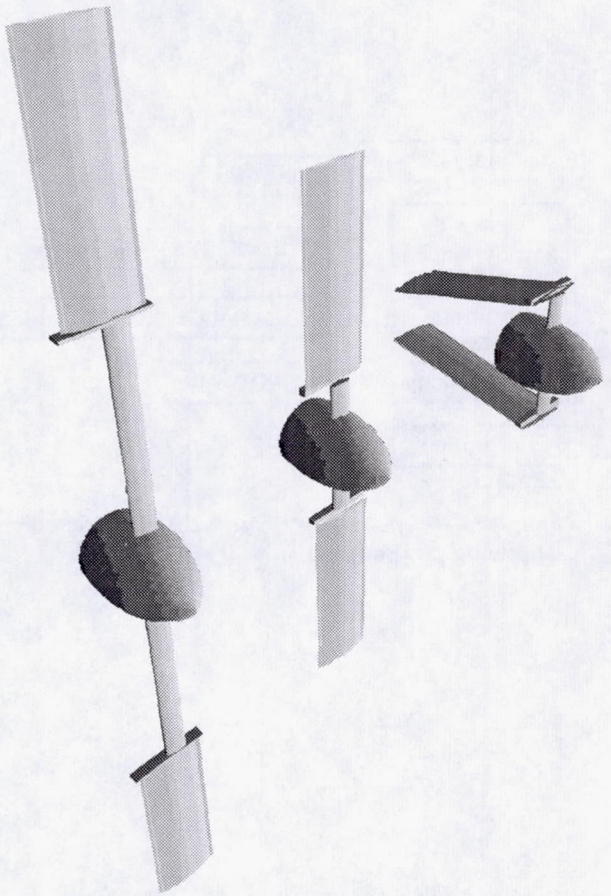

Figure 14.—Propeller concept and deployment sequence.

A diagram of the process of designing and optimizing a propeller for this application is shown in figure 15. It is an iterative approach between the aerodynamic and structural designs. The process was started with a preliminary design phase using a simple approach that has been implemented in a FORTRAN program named IDLEFF. The IDLEFF program calculates the "ideal" (i.e., no viscous loss) efficiency of a propeller, which is dependent on the number of blades, tip speed, and loading. This program quickly gives the effect of tip speed, cruise speed, and diameter changes. Once a rough propeller design has been created, a more detailed analysis can be accomplished using increasingly complex tools, such as a strip theory analysis (e.g., XROTOR, ref. 4) or a three-dimensional Navier-Stokes CFD analysis (ADPAC, ref. 5).

With a detailed aerodynamic design, and anticipating that the blade will be all composite (high strength, low weight), the COBSTRAN code (ref. 6) can be used to take a proposed ply layup schedule and generate material properties for a finite-element structural analysis such as NASTRAN or MARC. Once the steady-state mechanical design is acceptable, an aeroelastic analysis can be performed at the high Mach number-low Reynolds number operating condition using the TURBO-AE code (ref. 7).

There are a number of tradeoffs in the propeller design. For example, a larger diameter is beneficial for flight within the low-density atmosphere of Mars and increases efficiency by reducing axial momentum losses. Figure 16 shows how an increase in power loading (either by an increase in power to the propeller or by a decrease in diameter) reduces the ideal efficiency. The increase in ideal efficiency with diameter is asymptotic though, as shown in figure 17, and structural, weight, or tip speed constraints quickly limit the maximum diameter that can be used. Note that each curve in figures 16 and 17 represents a different set of three numbers: blade number, cruise Mach number, and blade tip Mach number. For example, the uppermost curve in the figures is for a two-bladed propeller with a free-stream Mach number of 0.8 and a helical tip Mach number of 1.05. These figures represent ideal efficiencies and are useful in demonstrating the gross effects on performance of a change in blade number, cruise speed, tip speed, or power loading. They do not predict the actual propeller performance because they do not take into account viscous losses, compressible-shock losses, or low Reynolds number effects. As the diameter increases for a given rpm, the tip velocity will increase. The increase in tip velocity reduces the swirl losses, but the overall propeller efficiency suffers because of compressibility effects at the blade tip. If the blade tip speed approaches Mach 1, then the formation of shock waves on the suction side will significantly reduce the propeller performance.

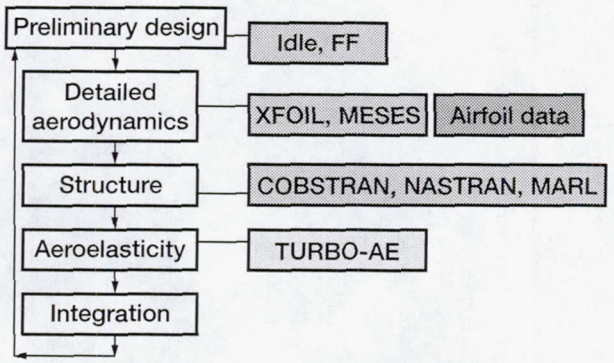

Figure 15.—Propeller design process showing corresponding program tools.

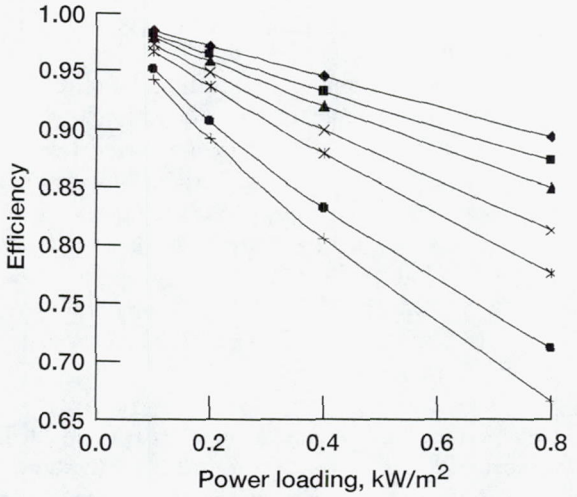

Figure 16.—The effect of power loading on ideal efficiency.

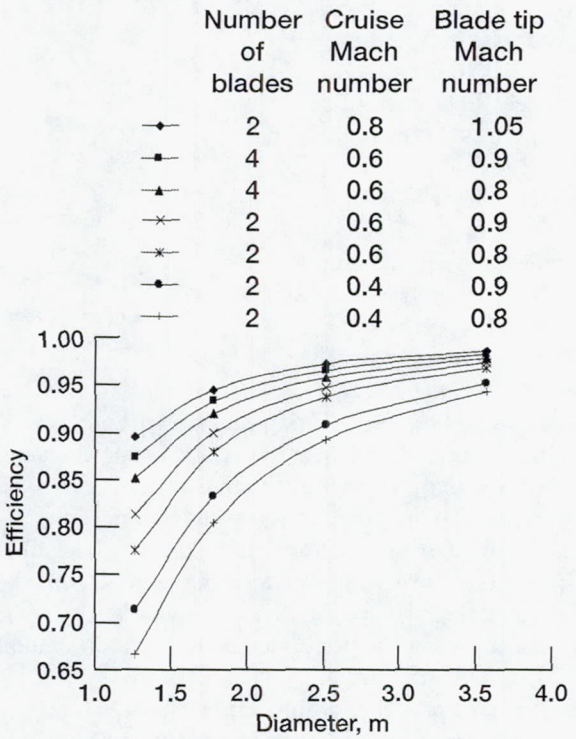

Figure 17.—Ideal efficiency power loading at P = 1 kW.

For the initial design, it was assumed that there would be two blades. The anticipated cruise speed would be Mach 0.6, and a tip speed of Mach 0.9 was intentionally set to keep the tip subsonic and thereby reduce shock losses. It was also desired to have a propulsive efficiency of about 90 percent. Knowing from general aviation propeller work that viscous losses reduce efficiency by about 5 percent, a target ideal efficiency of 95 percent was selected. Reading from figure 16, the limit on power loading is roughly 0.2 kW/m (ref. 2). The tip diameter is set by the power required. An initial propeller design can be made by assuming that the power required is 1.5 kW, which sets the tip diameter at roughly 2.75 m, for a tip radius of about 1.38 m. If this is a telescoping or folding blade, as shown in the concept sketch (fig. 14), and has a 0.7-m tip section at the end of a 0.75-m spar, it appears to be possible to fit it in the design envelope and meet the design constraints.

The next step in the design process is to use the XROTOR code to design the chord and twist along the blade. To do so requires knowing the properties of a low Reynolds number-high Mach number two-dimensional airfoil section. The XROTOR code will calculate an optimal circulation distribution and then find the maximum lift and drag (L/D) of the airfoil section(s) to set the operating lift coefficient and chord length along the blade. At very low Reynolds numbers, the maximum lift coefficient drops quickly with the decreasing Reynolds number. To increase performance range and reduce the design issues (shape sensitivity and unknown operating characteristics) with a low Reynolds number airfoil, the propeller chord can be increased (and C_l decreased to a nonoptimal value) to increase the local Reynolds number. The drag of the airfoil is thereby increased. Figure 18 shows the increase in drag and Reynolds number with increasing chord length. The objective in this trade-off is to increase the operating range and move the airfoil to a Reynolds number range (~100 000) where some data exists. Figure 18 shows that to increase the chord Reynolds number to 100 000 nearly triples the drag.

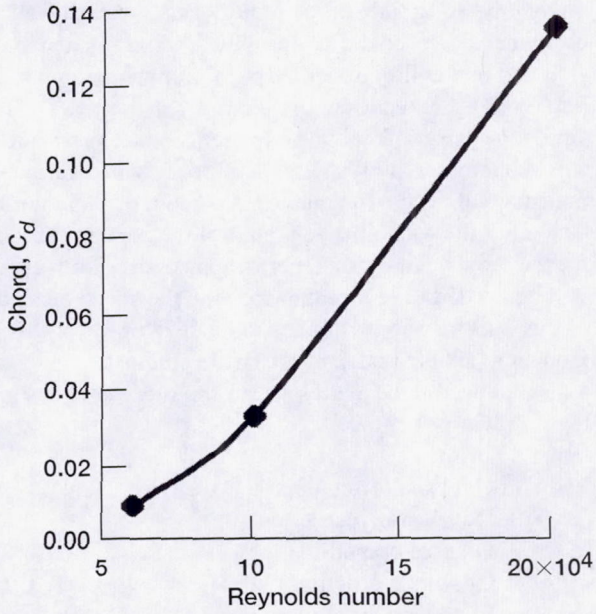

Figure 18.—Effect of increasing chord length on Reynolds number and drag.

Electric Motor and Gearbox

The electric motor selected was a brushless dc motor. This type of motor is a highly efficient way to translate the stored electrical energy into rotational energy for the propeller. Brushless dc motors are from 85 to 90 percent efficient. This compares to approximately 75- to 80-percent efficiency for a brushed motor. Brushless motors are more efficient at lower current levels (less than ~20 A) than are brushed motors because of the friction caused by the brushes. However, as the operating current increases, the losses due to the added electronics that are necessary in a brushless motor begin to decrease its efficiency. This tradeoff can be seen in figure 19 (ref. 8). For this mission, it would be preferable to operate at a lower current level (<20 A) and the corresponding higher voltage to keep the power transmission lines as thin and light as possible. Another advantage of the brushless motor is that there is no risk of the arcing that can occur with a brushed motor. The concern about arcing is due mainly to the rarefied atmosphere in which the aircraft will be flying. The thinner the atmosphere, the lower its electrical resistance and, therefore, the greater the chance of arcing. Other features of a brushless dc motor are listed below:

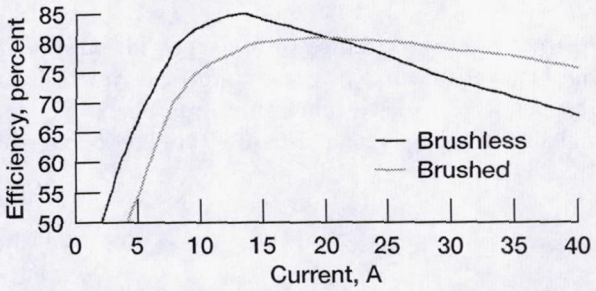

Figure 19.—Current versus efficiency for brushless and brushed dc motors.

- Compact lightweight design
- Power density on the order of 4 kW/kg
- Technology well understood, and sources from multiple manufacturers
- Custom designs available for a reasonable cost and within a reasonable timeframe

The risks associated with the use of this motor are all related to the fact that no motor of this type has ever been operated in a similar environment. Because of the thin atmosphere, the heat transfer from the motor to the environment will be poor. This poses a possible thermal problem during operation. The severity of this problem will depend

on the operating time of the motor. This issue, as well as most others relating to the operating environment, could easily be addressed during feasibility testing in an environmental chamber. The motors should be tested for outgassing and operability under Mars environmental conditions. This testing should include monitoring of the temperature, voltage, and current draw during operation. The motors should also be exposed to environmental conditions similar to those that will be experienced during transit, such as vacuum, thermal, and vibrational conditions. Unlike a brushed motor, a brushless dc motor requires various electrical components for the motor to operate. These components will need to be manufactured out of radiation-hardened electronics. None of the motor manufacturers contacted has the capability to do this at the present time. This requirement will add cost and increase the delivery time for the motor. For optimal performance, the motor should have a rotational speed of about 20 000 rpm. A gearbox will be needed to reduce this speed to the speed needed by the propeller (~1000 rpm).

A 20:1 gearbox will need to be developed for this application. There is no present-day off-the-shelf gear reducer available that can satisfy the unique design constraints presented by this mission. The major potential problems that need to be addressed for the successful design of a drive system for this Mars micromission aircraft are the following:

- Cold soak from deep space environment
- Outgassing restriction
- Oil-free operation
- Cooling restriction
- Low weight requirement
- High speed ratio
- Dry lubricated bearings
- Heat generated from gear and bearing friction

The design of the gearbox will need to take into account these concerns. The initial steps in meeting these requirements would be taken using coupon testing and component operation under simulated environmental and operational conditions.

After the termination of the 2003 Mars micromission aircraft project, no data was produced on development of the electric motor or gearbox.

COMBUSTION ENGINES

Aside from an electrically driven propulsion system, there are few choices for propeller-driven flight on Mars. This is mainly due to the very low atmospheric density and the lack of oxygen of the Mars atmosphere, which make a conventionally fueled combustion or turbine engine infeasible. However, there are a few alternatively fueled engines that have potential for use. A brief description of these is given below.

Akkerman Piston Hydrazine Engine

The Akkerman engine is a reciprocating combustion engine that burns hydrazine fuel in a catalyst bed chamber. A single prototype engine was developed in the mid-1970's for the remotely piloted Mini-Sniffer aircraft. The prototype was wind tunnel tested and flight tested to altitudes of 20 kft. The engine was designed to provide 22 kW (30 hp) of power to the propeller. A scaled-down version of this engine was proposed for use in a Mars aircraft by Development Sciences, Inc. while under contract to JPL in the late 1970's. Their estimate for the scaled Akkerman engine was that it would produce 11 kW (15 hp) of power and weigh 6.8 kg (15 lb). No prototype of this scaled-down engine was ever produced. The best measured specific fuel consumption for the original prototype engine was 2.7 kg/kWhr (4.5 lb/hp-hr).

Based on preliminary results from tests of this engine performed at the NASA Ames Research Center, the use of a hydrazine-powered engine can significantly increase the payload carrying capability, range, and endurance of the aircraft. The main issue associated with this power plant is that the one operational prototype that was produced operated at a power level approximately three times that needed for the proposed mission. Because of the risks associated with the use of this type of powerplant and the short time line of the project, it was decided not to pursue the Akkerman engine for the Mars micromission aircraft. These risks are summarized as follows:

1. The ability to scale the original engine design to the required power levels is uncertain. There is not much development history for this type of engine.
2. Significant development would be needed to produce a flight-qualified engine. Most of this development would need to take place internally because there is no outside company presently constructing this type of engine.
3. Because of the hydrazine fuel, the testing of this engine would need to be done under restricted conditions and at specialized locations.
4. The use of hydrazine fuel would require heated fuel tanks because the fuel must be maintained at a temperature between −1 and +4.5 °C (30 and 40 °F) to keep it from freezing. Also, the increased weight of the power system required to operate heaters may make this fuel choice unrealistic. If this is the case, then an alternative fuel would need to be chosen and another engine to use the new fuel would need to be developed.

Piston Expander

The piston expander engine can burn almost any mono- or bipropellant. This type of engine is used extensively by the Navy for torpedo propulsion. Because of its light weight and ability to burn several different types of fuel, this engine may be well suited for a Mars aircraft application. The engines presently used by the Navy would not be directly usable in a Mars aircraft. Several development issues would need to be addressed to apply this type of engine to the proposed micromission aircraft.

The two main obstacles to use of the engine are cooling and scaling to the correct power level. The torpedo motor is cooled during operation by circulating sea water through passageways within the engine. This would not be possible for a Mars aircraft, and an alternative cooling scheme would need to be devised. Additionally, the amount of power produced by the smallest production torpedo motor is greater by orders of magnitude than the power that would be needed for the proposed Mars aircraft. Therefore, the engine would need to be significantly scaled down to meet the power and corresponding weight requirements for this type of aircraft and mission, which would entail significant development time and cost. Because of this, the piston expander was eliminated as a potential candidate for the proposed Mars micromission aircraft.

Turbojet

This concept takes advantage of the recent developments in engine miniaturization. The turbojet would be similar to the jet used for model aircraft, except that it would be modified for operation with a monopropellant or a bipropellant. A significant amount of development would be needed to determine whether this concept is feasible. Significant modifications to present-day miniature turbine engines would be necessary to adapt for operation using the monopropellant or bipropellant fuels. Because of the limited mission timeline and the extensive development that would be necessary, this concept was not considered viable for the Mars micromission aircraft.

Situ Turbojet

Potentially, the Martian atmosphere could be used as an oxidizer in a turbojet engine, which would turn a liability into an advantage. This concept was developed by Wickman Spacecraft & Propulsion Co. (Wickman, John H., In Situ Martian Rocket and "Air Breathing" Jet Engines. Phase II Final Report, Wickman Spacecraft & Propulsion Co., Casper, WY, 1998) under funding from JPL and utilizes a magnesium-CO_2 mixture for combustion. This type of engine is very interesting for Mars aircraft applications because it could take advantage of the chemistry of the Mars environment. This is a big benefit because it eliminates the need to carry an oxidizer. Although the turbojet would be an innovative method of propulsion for a Mars aircraft, the development required to produce a viable flight-qualified engine is not reasonable for the timeframe of the proposed Mars micromission aircraft. Therefore, this engine was not considered as a candidate for this mission.

ROCKET PROPULSION SYSTEM

A rocket propulsion system was initially considered as a backup option to an electric propeller propulsion system for the Mars micromission aircraft. However, as the risks with the propeller option became more evident, rocket propulsion became the baseline approach for the 2003 mission. Several monopropellant, bipropellant, and solid rocket propulsion options could be considered for planetary aircraft propulsion. However, the propulsion system for the 2003 Mars aircraft had to be developed under the following constraints:

- Rapid flight development schedule (November 2002 launch)
- 8.9 N thrust level
- Total burn duration up to 20 min
- No power for active thermal management
- Long duration (months) in space before system activation
- Steady-state or pulse-mode operation
- Limited volume and mass envelope

Given the schedule, it was apparent that a relatively mature technology had to be selected. The current state-of-the-art propulsion systems, in the relevant thrust class, were monopropellant hydrazine (N_2H_4), the bipropellant combinations of nitrogen tetroxide (NTO)/monomethylhydrazine (MMH), and a combination of NTO and N_2H_4 (NTO/N_2H_4). The industry-standard NTO propellant is actually composed of 3 percent mixed oxides of nitrogen and is referred to as either NTO or MON–3. While these propulsion systems are an off-the-shelf technology, N_2H_4 and MON–3 require active thermal management (heaters) to keep temperatures well above their freezing points (N_2H_4, 2 °C; MON–3, –15 °C). This was unacceptable under the 2003 mission constraints. Solid rocket motors were considered, but a long-burning (tens of minutes), low-thrust (8.9 N) motor would require significant development.

The next best option was a bipropellant combination of MMH and an oxidizer composed of 75 percent NTO and 25 percent MON, or MON–25. Both MMH and MON–25 have freezing points under –50 °C, which means that the MON–25/MMH propulsion system could safely operate at –40 °C. The JPL pursued the development of MON–25/MMH technology for Mars ascent propulsion precisely because of its low-temperature capability (ref. 9). The JPL-sponsored testing demonstrated the fundamental feasibility of cold operation and provided a sound basis to baseline a MON–25/MMH system for the 2003 Mars aircraft mission.

To ensure the operation of a MON–25/MMH propulsion system, a number of risk-reduction activities were suggested:

1. A comparison of rocket propulsion options, including solid, monopropellant, and bipropellant. This activity would examine the applicable options and lay out the benefits and risks of each, although MON–25/MMH had already been selected as the baseline. This would be done to clearly point out propulsion options to mission planners and give consideration to accommodating other options by changing the 2003 mission constraints.
2. Testing of a NTO/MMH, 2-lbf thruster using MON–25/MMH propellants at temperatures down to –40 °C. This was viewed as the most critical risk-reduction activity because it would demonstrate performance and long-duration operation at the relevant temperature using off-the-shelf thrusters. This activity would identify the need for any major injector modifications, the thruster development task with the longest lead time.
3. Qualification of pyrovalves with MON–25, at –40 °C. Assuming positive isolation was needed in the propulsion system (see discussion below under Pyrovalve Testing), pyrovalve qualification with MON–25 was a long-lead item that would be required before incorporation into any flight system.
4. Preliminary system design of the Mars aircraft propulsion system. This was initially viewed as a risk identification task. That is, any off-the-shelf components that were not viewed as compatible with MON–25 or with cold temperature operation would be identified. Specific design was to be left to the flight development program, although preliminary sizing numbers were to be specified. It quickly became clear that there would be no compatibility issues with MON–25 or cold temperatures for system components. This activity then focused more on system sizing studies.

The selection of MON–25/MMH as the baseline propulsion system was felt to be the best balance between technical maturity and meeting the requirements of the 2003 mission. However, consideration needed to be given to other propulsion options, to allow mission planners the opportunity to trade off among different parameters. For example, an off-the-shelf monopropellant N_2H_4 system would greatly reduce development risk, but at the cost of providing power to maintain the propellant at 10 °C. Propulsion options were examined qualitatively in terms of technical maturity (development risk), system complexity (operational risk), thermal limits (power requirements), performance (mass requirements), and density (volume requirements). This discussion is summarized in table V. The properties of the liquid propellant options are shown in table VI.

Solid rocket motor.—Solid rockets are common for boost, upperstage, and tactical propulsion applications. A solid rocket motor would be the simplest (i.e., lowest risk operationally) propulsion option because the motor constitutes the entire propulsion system. There would be no concern about storing a solid at cold temperatures, so thermal management would not be necessary. There would have to be a demonstration of the rocket initiator at cold temperatures, but this was not expected to be a concern.

The drawback to any solid motor is that it can be fired only once, and there is no opportunity to shut it off. This would be limiting in defining the profile of the Mars aircraft mission but certainly did not preclude the use of a solid motor. A more pressing concern was that a long-duration 8.9-N solid rocket motor did not exist (according to the authors' knowledge). The existing lower thrust (<4500 N) motors were too large and heavy for the Mars aircraft

TABLE V.— COMPARISON OF CANDIDATE PROPULSION SYSTEMS

Propulsion option	Technical maturity*	System complexity	Thermal management (operating temperature, °C)	Engine performance	Propellant density
Solid	Low	Lowest	None (< –50)	Moderate	Highest
MON–3/MMH	Off-the-shelf	Moderate	High (0)	High	Moderate
MON–25/MMH	Moderate	Moderate	Little or none (–40)	High	Moderate
O2/H2	Moderate	Highest	None (< –50)	Highest	Lowest
N2H4	Off-the-shelf	Low	High (10)	Low	Moderate
HPB–1808	Moderate	Low	Moderate (–10)	Low	Moderate
H2O2	High	Moderate	High (0)	Lowest	Moderate
HAN-Glycine	Moderate	Low	Moderate (–25)	Low	Moderate
Advanced monopropellant	Low	Low	None (< –50)	Moderate	Moderate

TABLE VI.—PROPERTIES OF CANDIDATE LIQUID PROPELLANTS

Propellant	Freezing point, °C	Boiling point, °C	Density at 25 °C, g/cm^3
Hydrazine	2	113	1.004
Nitrogen tetroxide, MON–3	–15	21	1.433
MON–25	–54	–9	1.379
Monomethylhydrazine	–52	87	0.874
Hydrogen	–259	–252	0.083 (gas)
Oxygen	–218	–183	1.331 (gas)
Hydrazine propellant blend (HPB); HPB-1808	–20	100	1.080
90 percent hydrogen peroxide	–11	141	1.387
61 percent hydroxylammonium nitrate, 14 percent glycine	–35	100	1.439

envelope, and this at significantly shorter burn durations than 20 min. Thiokol, under a NASA Goddard Space Flight Center (GSFC) nanosatellite technology program (ref. 10), developed a low-thrust (356 N thrust) solid motor for an envelope 15.2 cm in diameter by 15.2 cm in length (comparable to the Mars aircraft). The burn duration of this motor, however, was well under 1 min (according to a personal communication from Dr. Michael Rhee, GSFC, September 1999). An 8.9-N solid rocket could likely be developed for a Mars aircraft, but a compromise would have to be made on the burn duration. The development of such a solid rocket was suggested as a fiscal year 2000 risk-reduction activity for a potential backup system.

Monopropellant N_2H_4.—Spacecraft propulsion systems have been using the monopropellant N_2H_4 for the past 3 decades, particularly in small total impulse missions such as the Mars aircraft. Off-the-shelf, 8.9-N N_2H_4 propulsion systems are currently available, with an extensive flight heritage for all of the components. Monopropellants represent the simplest of liquid propulsion systems because, of course, they use only one propellant. For the Mars aircraft mission, a pressurization system may not be necessary (most N_2H_4 systems operate in blowdown mode), allowing the use of an even simpler propulsion system.

The major drawback of monopropellant N_2H_4 for the Mars aircraft was that the system needed to be maintained above 10 °C (N_2H_4 freezes at 2 °C). The power costs of this could be minimized by not activating the system until just before the mission, meaning that thermal control would only be needed in the propellant tank. A secondary consideration was that N_2H_4 (and monopropellants in general) is relatively low performing (specific impulse (isp) of 210 sec at 30:1 area ratio).

Hydrazine propellant blends.—Hydrazine propellant blends (HPB's) represent a family of monopropellant formulation composed of N_2H_4, hydrazinium nitrate (HN), and water. The addition of HN and water serve to depress the freezing point and increase the performance of N_2H_4 (ref. 11). Several HPB's were developed and tested in the 1960's and 1970's, primarily for military applications. HPB's are receiving renewed attention as low-freezing-point monopropellants. The HPB 1808 (18 percent HN, 8 percent water) has a freezing point of –20 °C. Recently, NASA GSFC sponsored HPB development work at Primex Aerospace Company, under a NASA Glenn technology program.

HPB 1808 technology is relatively mature, although it has not achieved flight status. There is some question about material compatibility with HPB's, particularly of the bladder material in the fuel tank. With an isp of at least 230 sec, performance would be better than N_2H_4. The HPB 1808 would lessen (though not eliminate) thermal management because the system could safely operate at –10 °C. There are HPB's with freezing points as low as –54 °C, but they are damaging to existing catalysts and chamber materials and would have limited lifetimes. Investigation of the lower temperature HPB's could have been conducted as a risk-reduction activity.

Hydrogen peroxide.—Hydrogen peroxide (H_2O_2) has a flight heritage dating back to the 1930's, although until recently, the technology has been dormant. H_2O_2 is seeing a revival of sorts (ref. 12), primarily as an oxidizer in a bipropellant combination, but also as a monopropellant. No off-the-shelf, 8.9-N H_2O_2 monopropellant thruster exists now, but similar thrusters have flown extensively in the past, and NASA and the U.S. Air Force are investing significantly to reactivate the technology. H_2O_2 monopropellants are diluted with water; a useful rocket propellant requires a minimum of 70 percent H_2O_2. H_2O_2 represents a nontoxic alternative to N_2H_4 because it poses no vapor or flammability hazards.

High-purity H_2O_2 (>95 percent) has experienced spontaneous detonation, and generically, H_2O_2 has long-term storability problems. As with N_2H_4, propulsion systems would have to be maintained above 0 °C because H_2O_2 freezes at –11 °C. Furthermore, H_2O_2 is relatively low performing (isp of 190 sec) compared to N_2H_4.

Advanced monopropellants.—A family of monopropellant formulations composed of the oxidizer-rich salt hydroxylammonium nitrate (HAN), water, and a fuel component has been under development by NASA (ref. 13). The HAN-based monopropellants offer a high-density, low-freezing-point, nontoxic alternative to N_2H_4. The density and freezing point benefits would be of particular interest to a Mars aircraft. The most developed advanced monopropellant formulation is composed of 61 percent HAN, 14 percent glycine, and 26 percent water. Under a NASA Glenn contract, Primex Aerospace Company demonstrated a 4.45-N thruster on HAN/glycine for over 8000 sec of operation (ref. 14). Storage and system-level issues were also addressed in the program. This HAN/glycine mixture was selected because its combustion temperature is compatible with currently available catalysts. As a result, its performance (isp ≥ 190 sec) is lower than N_2H_4.

Generically, HAN-based monopropellants are 40 percent denser than N_2H_4 and have freezing points well below 0 °C. The 61-percent HAN/14-percent glycine formulation has a freezing point of –35 °C, which would lessen (though not eliminate) thermal management in a Mars aircraft system. HAN-based monopropellants with freezing points down to –60 °C have been formulated, but they are less developed than the baseline HAN/glycine.

There are HAN-based formulations with performance greater than N_2H_4. Furthermore, the U.S. Air Force has developed monopropellant formulations based on other oxidizers that perform better than N_2H_4. However, the combustion environments of these advanced monopropellants are too severe for current catalyst materials and would require the development of more robust catalysts or noncatalytic decomposition methods.

NTO(MON–3)/MMH.—NTO (MON–3)/MMH represents the state-of-art spacecraft bipropellant combination (along with NTO/N_2H_4). Like for the monopropellant N_2H_4, off-the-shelf, 8.9-N NTO/MMH systems are currently available. There is an extensive flight heritage with NTO/MMH propulsion system components. Specific impulse performance would be expected to be at least 280 sec.

However, as with the monopropellant N_2H_4, there would be a need for thermal management because MON–3 freezes at –15 °C. Also, bipropellant systems are usually operated in regulated mode, which implies a helium pressurization subsystem. The primary reason for operating bipropellants in regulated mode is mixture-ratio control, because off-nominal mixture-ratio operation could be catastrophic for the thruster. However, careful sizing of the propellant tanks could allow for blowdown mode operation and elimination of the pressurization subsystem.

Oxygen/hydrogen.—The bipropellant combination of oxygen/hydrogen (O_2/H_2) is common for large thrust (>450 000 N) applications but has never been flown in space at low-thrust levels. However, O_2/H_2 has looked attractive for a number of low-thrust applications. Over the past three decades, there has been extensive technology development of O_2/H_2 systems at thrust levels down to 0.45 N (ref. 15). Assuming propellants are stored and fed in the gaseous state, thermal management concerns are virtually eliminated. Gaseous O_2/H_2 offers a relatively simple propulsion system, without the need for helium pressurization. O_2/H_2 also offers high performance with specific impulses (depending on the mixture ratio) above 300 sec.

The drawback to using O_2/H_2 for in-space applications has always been volume. H_2, in particular, is a light gas requiring large tanks for storage, even at high pressure. Operation at oxygen-rich mixture ratios would mitigate H_2 storage requirements, but this is a riskier operating regime for the thruster. Storing propellants as liquids rather than gas would reduce storage volumes (ref. 16). However, zero boiloff tank technology would likely be needed for cryogenic storage (particularly for H_2), which would impose some power requirements on the system. Furthermore, cryogenic O_2/H_2 thruster technology is less mature than gaseous thruster technology.

Rocket Propulsion Testing

The JPL sponsored testing at Kaiser Marquardt (ref. 17) and GenCorp Aerojet (according to a personal communication from Mr. William Boyce, GenCorp Aerojet, June 1999) to demonstrate the feasibility of MON–25/MMH operation at –40 °C for a Mars ascent engine. This was accomplished with a 22-N thruster, although 150 N was the thrust level of interest for Mars ascent. The program demonstrated the fundamental feasibility of cold operation: the propellants were still hypergolic at –40 °C, and the ignition delay was minimal (less than 5 msec) compared to ambient temperatures. Testing also showed that MON–25 performance at –40 °C was no worse than MON–3. The Mars ascent program ultimately opted for a solid rocket propulsion system for a near-term mission, and further development of the MON–25/MMH system was not pursued. However, it was felt that these efforts provided the basis for pursuing MON–25/MMH for the 2003 Mars aircraft mission.

Modification of injectors is the most time-consuming developmental task in low-thrust rockets, because injector and chamber design is based almost completely on empirical observations. Extrapolation into different operating regimes (or propellants) is not easily accomplished without significant testing and iteration. For this reason, the key to reducing the development risk was to demonstrate the operation at –40 °C of existing 8.9-N MON–3/MMH thrusters on MON–25/MMH propellants.

The activity was to generate as much data as possible on the thruster operational envelope, so testing over a range of inlet pressures and temperatures was desired. Since duty cycles were not yet firmly defined, steady-state (up to 20 min in duration) and pulse testing were requested. The thruster was to have sufficient instrumentation to determine performance parameters, ignition response, and thermal and vibration characteristics.

NASA Glenn did not have established facilities to test MON–25/MMH propellants in a timely manner, so the work was contracted out. To meet the rapid development schedule of the 2003 mission, a limited competition solicitation was released. The purpose of this risk-reduction activity was to provide data, not to select a propulsion subcontractor for the flight. Competition was limited to those companies that had existing 8.9-N MON–3/MMH thrusters and could manufacture their own propellants in a timely manner (this was an important point because MON–25 is not commercially available). Atlantic Research Corporation and Kaiser Marquardt each claimed to meet both of these criteria and were awarded contracts.

Rocket testing at Atlantic Research Corp.—Details of the facility setup, procedures, and results at Atlantic Research Corp. can be found in the final report to NASA (ref. 18 and appendix A). The report is summarized as follows.

Atlantic Research Corp. conducted testing using a 9.4-N thruster (LEROS 10) that has been flight qualified and flown (50 on-orbit flights). The thruster (fig. 20) consisted of three major components: the propellant valves, the injector, and the chamber-expansion cone. The thruster used two Moog series-redundant solenoid valves that were normally closed. The injector had three unlike doublets in the core region and six fuel-film coolant holes equispaced on the periphery. The thruster was designed to run cool (for long life), so it used 58 percent of the total fuel flow for barrier cooling. The thrust chamber was manufactured from a niobium (C103) alloy and was coated with a disilicide for oxidation protection. The expansion nozzle was machined from a titanium alloy (Ti-6Al-4V) and welded with an electron beam to the thrust chamber.

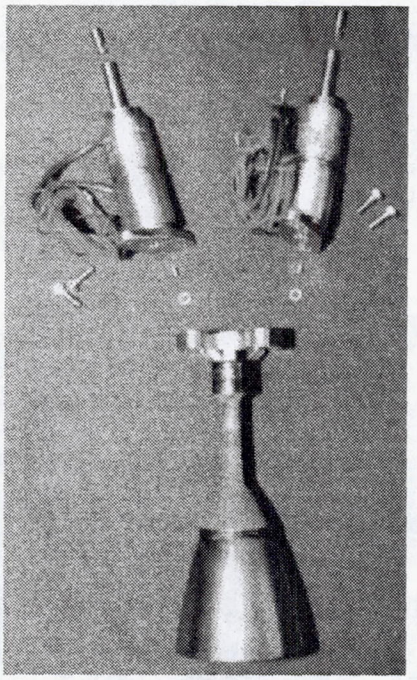

Figure 20.—LEROS 10 thruster, Atlantic Research Corporation.

MON–25 was produced by adding gaseous nitric oxide (NO) to MON–3. Since this addition of NO results in an exothermic reaction, Atlantic Research Corp. employed a cooling chamber during the mixing operation to limit the temperature increase. Analysis of propellant samples verified a NO content between 25.0 and 25.3 percent.

Testing was conducted in an Atlantic Research Corp. vacuum facility. Figure 21 shows the thruster during a test firing. Modifications were made to continuously deliver cold propellants to the thruster during testing. Liquid carbon dioxide was used to cool a heat exchanger fluid (ethylene glycol and water). This fluid, in turn, was delivered to heat exchangers to cool the propellants to the desired temperatures just before delivery to the thruster. Cold carbon dioxide was sprayed on the valve body and injector (the two largest thermal masses) before testing to maintain the thruster at the appropriate temperatures. The thruster was mounted and fired vertically. Most of the testing was conducted at vacuum conditions, although some testing was done at a pressure of 10 torr to simulate the Martian atmospheric pressure.

A total of 44 tests were conducted at propellant temperatures from –42 to +25 °C, over a range of inlet feed pressures from 690 to 2068 kPa. Testing consisted primarily of 30- and 60-sec-duration runs, although 600- and 1200-sec runs were also accomplished. Four pulse series were conducted, all of them consisting of 20 pulses. Two series were 0.1 sec on/0.1 sec off, while a third series was 0.2 sec on/0.2 sec off. A fourth series, 0.5 sec on/0.5 sec off, was terminated early.

The LEROS 10 was originally designed for extended life by sacrificing performance. The maximum chamber temperature achieved in testing was 912 °C, far below the 1370 °C temperature limit of the disilicide-coated C103 chambers. The excess amount of film cooling resulted in less than maximum performance because a large amount of fuel exits the nozzle without participating in the combustion process.

When operating at –40 °C, the mixture ratio of the thruster shifted from the nominal value of 1.65 to about 1.85. Atlantic Research Corp. suggested that this shift was caused by an increase in MMH viscosity, with a corresponding reduction in MMH flowrate and increase in mixture ratio. It was recommended that the injection orifices be redesigned or that a different set of trim orifices be used upstream of the valve to compensate for the shifting mixture ratio.

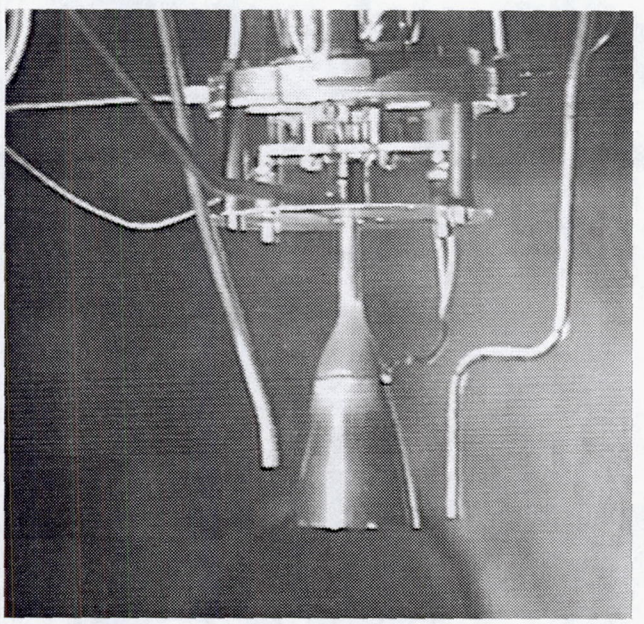

Figure 21.—LEROS 10 thruster firing in vacuum facility.

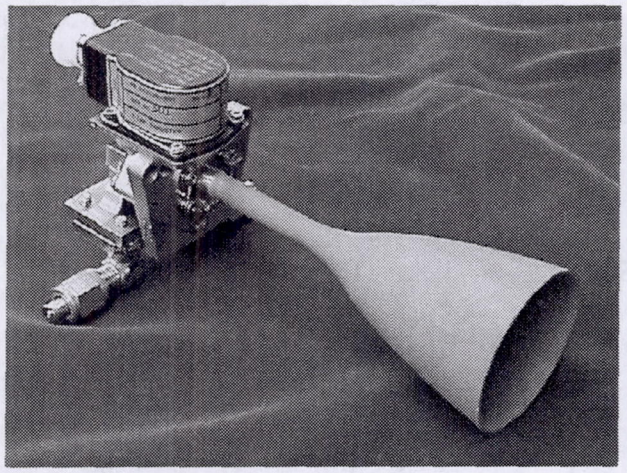

Figure 22.—Kaiser Marquardt R–53 thruster.

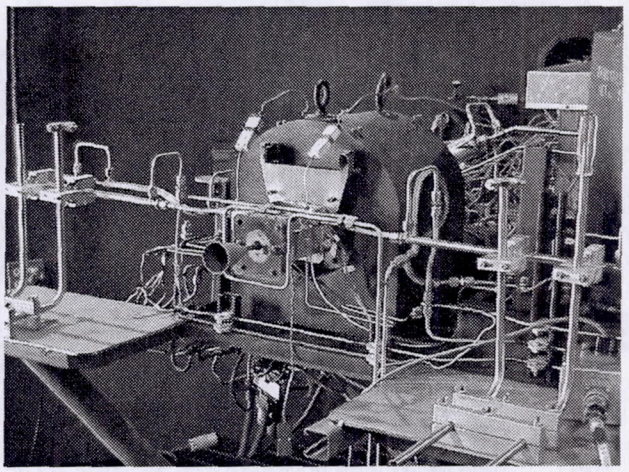

Figure 23.—R–53 thruster mounted on thrust stand.

Specific impulse at –40 °C (at nominal feed pressures) was 267 sec, while performance was 277 sec at 21 °C. The difference in specific impulse at 21 °C and –40 °C was attributed, in part, to the mixture-ratio shift. That is, the shift from a mixture ratio of 1.65 to 1.85 resulted in a decrease of at least 5 sec in specific impulse.

Rocket testing at Kaiser Marquardt.—Details of the facility setup, procedures, and results at Kaiser Marquardt can be found in the final report to NASA (ref. 17 and appendix B). The report is summarized below.

Kaiser Marquardt conducted testing using a flight-qualified 8.9-N thruster (R–53). The thruster (fig. 22) consisted primarily of an engine control valve, injector, and chamber-nozzle assembly. The control valve was a Moog torque-motor bipropellant type, which simultaneously controlled the flow of the oxidizer and the fuel. The injector consisted of a single unlike-doublet with two separate injection ports for fuel-film cooling of the combustion chamber wall. The injector was designed for 30-percent fuel-film cooling, but as a result of manufacturing difficulties, only 20 percent of the fuel flow was used. The chamber and nozzle consisted of a single piece of forged niobium (C–103) alloy with a disilicide coating to prevent oxidation.

MON–25 was produced by the addition, from a cylinder mounted on a weight balance, of gaseous NO to a known quantity of MON–3. The storage tank temperature was lowered to –7 °C to lower the vapor pressure of the mixture, accelerating the production process. A tank-stirring mechanism was also used to accelerate the mixing process. Compositional analysis of propellant samples verified that the proper amount of NO was added.

Testing was conducted in a Kaiser Marquardt vacuum facility. Figure 23 shows the thruster installed on the Kaiser Marquardt thrust stand. An Environmental Industries refrigeration system, capable of chilling propellants to –7 °C, was used in combination with a Government-supplied, FTS thermal conditioning system to provide propellants down to temperatures below –46 °C. Conditioning was achieved using a system of coannular plumbing, where propellants were passed through an interior passage encased in an outer tube of flowing refrigerant. The Environmental Industries refrigeration system served as the first conditioning stage, using ethylene glycol as the refrigerant to condition propellants in the storage tanks and in the lines up to the test cell. The FTS refrigeration system served as the second stage, using a silicon-based refrigerant to condition propellants from just inside the test cell wall up to the engine inlets. A one-gallon chilled accumulator was installed serially inline with the propellant supply lines and was controlled by the second-stage conditioning system. This ensured a stable propellant temperature during long-duration testing and provided a buffer between the higher temperature first-stage propellant and the cold propellant at the engine inlet. A cold gaseous nitrogen purge was sprayed on the engine valve, injector, and chamber to maintain the hardware at cold temperatures. A spray bar was used also to cool the engine inlets and the short sections of unconditioned, flexible propellant lines.

Fifty-five tests were conducted at propellant temperatures of –40, –18, and –7 °C and over a range of inlet feed pressures from 723 to 2315 kPa. Total firing time on the thruster was nearly 8600 sec. Testing consisted primarily of 10-sec runs, but durations up to 1200 sec were also conducted, as well as three pulse series, each consisting of twenty pulses, 0.1 sec on and 0.1 sec off. Most of the testing was conducted at vacuum conditions (<0.15 kPa), although one test was done at 1.5 kPa to simulate the Martian atmospheric pressure.

Because the fuel-film cooling percentage was less than design, this engine ran at high temperatures (a maximum of 1420 °C) for a C–103 chamber. However, the engine survived the entire test matrix with no obvious signs of degradation. The nominal test conditions included a thrust level of 8.9 N and a mixture ratio of 2.1. The nominal inlet feed pressures for these conditions normally would be 1517 kPa; however, problems with the flow trim orifices required oxidizer and fuel inlet pressures of 1551 and 1827 kPa, respectively, to achieve nominal conditions. At the nominal conditions and –40 °C temperatures, ignition delay was about 8 msec, similar to that for MON–3/MMH at ambient temperatures. At thrust levels below 6 N, there was a 10-msec delay during which the engine produced very little thrust, followed by an abrupt change to the steady-state value. This happened when propellants accumulated in the chamber, accompanied by a detonation and momentary spike in the thrust. The engine was not damaged by this phenomenon.

At thrust levels above 8.9 N (at a constant 2.1 mixture ratio), the C* efficiency was nearly constant, at 93 percent, dropping sharply at thrust levels below 7 N. When thrust was held constant at 8.9 N and the mixture ratio was varied, the C* efficiency initially increased from 92.6 percent at 1.61 to a maximum of 93.3 percent at 1.99, after which it decreased to 87.1 percent at 2.75. Because the thrust coefficient was nearly constant (assuming a nozzle efficiency of 97 percent), the specific impulse was directly proportional to the C* efficiency and showed the same trends, with a performance of 298 sec at thrust levels above 8.9 N and a mixture ratio of 2.1. The maximum specific impulse of 300 sec was achieved with a mixture ratio of 1.99. When regression analysis was applied, the optimal mixture ratio was at 1.87, although more data would be needed to validate that number because the data acquired so far shows an optimal closer to 2.0.

In the 1200-sec runs, the chamber and the injector-to-chamber interface temperatures reach steady-state values. However, the valve and propellant temperatures did not achieve steady-state values, even after 1200 sec. It was not possible to maintain the –40 °C propellant inlet temperature in the long-duration tests, which resulted in a steady decrease in the mixture ratio.

A single run was conducted at a facility pressure of 1.4 kPa to simulate the Martian atmospheric pressure. As expected for a nozzle design for vacuum operation, the flow in the nozzle separated and performance dropped off significantly. If the R–53 were to be used for the Mars aircraft, the nozzle would have to be optimized for the higher Martian exhaust pressure.

An accelerometer was attached to the back of the engine control valve to ascertain the system vibration characteristics. The highest amplitude vibrations were experienced during the first 2 msec of startup, after which the vibration was significantly reduced.

Rocket testing conclusions.—The risk reduction effort provided testing of two thrusters in two different facilities to assess the feasibility of adapting an existing 8.9-N MON–3/MMH thruster to run MON–25/MMH. Both thrusters demonstrated stable long-duration operation in steady-state and pulse mode on MON–25/MMH at temperatures down to –40 °C. Neither thruster was designed to operate with the MON–25 oxidizer or at cold temperatures. However, neither thruster experienced a significant ignition delay due to the different oxidizer and operating temperature. As expected, the nozzle for these thrusters, which was designed for vacuum operation, would have to be optimized for the Martian atmospheric pressure.

There were differences in performance and optimal mixture ratio between the two thrusters, despite the fact that both used the same fundamental injector approach (unlike doublets). There were differences, however, in the number of elements used (the Atlantic Research Corp. LEROS 10 had three, whereas Kaiser Marquardt's R–53 had one) and amount of fuel-film cooling used (by design, LEROS 10 had an excessive amount, whereas the R–53 thruster used less than the design percentage). Furthermore, there were difficulties in maintaining cold propellant temperatures in long-duration (1200-sec) testing. Although both test series demonstrated that MON–3 thrusters can be adapted for MON–25 operation, there are injector issues that still must be resolved. The data generated from this testing (detailed in appendixes A and B) should provide a firm basis for modifying existing thrusters for the Mars aircraft mission.

Pyrovalve Testing

Explosively actuated valves called pyrovalves (which are normally closed) are often used on spacecraft to isolate key segments of the propulsion system until needed (ref. 19). Positive isolation can be of critical importance for spacecraft propulsion systems with long dormant periods to prevent pressurant loss, overpressurization of the propellant tanks, propellant leakage from the tanks, and/or to avoid the mixing and combustion of hypergolic vapors.

Normally closed pyrovalves are the only way to ensure this isolation, as all other valves will leak to some degree. A closed pyrovalve design would typically consist of tube fittings with shear nipples welded to the housing to provide a seal. When a pyrovalve is initiated, an explosive charge or gas generator is fired to accelerate a translating ram into the line at high velocity. The ram shears off the tube nipples and wedges into a tapered section of the housing. This action opens up the line to fluid flow, with the ram and housing providing a metal-to-metal seal. "Blowby" of the hot charge gases into the propellant has been responsible for a number of spacecraft failures, although this has spurred the spacecraft community to make improvements in pyrovalve designs.

The use of pyrotechnic devices on the Mars aircraft is not especially desirable, but may be necessary. If a hypergolic bipropellant system is used (such as the baseline MON–25/MMH), then the migration of propellant vapors from the tanks and through the thruster valves would have to be prevented. The aircraft will be spending the majority of the mission inside an aeroshell. Any burning and/or detonation of propellants inside this closed compartment could lead to catastrophic failure. If a common helium pressurization subsystem were used, then pyrovalves would also be needed to isolate the fuel side from the oxidizer side. Otherwise, migration of propellant vapors from the tank into the common line of the pressurization system would be possible.

It is possible that burst disks could accomplish the same task as the pyrovalves, that is, positively isolate segments until the propulsion system is activated. The critical issue then would be determining the amount of pressure that would build against the burst disk over the mission life. This would be a function of the latch valve leakage rates and the thermal environment of the propellant lines over time. If it could be confidently predicted that the pressure against the disks would not be a significant fraction of the system activation pressure, then burst disks could probably be used; but if there were any question about the burst disks releasing prematurely, then pyrovalves would likely be the safer option. This would have been an issue to resolve in the design of the flight system.

Although the issue of whether or not to employ pyrovalves for the Mars aircraft was not settled, qualification with MON–25 at –40 °C still needed to be conducted early on. The fabrication of pyrovalves was a long-lead item (6 to 9 months), and the valves needed to be qualified before they could be incorporated into a flight system. If pyrovalves were to be used for the Mars aircraft, these activities would have to be initiated as soon as possible to meet the November 2002 launch date. If the valves were not used for the Mars aircraft, the data generated from the activity would be of high interest to the space community, particularly JPL.

Testing was to be done at NASA Johnson Space Center's White Sands Test Facility (WSTF). The WSTF is the designated NASA center for hypergolic propellant research and conducts tests of pyrovalves for the aerospace community. Initial discussions with WSTF personnel indicated that WSTF could have conducted the MON–25, –40 °C pyrovalve testing with little modification to existing facilities (according to a personal communication from Mr. Regor Saulsberry, WSTF, June 1999).

A procurement of a pyrovalve lot (10 items) was initiated, then halted when the 2003 mission was cancelled. These were so-called "low blowby" pyrovalves, designed to minimize interaction between the explosive charge gases and the fluid (a design that came about after a series of pyrovalve-related spacecraft failures). There was some discussion about using titanium (as opposed to stainless steel) pyrovalves to provide mass savings. However, it was decided that the experience base with titanium pyrovalves was limited and that the stainless steel pyrovalves should be baselined for reduced developmental risk. Still, it was planned to include an available titanium pyrovalve in the test sequence.

Rocket Propulsion System Trade

The intent of this task was to provide mission planners with an idea of the propulsion system sizing as a function of mission duration. Initial feedback to mission planners had been on the basis of propellant and tank mass. For larger propulsion systems, propellant and tank mass would dominate the mass of the system and would be a good first-order approximation. However, considering that the vehicle mass would be less than 20 kg, the mass of the propulsion system components would be even more significant. Furthermore, the masses of the contingency propellant, support structure, and lines were not accounted for initially, though all would have a significant impact on system mass.

A more complete propulsion system model was made for preliminary sizing of the propulsion system. There was no attempt to optimize the system for the Mars aircraft envelope, and redundancy requirements were not accounted for in any critical fashion.

Propulsion system model.—The propulsion system dry-mass model was based on the Near-Earth Asteroid Rendezvous (NEAR) spacecraft propulsion system. This model was recently used to evaluate liquid propulsion system options for Discovery-class spacecraft (ref. 20). Although the NEAR spacecraft was much larger (>800 kg) than the Mars aircraft, the basic model was felt to be representative of spacecraft propulsion systems and provided for a conservative estimate. There have been recent efforts to develop low-mass propulsion system components for kinetic kill vehicles, but these had lifetimes under 1 min. There are efforts to develop new longer life, lightweight components (ref. 21), but components with a flight heritage were considered to represent the development path with the lowest risk.

There were three system designs evaluated:

1. Blowdown MON–25/MMH system: This system consisted of the fuel and oxidizer tanks (each loaded with helium pressurant for a 4:1 blowdown ratio), a pyrovalve for each propellant leg, and the thruster. Propellants were assumed to be loaded to the pyrovalve before system activation. When the pyrovalves are actuated, propellant is brought to the engine valves, which controls system operation. Latch valves could be used instead of pyrovalves, but the latch valves would be heavier and would not ensure against leakage. The system had a transducer for the chamber pressure (thruster performance) and thermocouples for the propellant tanks. This represents the simplest possible design but also entails the most risk from an operation standpoint.
2. Regulated MON–25/MMH system: This system had a 20 685-kPa helium bottle that was used to pressurize the fuel and oxidizer tanks. Pyrovalves were placed between the fuel and pressurant tanks and between the pressurant tanks and the oxidizer to prevent mixing of hypergolic vapors in the pressurization subsystem. Check valves were also in place in the fuel and oxidizer lines. The pyrovalves were downstream of the propellant tanks where, similarly to the blowdown system, they act as tank valves until the system is activated. The system had a transducer for the chamber pressure (thruster performance) and thermocouples for the propellant tanks. This design had more components, but lower risk than the blowdown bipropellant system.
3. Blowdown HPB–2517 system: This system was included to illustrate the difference between bipropellant and monopropellant systems. The HPB–2517 (25 percent hydrazinium nitrate, 17 percent water) was selected as a low-freezing-point monopropellant. Although HPB-2517 was not as developed as HPB-1808 or HAN/glycine, its freezing point (–54 °C) was low enough that it could operate at –40 °C, as the MON–25/MMH system would. The system consisted of a single tank loaded with helium pressurant for a 4:1 blowdown ratio, a pyrovalve that acted as a tank valve until system activation, and the thruster. The system had a transducer for the chamber pressure (thruster performance) and thermocouples for the propellant tanks.

The mass of the components in this propulsion system model is given in table VII.

Assumptions were made that were common to all of the above system designs. The propellant tanks were assumed to be spherical surface-tension tanks composed of a titanium alloy (Ti-6Al-4V). Engine valves were counted as part of the engine mass. The propellant requirements were based on the engine performance, mission duration (2, 5, 10, 15, and 20 min), and an 8.9-N thrust level. Propellant requirements were further augmented with a 5-percent contingency and an assumption of 97-percent ullage in the propellant tanks. Helium pressurant requirements were calculated based on propellant requirements, assuming that pressurant and propellants would be at the same temperature. The support structure for the system components was assumed to be 10 percent of the propulsion system dry mass. The mass of the lines and fittings was also assumed to be 10 percent of the propulsion system dry mass. Another 1 percent of the dry mass was added for miscellaneous hardware or supports not accounted for. For the regulated bipropellant system, the helium pressurant tank was assumed to be a spherical, carbon composite overwrapped pressure vessel with a thin aluminum liner. Engine performance for the MON–25/MMH system was assumed to be 295 sec, while HPB–2517 was assumed to have a specific impulse of 220 sec.

TABLE VII.—COMPONENT MASS FOR PROPULSION SYSTEM TRADE

Component	Mass model, kg
Propellant tank	Spherical, surface tension, Ti-6Al-4V (ref. 22)
Pressurant tank	Carbon composite overwrapped with titanium liner (ref. 23)
Thruster	0.50
Pyro valve	0.15
Latch valve	0.75
Check valve	0.22
Manual valve	0.22
Regulator	1.20
Filter	0.13
Thermocouple	0.009
Pressure transducer	0.45

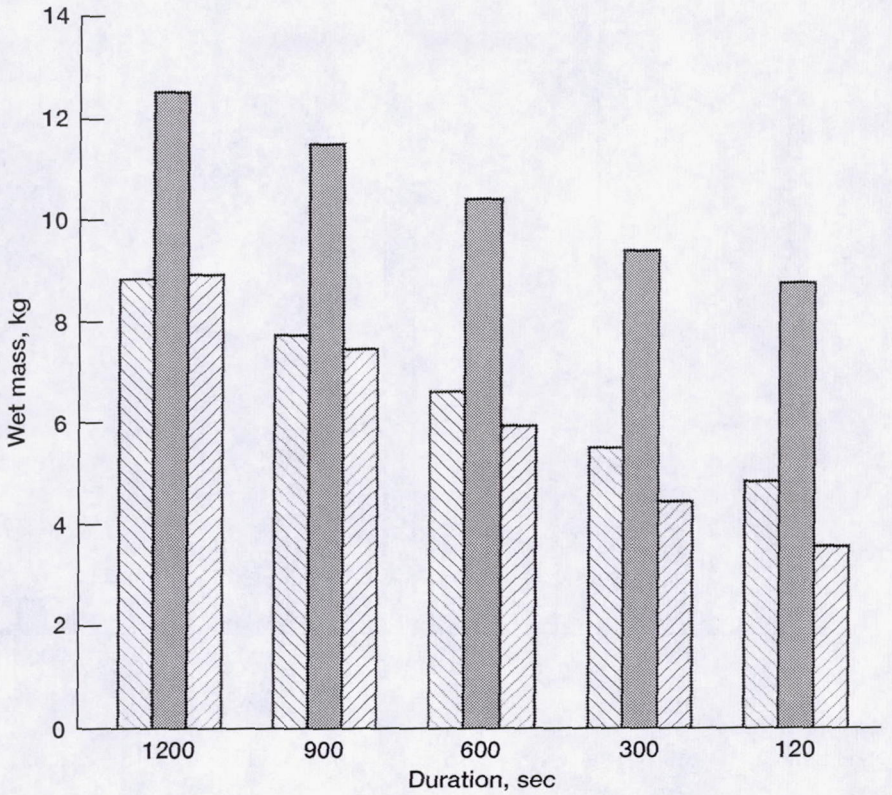

	1200	900	600	300	120
Blowdown MON–25/MMH	8.85	7.75	6.65	5.54	4.88
Regulated MON–25/MMH	12.53	11.49	10.45	9.41	8.79
Blowdown HPB–2517	8.95	7.46	5.96	4.46	3.56

Figure 24.—Propulsion system wet mass trade as a function of total mission duration.

Propulsion system trade results.—Figure 24 shows the propulsion system wet mass as a function of mission duration. Figure 25 shows the volumes of the tanks, which will dominate the propulsion system volume. Although this was not a rigorous trade study, some general conclusions could be drawn about liquid rocket propulsion options for the Mars aircraft:

- It will be difficult to meet the Mars aircraft mass and volume constraints without reducing the total burn duration from 20 min.
- The HPB monopropellants generally offer a lower propulsion system wet mass than the bipropellants.
- MON–25/MMH offers a lower propellant volume than monopropellants, although the bipropellant requirement for two tanks hinders packing efficiency.

If mission planners have to maintain the 20-min burn duration requirement, then an aggressive program would have to be implemented to accelerate low-mass component development and nonconventional tankage. Alternatively, efforts could focus on developing a 20-min-burning, 8.9-N solid rocket motor. Reducing the burn duration would make the liquid propellant systems more acceptable using flight hardware. The shorter the burn duration, the more feasible it will be to develop 8.9-N solid rocket motors. The solid option will always be the most desirable in terms of system simplicity, assuming a single burn is acceptable.

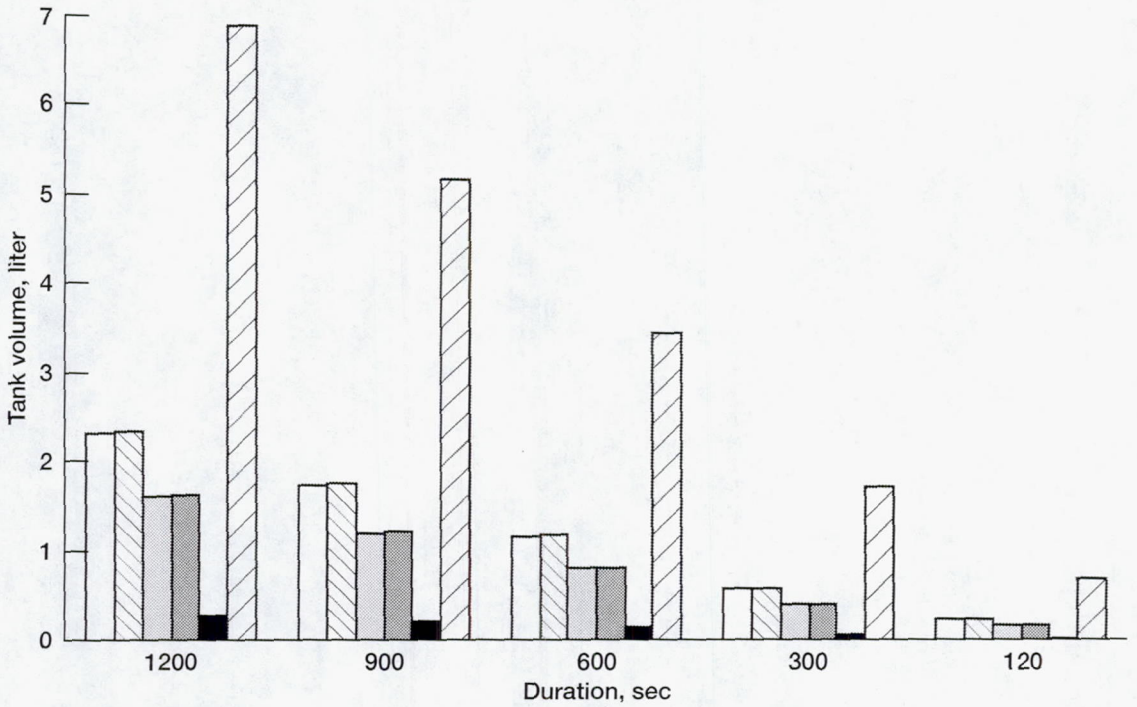

	1200	900	600	300	120
Blowdown MMH tank	2.33	1.75	1.17	0.58	0.23
Blowdown MON–25 tank	2.36	1.77	1.18	0.59	0.24
Regulated MMH tank	1.62	1.21	0.81	0.40	0.16
Regulated MON–25 tank	1.63	1.23	0.82	0.41	0.16
Regulated He tank	0.289	0.217	0.145	0.072	0.029
HPB–2517 tank	6.89	5.17	3.45	1.72	0.69

Figure 25.—Tank volume trade as a function of total mission duration.

FUTURE OPTIONS

Beyond the propulsion systems listed in the previous sections there are other options that can be pursued for future aircraft. These options are longer term projects and require considerable development before they can be used. However they do offer the potential for significantly more capable aircraft; if perfected, they would enhance the ability to perform science from a flying platform.

Solar-Powered Vehicle

The ability to utilize a renewable power source to propel an aircraft is very enticing. This would enable the aircraft to fly for extended periods of time and eliminate the restriction of carrying significant amounts of fuel. One approach is to produce an aircraft that can generate and store enough power during the day to fly continuously throughout the night. An aircraft so designed would be able to fly continuously for months or even years without needing to land. This opens up a whole world of possibilities for scientific exploration. To accomplish this, the

aircraft would need to carry a rechargeable energy storage system such as a fuel cell or battery. This concept has been previously studied and is feasible for flight on Mars. The previous analysis can be found in reference 2, and a conceptual drawing of such an aircraft is shown in figure 4. This type of aircraft, however, would require energy storage capabilities well beyond what is presently available or projected in the near term for either fuel cells or batteries. Also, the aircraft would be large, with greater than a 150-m wingspan. The deployment of an aircraft this size presents a number of issues that would require substantial development, as well as possibly the implementation of infrastructure onto the Martian surface. Because of these issues, this type of aircraft would not be feasible for a near-term mission.

To bring the solar-powered aircraft closer to near-term use, it may be possible to develop an aircraft that operates on solar power but requires no energy storage system. This type of aircraft would be limited in the location and duration of its flight, but it would still have greater endurance than a battery-powered or -fueled aircraft. It is estimated that an aircraft may be capable of sustained flight for 7 days without energy storage if flown near the poles during the summer months when the Sun is above the horizon all day (Gefford, L., internal NASA Glenn Research Center report. March 1999).

This aircraft would require approximately a 6- to 12-m wingspan, depending on the structural design and payload. Because of this fairly large wingspan, other less conventional deployment schemes would need to be developed. The leading contender is an inflatable wing structure that becomes rigid upon deployment. There are some rigidizing inflatable structures being developed for space applications that may be appropriate for this type of aircraft. A drawing of the aircraft concept is shown in figure 26.

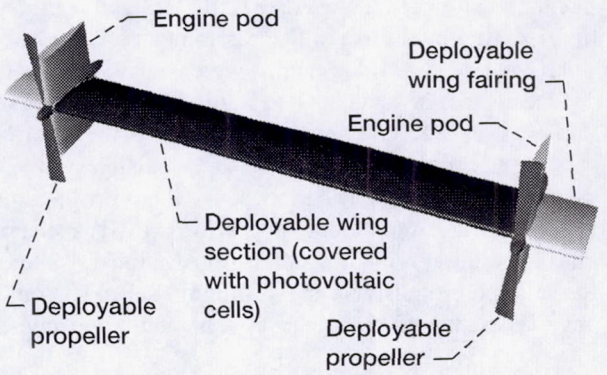

Figure 26.—Inflatable solar PV aircraft concept.

Entomopter

One of the main obstacles to flight on Mars is the very low atmospheric density. This low density requires an aircraft to fly within a very low Reynolds number-high Mach number regime. This low Reynolds number problem is compounded by the size restrictions for the aircraft, which must fit and deploy from an aeroshell, especially if it is a Mars micromission capsule. As a possible way around this low Reynolds number problem, the concept of using an entomopter (mechanical insect) as the flight vehicle for a future Mars aircraft exploration mission has a number of potential advantages. The basis behind this type of aircraft is that, according to conventional aerodynamics, insects should not be capable of generating sufficient lift to maintain flight. This is due to the size of the insect's wings and the Reynolds number they are operating in. Work was done in 1994 by Charles Ellington at the University of Cambridge to investigate how insects generate lift to stay aloft. It was determined that a microscale vortex that adhered to the wing's leading edge during the downstroke was the source of the lift. Because of this vortex and the geometry and motion of an insect's wing, insects are capable of generating lift coefficients on the order of 5. This effect is suspected to diminish when progressing from insects to the size of small birds (when the flight Reynolds number increases). A Mars aircraft with an approximate 1-m wingspan would be operating at a similar Reynolds number as insects do here on Earth. Flight within the Mars environment could enable taking advantage of the same lift-producing mechanism that insects employ and may be an elegant way of producing an aircraft to fly on Mars. The fact that Mar's gravitational force is a third of that on Earth is an additional advantage here. This reduced gravity enables thinner, lighter structures to be used, which could be an important factor in the feasibility of this concept.

Presently, work is being done at a number of universities and some private companies on developing entomopters for Earth applications. This work is mainly supported by an ongoing program at the Defense Advanced Research Projects Agency. One of the research institutes involved with this is the Georgia Institute of Technology. They are presently developing prototype entomopters and hope to have an operational one within 1 to 2 years. Based on their work, the possibility of flight on Mars with an entomopter looks feasible and may in fact be easier to accomplish there than on Earth because of the larger scale of the vehicle. If it proves to be feasible, a vehicle of this type on Mars would have the ability to take off, land, and hover, which would greatly enhance mission capability.

CONCLUSION

The environment of Mars must play a major role in selecting a propulsion system for a Mars-based aircraft. Because of the cold, low-density atmosphere, which is almost completely devoid of oxygen, most conventional aircraft engines will not operate there. An alternative or nonconventional propulsion system is needed in this environment. Other restrictions aside from the environment play a role in determining the type of propulsion system that can be used. These restrictions include the size and mass restrictions of the aircraft, the required mission duration, and the timeframe available to meet the required launch date. All of these issues were factored in while evaluating different types of propulsion systems for the proposed 2003 Mars micromission aircraft. Because this was a micromission, the limitations on the aircraft size and weight were significant. The propulsion system had to be a small-volume system with a mass limited to approximately 7 kg. Because of the small aircraft size and the low-density atmosphere, the aircraft would need to fly at a fairly high speed to generate lift, approximately 112 m/sec (250 mph). Also, due to the proposed launch date (fall 2002), all components used had to be off-the-shelf, requiring little or no development. Another aspect of the mission that affected the propulsion system selection was the available communications window. Several scenarios were examined; the one that showed the most promise was to use the carrier spacecraft to relay data back to Earth. Using this type of data transfer method, the available communications window was set at 15 to 20 min, and, therefore, the required flight duration was also 15 to 20 min. After considering these restrictions, the choice for the propulsion system was reduced to two candidates: a battery-powered electric system using silver-zinc batteries, and a bipropellant rocket system using 25-percent mixed oxides of nitrogen (MON–25) and monomethylhydrazine (MMH) as the oxidizer and fuel. In the final selection, the rocket system was chosen because of its overall lower operational risk and reduced development time. However, it should be noted that the selected propulsion system is highly dependent on the specified mission requirements and restrictions. Changing any of these requirements most likely would impact the system selection.

REFERENCES

1. Reed, R.D.: High-Flying Mini-Sniffer RPV—Mars Bound. Astro. Aeron., vol. 16, 1978, pp. 26–39.
2. Colozza, Anthony J.: Preliminary Design of a Long-Endurance Mars Aircraft. NASA CR–185243 (AIAA Paper 90–2000), 1990.
3. Greer, D.; Hamory, P.; Krake, K.; and Drela, M.: Design and Predictions for a High-Altitude (Low Reynolds-Number) Aerodynamic Flight Experiment. NASA TM–206579, 1999.
4. MIT Fluid Dynamics Research Laboratory: XROTOR. (Computer program). http://raphael/mit.edu/projects%26research.html. Accessed in 1999.
5. Hall, Edward J.; Heidegger, Nathan J.; and Delaney, Robert A.: ADPAC v1.0: User's Manual. NASA/CR—1999-206600, 1999. http://gltrs.grc.nasa.gov/GLTRS/. Accessed in 1999.
6. Lackney, J.J.; Murthy, P.L.N.; and Gotsis, P.K.: High Temperature Composite Analyzer (HITCAN) Theoretical Manual. NASA TM–106001, 1993.
7. Bakhle, Milind A.; et al.: Development of an Aeroelastic Code Based on an Euler/Navier-Stokes Aerodynamic Solver. NASA TM–107362, 1997.
8. Boucher, Robert J.: The Electric Motor Handbook: The Complete Handbook of High Performance D.C. Motors. AstroFlight, Los Angeles, CA, 1994.
9. Guernsey, Carl S.: Mars Ascent Propulsion System (MAPS) Technology Program—Plans and Progress. AIAA Paper 98–3664, 1998.
10. Panetta, Peter V.; et al.: NASA-GSFC Nano-Satellite Technology Development. Proceedings of the 12th AIAA/USU Annual Conference on Small Satellites (Logan, UT), Jan. 1998.
11. Schmidt, Eckart W.: Hydrazine and its Derivatives: Preparation, Properties, Applications. John Wiley & Sons, New York, NY, 1984.
12. Wernimont, E.J.; and Mullens, P.: Recent Developments in Hydrogen Peroxide Monopropellant Devices. AIAA Paper 99–2741, 1999.
13. Meinhardt, D.S.; et al.: Selection of Alternate Fuels for HAN-Based Monopropellants. 1998 JANNAF Propellant Development and Characterization Subcommittee and Safety and Environmental Protection Subcommittee Joint Meeting, vol. 1, 1998, pp. 143–151.
14. Meinhardt, Dennis; et al.: Performance and Life Testing of Small HAN Thrusters. AIAA Paper 99–2881, 1999.

15. Reed, Brian D.; and Schneider, Steven J.: Hydrogen/Oxygen Auxiliary Propulsion Technology. AIAA Paper 91–3440, 1991.
16. Shahnam, Mehrdad; et al.: Low Temperature Liquid Propellant—An Alternative Propulsion Source for Space Exploration. AIAA Paper 99–2463, 1999.
17. Fuller, Raymond: Mars Flyer Rocket Propulsion Risk Assessment. Final Report, Contract NAS3–99198, Kaiser Marquardt Rocket Propulsion Systems, Dec. 1999.
18. Mars Flyer Rocket Propulsion Risk Assessment. Final Report, ARC TR 80291, vol. 1—Test Report, Atlantic Research Corporation, Dec. 1999.
19. Julien, H.L.; et al.: Explosive Events Initiated by Pyrovalves. AIAA Paper 99–2309, 1999.
20. Schnieder, Steven J.: On-Board Propulsion System Analysis of High Density Propellants. AIAA Paper 98–3670, 1998.
21. Dyer, Keith; Yankura, George; and Acosta, Jesus: Low Mass Components for Mars Ascent Propulsion. AIAA Paper 99–2149, 1999.
22. Smith, P.; and Horton, M.A.: Advanced Propulsion Systems for Geostationary Spacecraft Study Results. AIAA Paper 84–1230, 1984.
23. Kawahara, Gary; and McCleskey, Stephen F.: Titanium-Lined, Carbon Composite Overwrapped Pressure Vessel. AIAA Paper 96–2751, 1998.

APPENDIX A: MARS FLYER ROCKET PROPULSION RISK ASSESSMENT

Atlantic Research Corporation

This report is being reprinted in its entirety as originally printed in April 2001. The reader should note that the original page numbers have been retained.

NASA/CR—2001-210709

Mars Flyer Rocket Propulsion Risk Assessment

ARC Testing

Atlantic Research Corporation
Niagara Falls, New York

Prepared under Contract NAS3–99197

National Aeronautics and
Space Administration

Glenn Research Center

April 2001

Trade names or manufacturers' names are used in this report for identification only. This usage does not constitute an official endorsement, either expressed or implied, by the National Aeronautics and Space Administration.

Available from

NASA Center for Aerospace Information
7121 Standard Drive
Hanover, MD 21076
Price Code: A04

National Technical Information Service
5285 Port Royal Road
Springfield, VA 22100
Price Code: A04

Available electronically at http://gltrs.grc.nasa.gov/GLTRS

TABLE OF CONTENTS

LIST OF TABLES

LIST OF FIGURES

1.0 INTRODUCTION

The purpose of this report is to describe the results from tests conducted at the Atlantic Research Corporation/Liquid Prolusion Division (ARC/LP) located in Niagara Falls, NY under the NASA Glen Mars Flyer Rocket Propulsion Risk Assessment Program. The technical objectives of this program were to provide test data on the operational characteristics of a 2 lbf thruster operating with MMH and MON-25 propellants cooled to –40C to simulate conditions expected to be encountered during the Mars Flyer mission.

The thruster used in this program was an ARC 10N (2.25 lbf) thruster which had been used in previous ARC development activities. The thruster was made available to this program at no cost and is described in Section 2.0. Since MON-25 is not available off-the-shelf, ARC manufactured a supply of MON-25 for this program and verified the NO content by assay using an independent company, Vicksburg Chemical. The procedure used to manufacture the MON-25 and the assay results are discussed in Section 3.0. For this program, ARC developed a propellant conditioning system which was capable of delivering –40C propellant to the thruster for tests of any duration. A description of this system is given in Section 4.0. The test plan is discussed in Section 5.0 and the results from the tests are discussed in Section 6.0. Conclusions are given in Section 7.0 and Recommendations in Section 8.0

This program can be summarized by indicating the manufacture of MON-25 was successful with two assays indicating the NO content of the propellant was 25.0 and 25.3%. After a series of development and calibration tests, the propellant conditioning system demonstrated the capability of delivering propellant to the thruster at the target temperatures of 21C (70F), -1C (30F), -18C (0F), -29C (-20F) and –40C (-40F) for tests of any run length, including three successive tests of 1200s duration of –40C. All but three of the tests in the original plan were conducted with testing being terminated with the depletion of the MON-25. Most tests were successfully completed including two where the test cell pressure was increased to 10 torr (0.2 psia) to simulate the Martian atmospheric pressure. The thruster ran well at

Figure 1. ARC 2 lbf Thruster

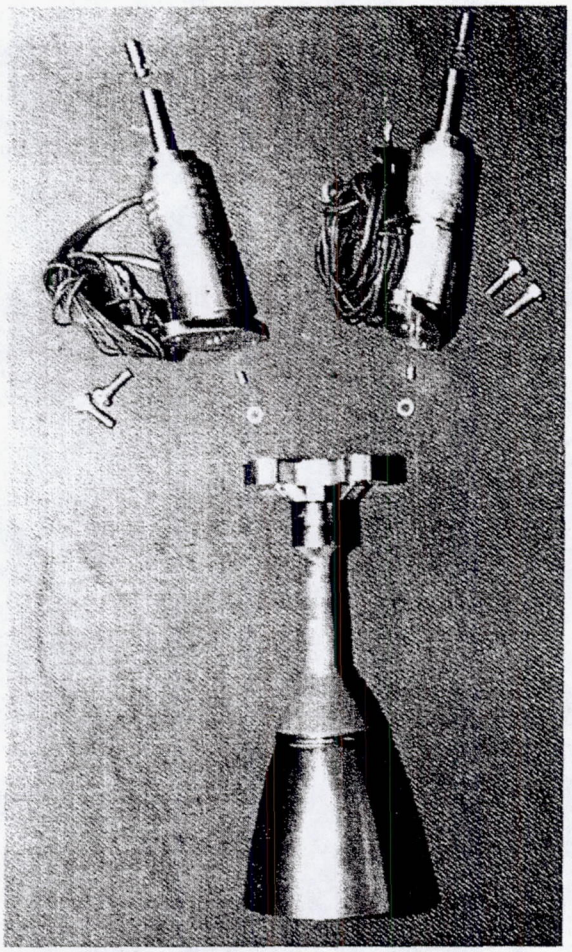

Design

- Propellants: MON-3/MMH
- Materials
- Disilicide Coated C-103 Chamber
- Titanium Injector & Cone
- Area Ratio: 336/1
- Mass: 0.62 kg
- Status
- Flight Qualified
- 210 Delivered
- 50 On-Orbit

Performance

- Thrust: 9.4N
- Feed Pressure: 13.8 bar
- Mixture Ratio: 1.65
- Specific Impulse: 274s
- Chamber Temperature: 900C
- Demonstrated Life
- 151,000s
- 587 kg throughput
- 1278 Cold Starts
- 1,120,000 Pulses

most conditions with the most notable result being that the cold propellant caused the nominal mixture ratio to shift from 1.65 to 1.90 as the propellant temperatures were reduced from 21C to –40C with a consequent small decrease in specific impulse. Details of the test results are given in Section 6.0 and Volume 2. These results show that there should be no significant problems operating this thruster with MMH/MON-25 propellants in the cold –40C environment.

2.0 THRUSTER DESCRIPTION

The 10N thruster, which was designed for MON-3/MMH propellants, is shown in Figure 1. The thruster is radiation cooled and uses fuel-barrier cooling to maintain chamber wall temperatures at levels sufficiently low to ensure the thruster meets propellant throughput requirements. The thruster was designed for stationkeeping on geostationary satellites and has been fully qualified for this mission using solenoid valves.

The thruster was designed for operation with propellants at a nominal temperature of 21C (70F). Orifices and flow passages were designed to provide a nominal mixture ratio of 1.65 with MMH and MON-3 propellants at 21C. Since propellant densities and viscosities are a function of propellant temperature, it was expected that operation with –40C propellants would result in changes in the thruster operational characteristics. These changes will be discussed shortly. It is important to note that the purpose of the tests described herein was to obtain an understanding of thruster operation with –40C propellants such that one could design a thruster optimized for these conditions at a later time.

The thruster is comprised of three major sub-assemblies: the injector assembly, thrust chamber and expansion cone and the propellant valves. The injector assembly consisting of the injector, distribution ring, thermal stand-off and oxidizer inlet tube are machined from 6Al/4V Titanium and electron beam welded together. The injector has three unlike doublets in the core region and six fuel film coolant holes equispaced on the periphery. Gold plated Inconel 'C' seals provide the sealing between the valves and the injector assembly..

The thrust chamber is manufactured from Columbium C103 alloy and is coated with the Hitemco R512E disilicide coating. The 336:1 area ratio expansion cone is machined from 6Al/4V Titanium and is electron beam welded to the thrust chamber.

This thruster has no Pc top so chamber pressures could not be measured. Chamber pressure was estimated by using measured thrust and an assumed value of the thrust coefficient Cf of 1.77.

The thruster uses two Moog Model 51-178 series redundant normally closed solenoid valves. The valve is a fail safe design that remains closed through spring pre-load until opened by electrical energisation. The valve features a teflon seat and no sliding fits. An outlet orifice is fitted into the valve flange for pressure drop control and there is a provision for an orifice in the inlet tube for final thruster trimming. The valve also incorporates a 25 micron absolute filter at the inlet.

2.1 Thruster Heritage

The thruster has been subjected to a very extensive qualification program using two thrusters. One thruster was used primarily for steady-state testing, while the second was used primarily for pulse mode testing. The scope of the qualification program included:

- Two thrusters
- 1400 burns
- Propellant temperatures: -7 to 54C
- Feed pressures: 8.3 – 19.8 bar
- Pulse trains of over 2700 pulses
- Hot restarts
- Variable pulse width pulse trains
- Thermal stability tests
- Gas Ingestion Tests
- Thermal Soakback Tests

Some results on the qualification program scope are included in Table 1. The thruster has successfully performed long burns of 1000s and it was expected that the thruster would be able to perform the 20 minute (1200s) burns required during this program without any problems.

Table 1. Qualification Test Summary

Parameter	Results	
	Qual Thruster 1	**Qual Thruster 2**
Total number of pulses	1,123,977	216,863
Thermal cycles (cold restarts)	1,278	426
Propellant throughput • Steady State • Pulse Mode	 417 877	 645 154
Propellant temperature range (C)	-10 to 59	-9 to 57
Injector pre-fire temp range (C)	-20 to 96	-11 to 97
Mixture Ratio	1.08 to 1.96	1.31 to 1.97
Thrust (N)	5.8 to 12.5	5.8 to 12.0
Longest SSF duration (s)	1,000	800
Longest PMF duration (s)	3,600	812
Total on time (s)	151,362	99,354
Total Impulse (N-s)	1,428,192	1,030,620

Figure 2 shows the fuel and oxidizer feed pressure envelope for which the thruster is qualified and the points at which tests were conducted. The qualification range was 8.3 – 19.7 bar (120-286 psia). The nominal operating conditions for the thruster are feed pressures for the fuel and oxidizer of 13.8 bar (200 psia) and a mixture ratio of 1.65. ARC plans to put trim orifices into the thruster which will result in a nominal feed pressure of 15.2 bar (220 psia).

Figure 2. Thruster Feed Pressure Qualification Box

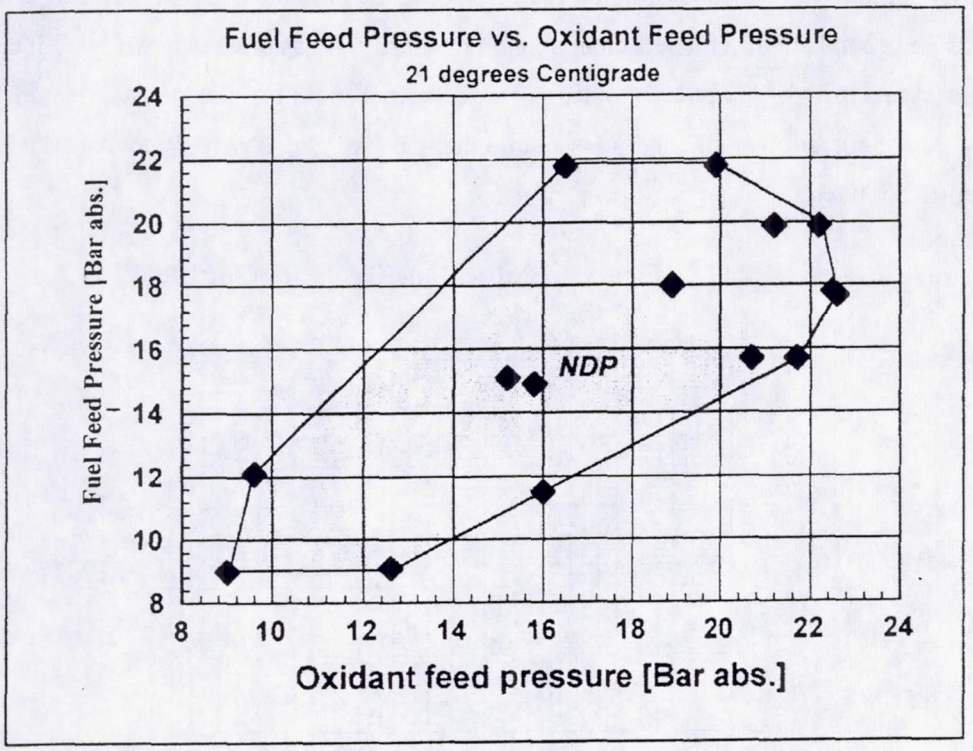

Figure 3 shows a map of the pulse mode tests which were conducted on the thruster in terms of the on-time and off-time for the pulses and the propellant temperatures at which these tests were conducted. The pulse mapping on this thruster was quite extensive and included long pulse trains (up to 4000 pulses) to demonstrate thermal stability. The thruster demonstrated successful operation at all conditions and no thermal limitations were discovered during the qualification tests.

Figure 3. Pulse Mode Operation Box

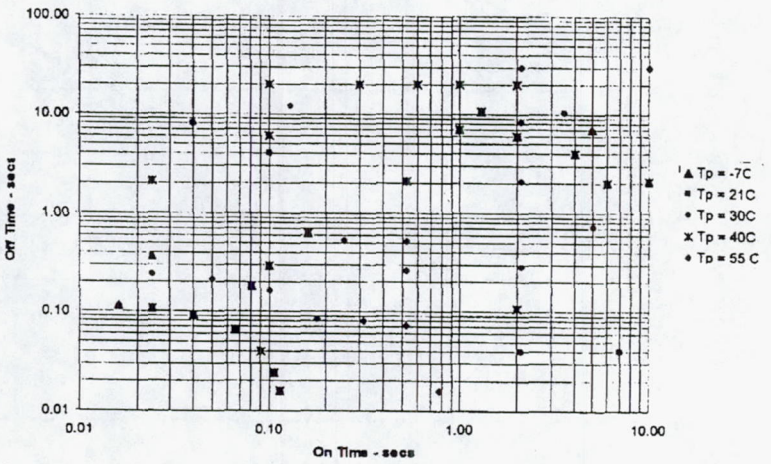

Figure 1 provides a brief summary of the operating characteristics of the thruster at the nominal operating condition. The specific impulse is 274s and the maximum chamber temperature is only 900C (1650F). This thruster was designed with a high fraction of the fuel in the barrier in order to produce a thermally robust thruster which could satisfy all high propellant throughput requirements for very demanding satellite missions. The thruster was designed to operate at a mixture ratio of 1.65 with MON-3/MMH propellants.

The thruster was designed to provide moderate performance in terms of Isp, but, more importantly, to operate without any thermal limitations over the entire range of duty cycles which could be encountered during satellite operation. The nominal mixture ratio for the thruster

is 1.65 with MON-3/MMH and the design has a high fraction of the fuel in the barrier. At nominal conditions, the Rupe Number for the doublet element core is about 1.75, rather than the more optimum value of 1.00; this is by design to obtain a wide operational envelope rather than a narrow envelope with higher performance. Rupe Number decreases toward a more optimum value of 1.0 as mixture ratio decreases below 1.65 and Isp increases slowly as MR decreases as shown by the data in Figure 4.

Figure 4. Variation of Specific Impulse with Mixture Ratio

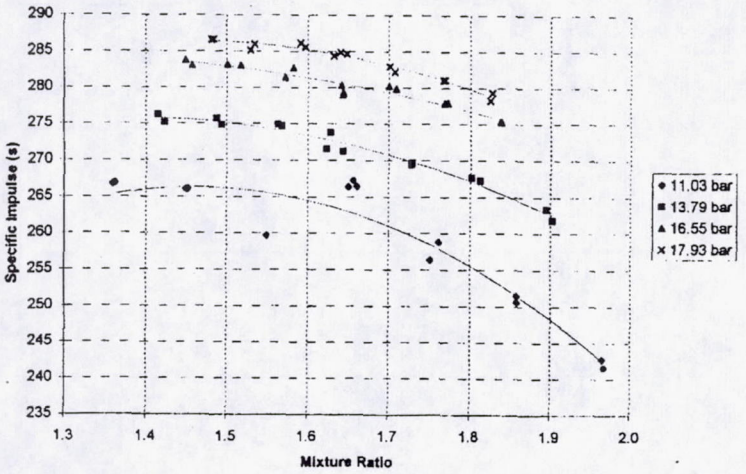

2.2 MARS FLYER TEST CONDITIONS

As mentioned earlier, the thruster was designed for operation with 21C propellants and some changes in operational characteristics were expected at the Mars Flyer conditions due to the change in propellant properties. The propellant properties which have the largest influence on thruster operation are density and viscosity.

Figure 5 shows how the density of MON-3, MON-25 and MMH vary with temperature over the –46C (–50F) to 49C (120F) range. All three propellants show the same trend of density increasing slowly as propellant temperature decreases. Note that MON-25 is somewhat less dense than MON-3 due to the higher NO content.

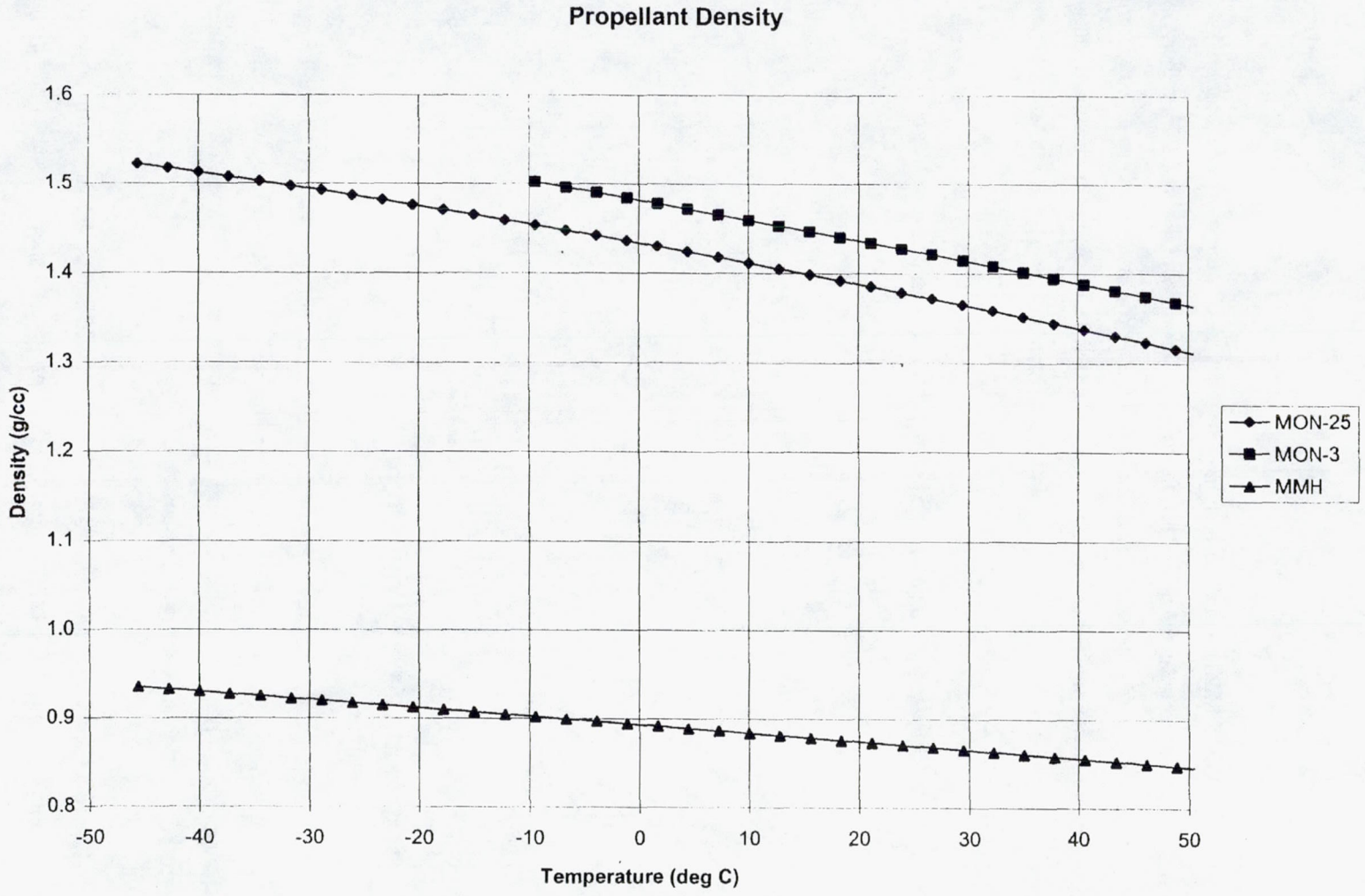

Figure 5. MON-3, MON-25, and MMH Density Variation with Temperature

In assessing performance of bipropellant thrusters, one of the most common design parameters is the Rupe Number given by

$$R = \frac{(\rho u^2 d)\,ox}{(\rho u^2 d)\,fuel} \qquad (1)$$

In Eq. (1), ρ is the propellant density, u is the orifice injection velocity and d is the orifice diameter; these parameters are for the injector core. Optimum bipropellant combustion is obtained for R = 1.0. Eq. (1) can be rewritten as

$$R = \left(\frac{\rho_f}{\rho_o}\right)\left(\frac{MR}{1-B}\right)^2\left(\frac{d_f}{d_o}\right)^3 \qquad (2)$$

where ρ_f and ρ_o are the fuel and oxidizer densities, d_f and d_o are the diameters of the fuel and oxidizer orifices in the injector core, MR is the mixture ratio, and B is the fraction of the barrier fuel injected into the thrust chamber wall. The parameter B is fixed by the ratio of the fuel core and barrier orifice diameters. Thus, for a given thruster design, R is affected by test conditions only through the density ratio and mixture ratio.

Figure 6 shows the oxidizer/fuel density ratio for MON-3/MMH and MON-25/MMH as a function of temperature. For MON-3/MMH at 21C, the density ratio is approximately 1.64 while for MON-25/MMH at –40C, the value is about 1.625. The difference between these two values in terms of their effect on Rupe Number is negligible. In fact, the variation of the density ratio for both propellant combinations over the range of temperatures shown in Figure 6 is sufficiently small that no significant effect on Rupe Number or thruster performance would be expected. The conclusion then, is that the thruster performance will not be affected to any significant degree by the propellant density changes associated with operating at –40C.

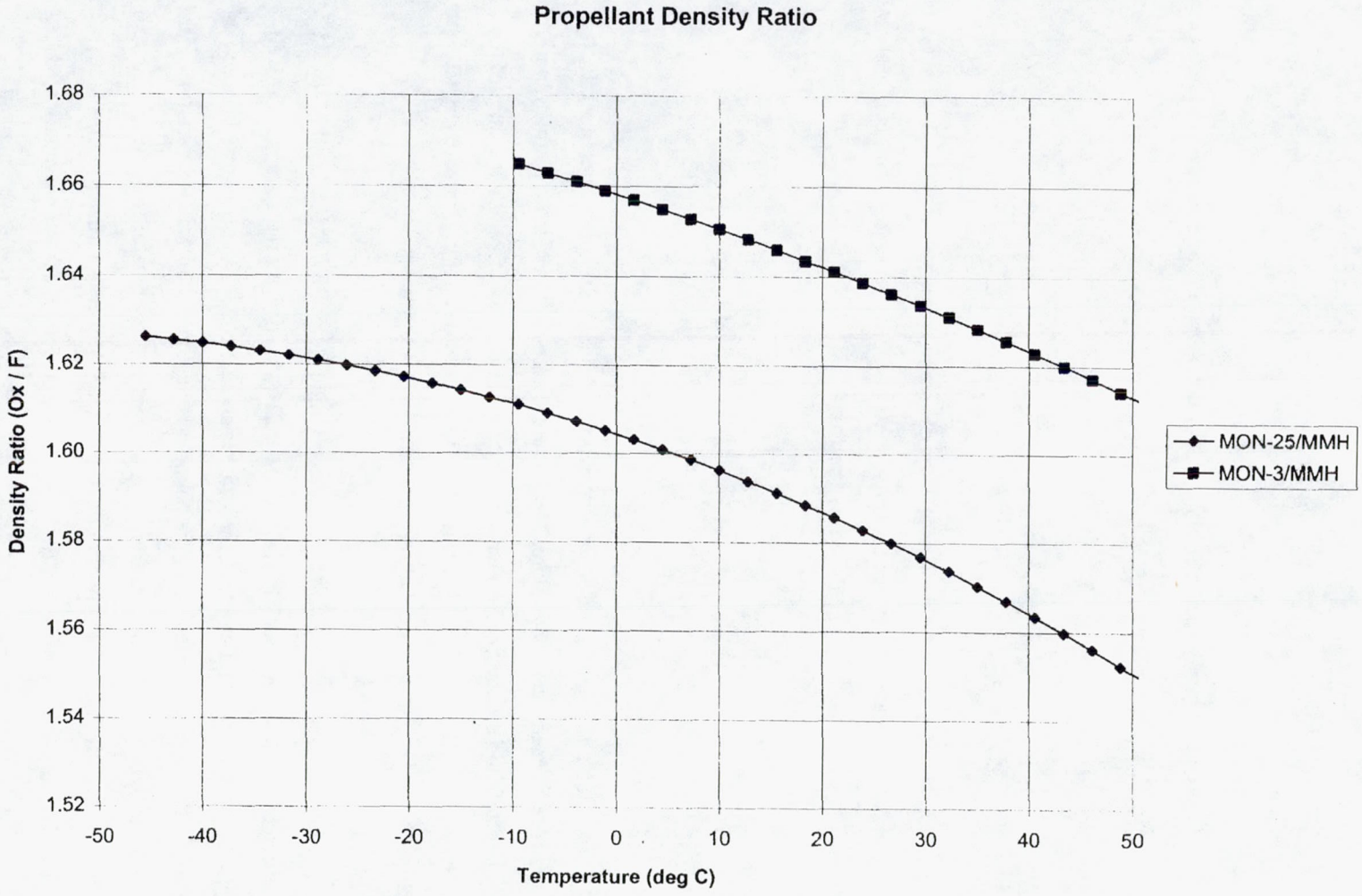

Figure 6. Fuel/Oxidizer Density Ratios

Figures 7 and 8 show the variation of viscosity of MMH and MON-3 with temperature. Note that the MON-3 data extends downward only to 2C (35F). No data is available for the viscosity of MON-25 so we will use the MON-3 data as an estimate. The data in Figure 7 show that in going from 21C to –40C, the viscosity of MMH increases by about a factor of 7. Using a straight line extrapolation of the data in Figure 8, in going from 21C to –40C, the viscosity of MON-25 would be estimated to increase by about a factor of 2.

For a thruster operating at a given feed pressure, an increase in propellant viscosity will result in an increase in the frictional pressure drops losses through the thruster flow passages and consequently, a reduction in propellant flowrate. Since the increase in the fuel viscosity as propellant temperatures are reduced to –40C is much larger than the increase in the oxidizer viscosity, the fuel flowrate will decrease more than the oxidizer flowrate. This will cause the nominal thruster mixture ratio to increase as propellant temperature decreases and as will be shown in Section 6, this is the trend that is observed in the test data.

The results in Figure 4 show that thruster Isp decreases slowly as mixture ratio increases and therefore, we would expect Isp to decrease as propellant temperature decreases because of the mixture ratio shift. This trend is also observed in the test data.

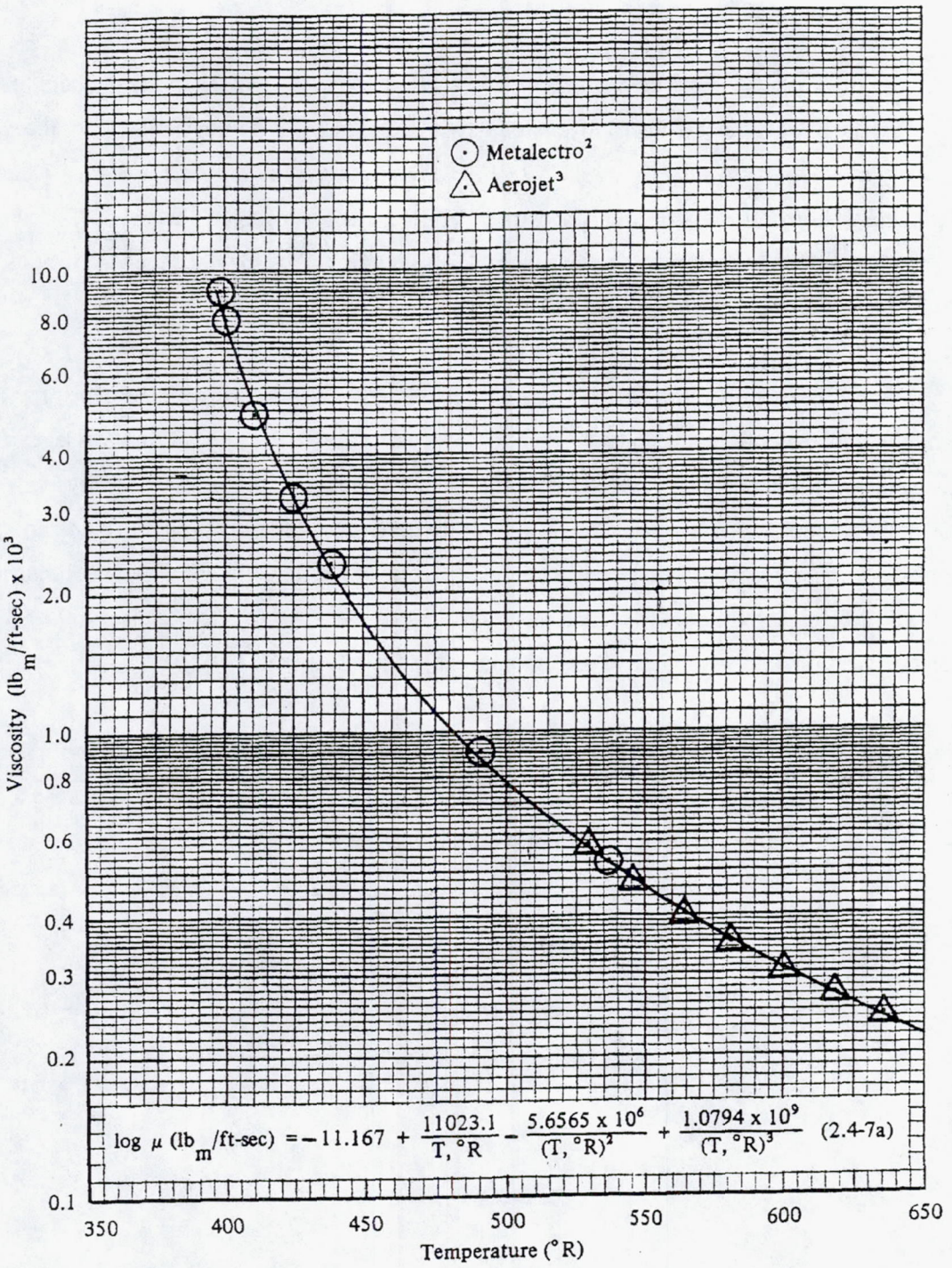

Figure 7. Variation of MMH Viscosity with Temperature

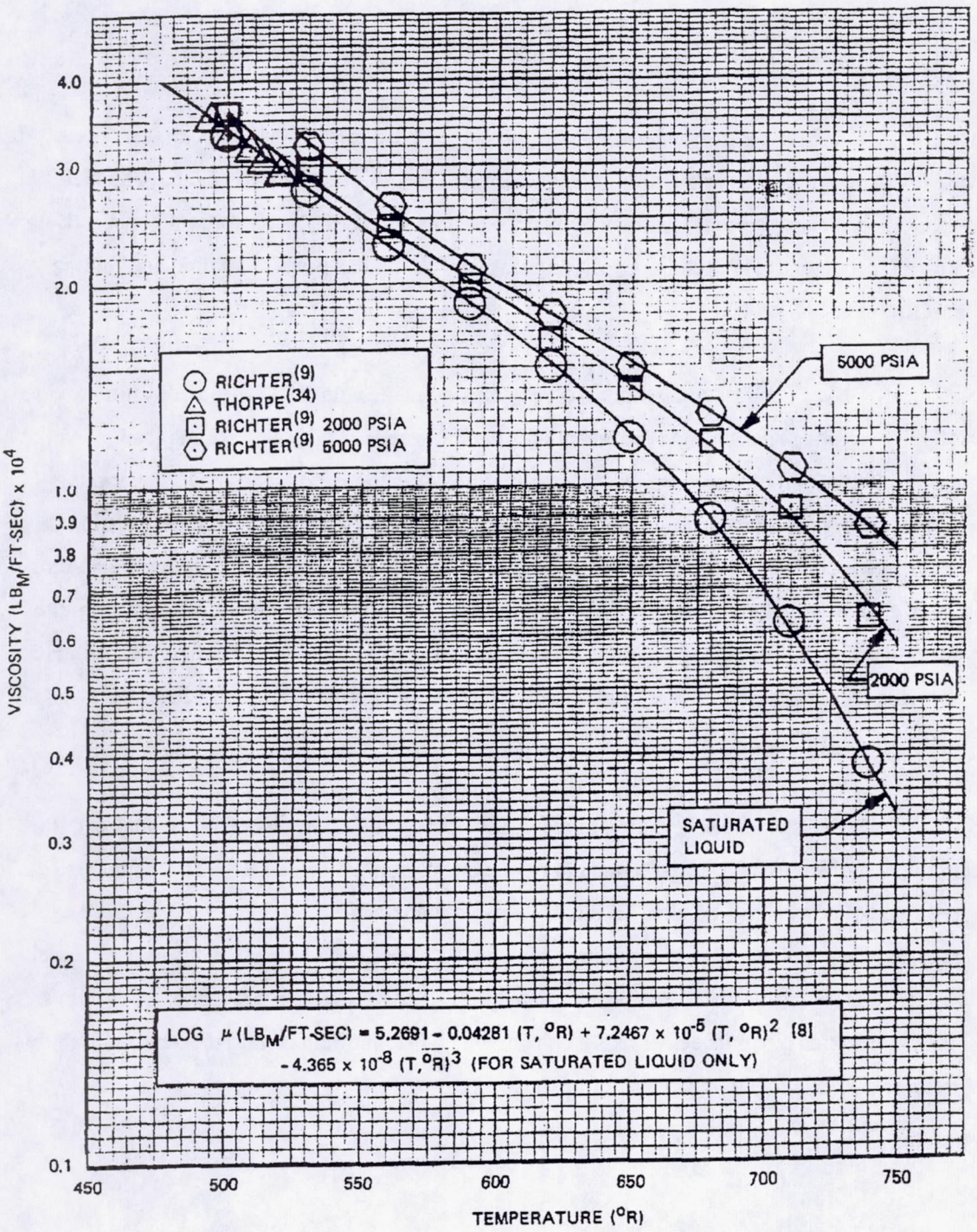

Figure 8. Variation of MON-3 Viscosity with Temperature

3.0 MON-25 PRODUCTION PROCESS

MON-25 is not available either commercially or from Kelly AFB stockpiles. Therefore, the MON-25 used in this program was manufactured by ARC/LP at our Niagara Falls facility. ARC/LP had experience in the manufacturing of MON-3 and MON-10 from previous and ongoing programs. The technique is straightforward as long as proper handling and mixing procedures are followed.

MON-25 consists of a mixture of 75% nitrogen tetroxide (N2O4) and 25% nitric oxide (NO) by weight. The starting constituents for the mixture are MON-3, which is readily available at our facility from other programs, and commercially available bottles of NO. The mixing process involves an exothermic reaction of the NO gas with N2O4 to create nitrogen trioxide (N2O3), which gives MON-25 its characteristic bluish-green color. ARC employed a cooling chamber during the mixing operation to both limit the oxidizer temperature increase from the reaction and to lower the vapor pressure of the resulting mixture to better utilize the available NO from its storage bottle. The initial temperature of the mixing bottle and MON-3 was approximately –1C (30°F).

Figure 9 shows a schematic of the mixing operation. All hardware associated with the production of MON-25 was passivated to ensure the minimization of MON-25 leaching excess iron into solution. This included all mixing vessels, transfer/feed lines and samples bottles. To minimize the transfer operations required for this test series, a common mixing/storage vessels was used. The mixing/storage vessel consisted of a standard cylindrical 9-gallon tank with a stand tube inside along its center axis. The gaseous NO is introduced into the tank through this perforated stand tube at the bottom of the tank.

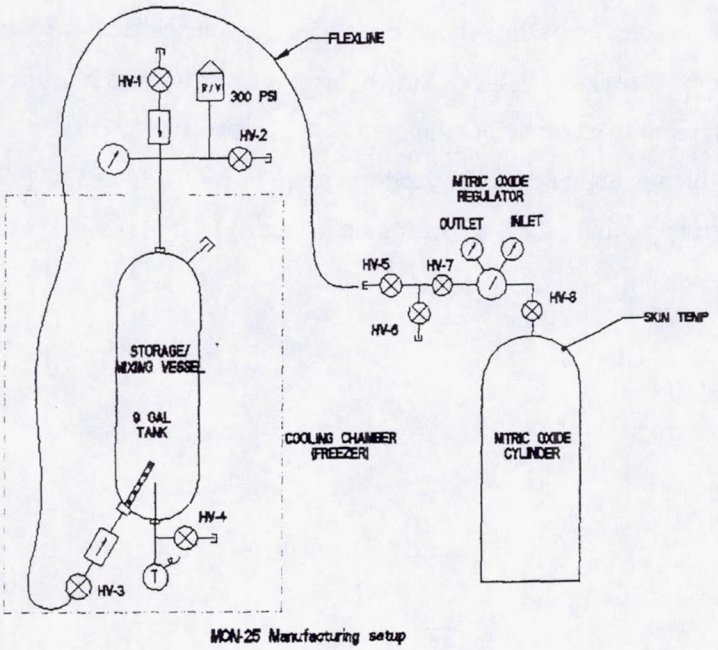

Figure 9. MON-25 Mixing Operation Schematic

The flow of NO into the tank was controlled by a NO gas regulator which limited the pressure of the NO to about 1.6 bar (23 psia), which is approximately the vapor pressure of the final mixture of MON-25 at –1C (30F). Both pressure and temperature were monitored during the mixing operation. Periodically, the NO flow was turned off to allow the reaction to reach completion and for the mixing/storage vessel to be recooled. The pressure and temperature of the NO bottles were monitored during this operation. The NO bottle was allowed to return to ambient temperature to calculate the mass of NO which has been introduced into the mixing/storage vessel through the use of the perfect gas law.

After it has been determined that sufficient NO has been added to the oxidizer, the oxidizer was sampled using an evacuated standard Hoke bottle. The sample was shipped to Vicksburg Chemical for chemical analysis per MIL-P-26539D to verify the NO content of the oxidizer. The two samples analyzed showed an NO content of 25.0% and 25.3%. Approximately 22.7 kg (50 lbm) of MON-25 was manufactured.

After completion of the mixing operation, gaseous helium was introduced into the mixing/storage vessel. This gas pressure blanket insures that the NO does not come out of solution preferentially at ambient temperatures. The pressure was maintained at about 8.6 bar (125 psia), which is higher than the vapor pressure of MON-25 at 32C (90F) (a maximum summer time temperature for the Niagara Falls facility).

4.0 PROPELLANT AND HARDWARE TEMPERATURE CONDITIONING SYSTEMS

To support the Mars Flyer program, ARC developed a propellant conditioning system with the capability to cool the propellants to –40C for tests of any run duration. A schematic of the propellant cooling system is shown in Figure 10.

In this system, liquid carbon dioxide (CO_2) is used to cool a bath filled with a mixture of approximately 60/40 ethylene glycol and water. The freezing point for this mixture is about –50C (-58F). This mixture was chosen as a tradeoff between the required temperature capability of the fluid and the ability to pump it to the propellant heat exchangers. For example, by reducing the water in the fluid, the freezing point could be reduced further, however, since the viscosity of the fluid increases rapidly as the ethylene glycol content is increased and temperature is reduced, it becomes difficult to pump an adequate supply of the fluid to the heat exchangers. After some experimentation, the 60/40 mixture was found to be satisfactory for these tests. The CO_2 circulates through the bath inside a set of copper coil tubing. It enters the coils as a liquid and exits as a gas; most of the cooling capability is, therefore, in the heat of vaporization of the CO_2. A mechanical agitator was also used in the bath to increase the heat transfer rate between the bath fluid and the liquid CO_2.

The glycol bath is located outside of the test cell. The cold bath fluid is pumped through an insulated line to the propellant heat exchanges inside the test cell. The cooling fluid is split inside the cell and directed to separate fuel and oxidizer heat exchangers. After leaving the propellant heat exchangers, the fluid is returned to the bath via a single line.

As shown in Figure 10, the propellant heat exchangers are located in the test cell downstream of the propellant tanks and flowmeters. Figure 11 shows the thruster mounted in the test cell with the propellant heat exchangers located just behind the thruster. The distance between the propellant heat exchangers and the thruster valve was approximately 10 cm. Thermocouples (FIT, OIT; See Figure 10) were located in the fuel and oxidizer lines just

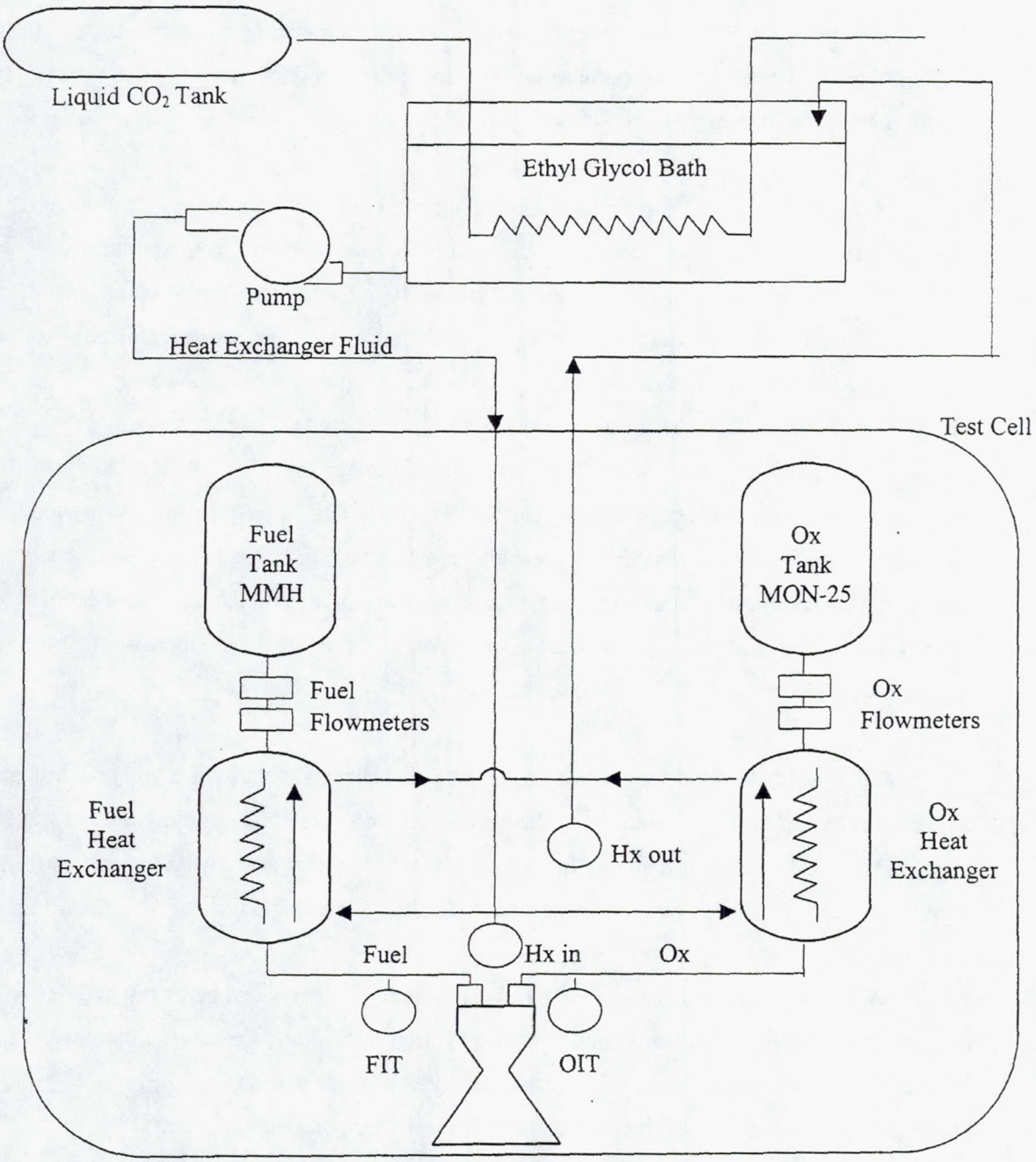

Figure 10. Propellant Cooling System in Test Cell

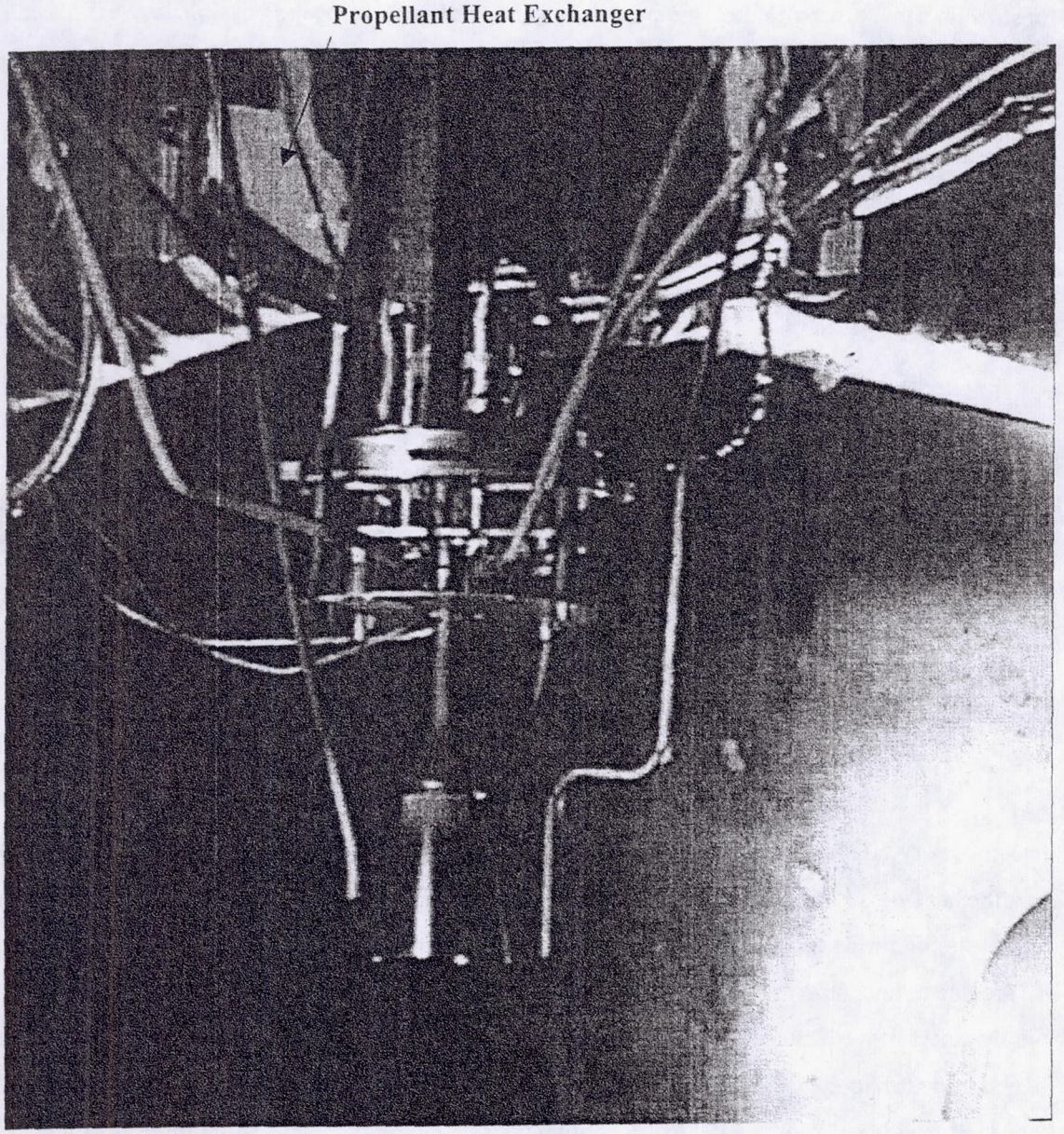

Figure 11. Thruster Mounted in Test Cell

upstream of the thruster to measure propellants temperatures as close as possible to the thruster inlet. The propellant heat exchangers contain copper coils through which the propellants flow. The cold glycol/water mixture flows around the outside of the coils and cools the propellant. The heat exchanger is a counterflow design with the cold glycol entering the heat exchanger at the location where the propellant exits to the thruster. Typically, the propellant enters the heat exchanger at about 21C (70F) and leaves at a temperature within about 1C (2F) of the entering glycol/water mixture.

Figure 12 shows a high resolution time history of the propellant temperatures for Test 35625 which was a 1200s run at the nominal 15.2 bar (220 psia) feed pressure with nominal –40C propellants. Except for a short period during the start transient, the propellant conditioning system maintained the propellants within ±1C (±2F) of 40C for the entire 1200s run. The start transient is due to the cleaning of the small amount of propellant in the short line between the propellant heat exchangers and the thruster. Before each test, a short bleed flow is conducted into a catch tank to clear the propellant in this line, however, bleed flow times on these tests was kept short due to the limited amount of MON-25 available for these tests.

As noted earlier, the mixture of ethylene glycol and water used as a heat exchanger fluid becomes very viscous at low temperatures. When conditioning propellants to –40C, it was found that the heavy load imposed on the pump by this viscous fluid would cause the pump to over heat and cycle off during long tests. The two valleys in the propellant temperatures shown in Figure 12 are due to the pump cycling off and then being restarted. Figure 13 shows the time history of temperatures of the heat exchanger fluid at the heat exchanger inlet and outlet for this test. These temperatures are quite constant over most of the test except for the two points where the pump cycles off and is restarted. Note that in cooling the propellant, the temperature increase of the fluid is only 1C (2F) from heat exchanger inlet to exit. The system was designed with a good deal of margin in terms of the thermal cooling capability of the propellant heat exchangers and because of this margin, even when the pump shuts down and is restarted, the propellant temperatures were maintained within 1C of the target –40C valve for the entire 1200s test.

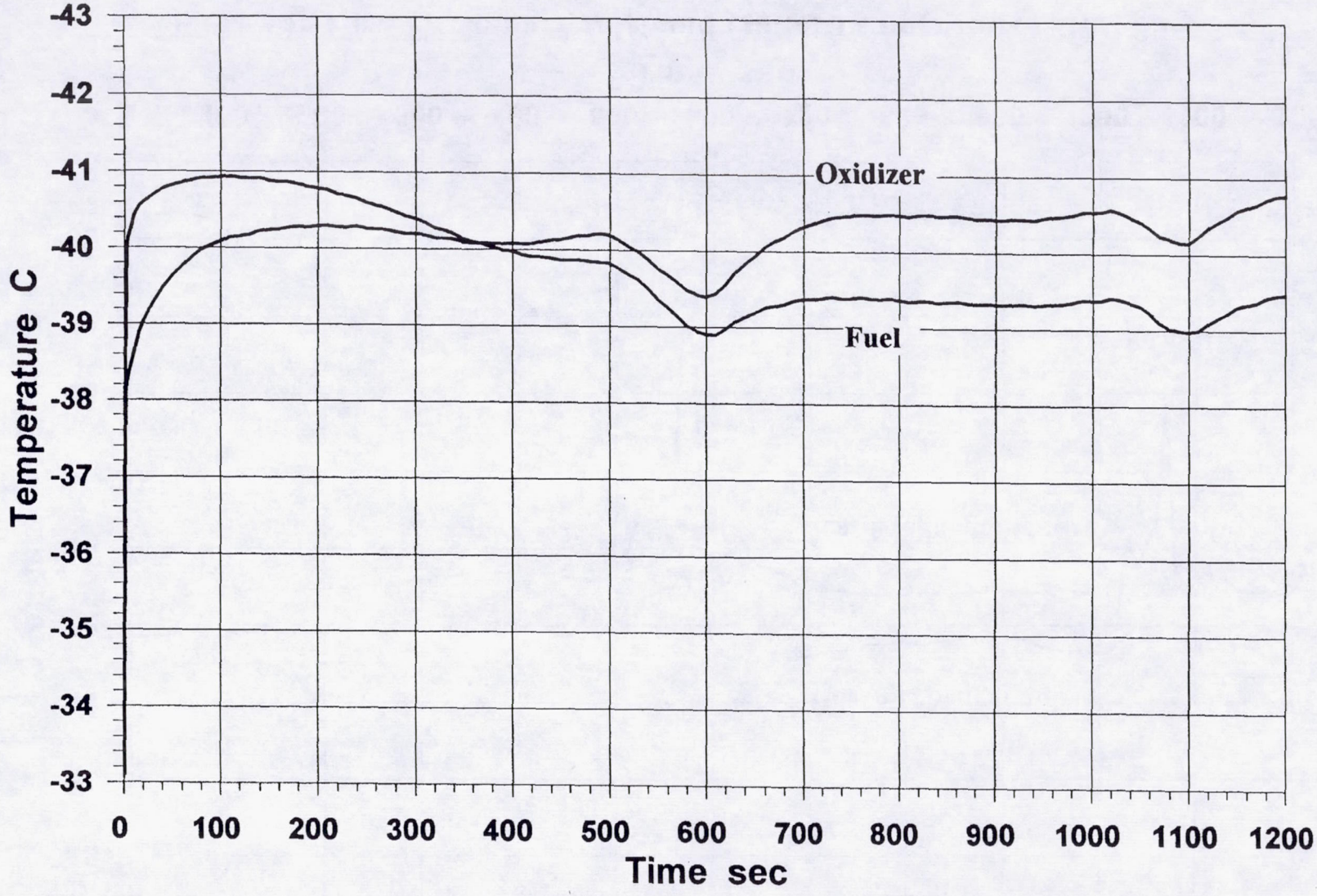

Figure 12. Propellant Temperature Time History, Test 35625

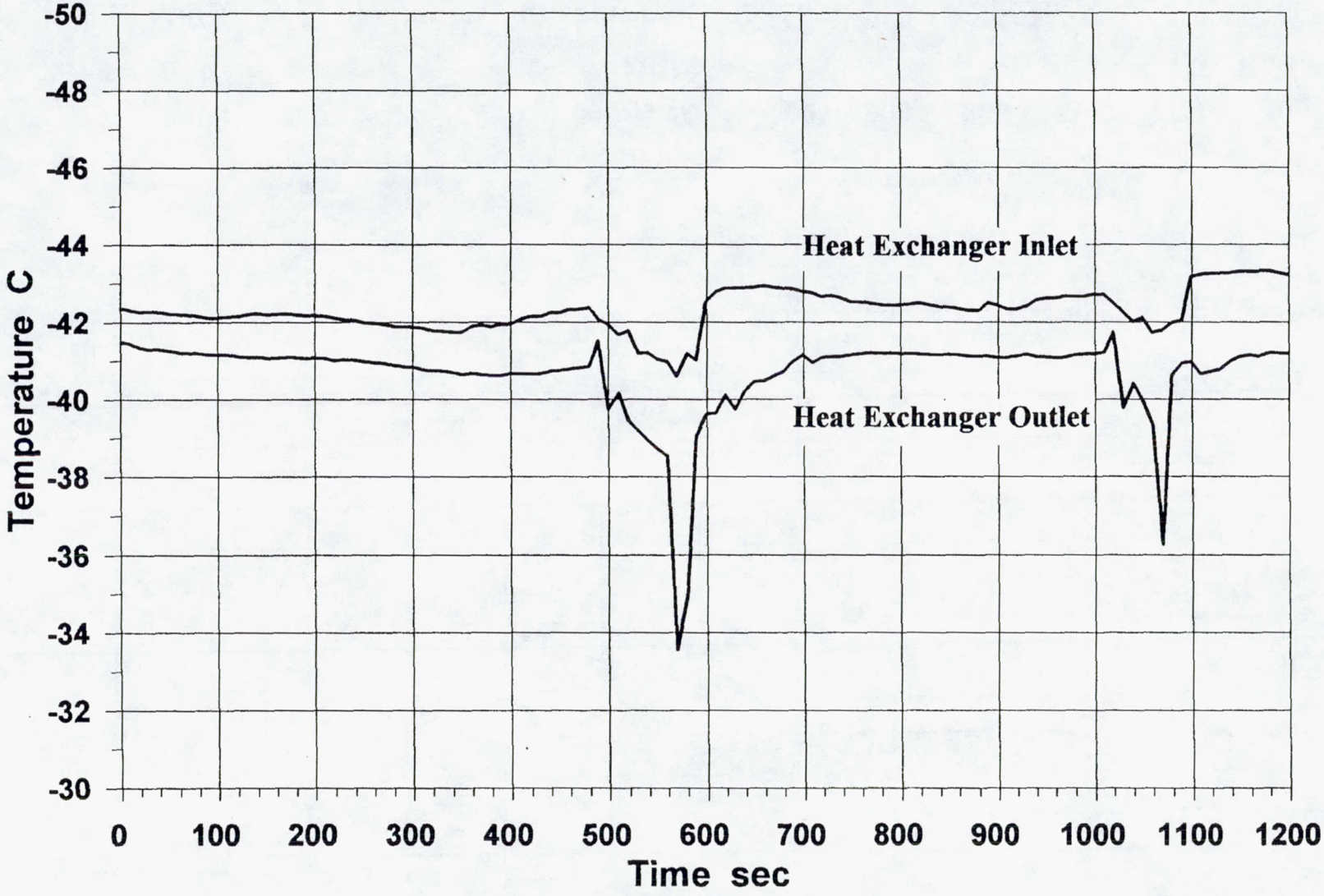

Figure 13. Heat Exchanger Inlet and Outlet Temperatures, Test 35625

Before each test, the thruster and valves were cooled to a temperature which was below the propellant temperature. It was difficult to cool the hardware with any degree of precision, however, the objective was hardware temperatures equal to or lower than the propellant temperatures, and this was achieved in all cases. Hardware temperatures were measured by thermocouples located on the back of the injector. The hardware was cooled by throttling liquid CO_2 through an orifice. In going through the orifice, the liquid flashed to vapor at the test cell pressure of about 1.5 torr (0.03 psia). This cold CO_2 gas was directed at the hardware through four lines, one at each valve and two at the injector from opposing sides. This cold gas injection system had independent valves for the valve and injector cooling circuits and they were cycled on/off until the desired temperatures were obtained. As noted earlier, it was difficult to achieve precise control of the hardware temperatures using this approach. The data shows that for all tests, hardware temperatures were below the propellant temperatures and for many tests, the hardware start temperatures were well below the propellant temperatures which represents a very severe environment. In any future testing, a system which provides more precise control of hardware temperatures should be developed.

5.0 TEST PLAN

The test procedures and test plan for this activity are documented in ARC PP-80704 (Test Procedure) and ARC PP-80704, Addendum 1 (Hot Fire Test Matrix). These documents were reviewed and approved by NASA before testing was initiated.

Tables 2, 3 and 4 show the planned tests. Table 2 shows the baseline tests with 21C (70F) propellants. The test matrix consists of tests a different feed pressures from 6.9 – 20.7 bar (100-300 psia), three tests to measure the effect of mixture ratio, and one test where the cell pressure was increased to 10 torr (0.2 psia) to simulate the Mars atmospheric environment. Shown in the last column is the ARC test number for the planned test. Table 3 shows the matrix for the tests to map thruster performance as a function of propellant temperature and feed pressure. Table 4 shows the matrix for testing with –40C propellants. All tests were completed except for Tests 6, 8, and 9 in Table 4. These tests were not conducted since of the MON-25 supply was exhausted.

Figure 14 shows the thermocouple instrumentation on the thruster. Two thermocouples (ICBT1, ICBT2) wee located on the backside of the injector. One thermocouple was located on each valve and valve mount and four thermocouples were located at the nozzle joint. These thermocouples were used to set pre-test hardware temperature and to monitor thruster behavior during hot fire testing.

Table 2
MON-25/MMH Baseline Test Matrix

Test No.	FFP/OFP (psia)	Run Duration		Temperatures (°F)			Flow Path	Comments	ARC Test Number
		On/Off (sec)	No. of Pulses	Propellant	Start				
					Valve	Inj.			
1	220/220	60 / -	1	70	≤104	≤104	Flowmeter	Baseline	35606
2	100/100	60 / -	1	70	≤104	≤104	Flowmeter	Pc Survey	35607, 35610
3	150/150	60 / -	1	70	≤104	≤104	Flowmeter	Pc Survey	35601
4	200/200	60 / -	1	70	≤104	≤104	Flowmeter	Pc Survey	35608
5	250/250	60 / -	1	70	≤104	≤104	Flowmeter	Pc Survey	35611
6	300/300	60 / -	1	70	≤104	≤104	Flowmeter	Pc Survey	35612
7	220/250	60 / -	1	70	≤104	≤104	Flowmeter	MR Survey	35613
8	220/190	60 / -	1	70	≤104	≤104	Flowmeter	MR Survey	35614
9	190/220	60 / -	1	70	≤104	≤104	Flowmeter	MR Survey	35615
10	220/220	0.1/0.1	20	70	≤104	≤104	Bellows	Baseline Pulse	35616
11*	220/220	60/-	1	70	≤104	≤104	Flowmeter	Mars Simulation	35617

Table 3.
MON-25/MMH Pressure and Temperature Mapping Tests

Test No.	FFP/OFP (psia)	Run Duration		Temperatures (°F)			Flow Path	Comments	ARC Test Number
		On/Off (sec)	No. of Pulses	Propellant	Start				
					Valve	Inj.			
1	100/100	60 / -	1	-40	≤-40	≤-40	Flowmeter	Pc Survey	35619
2	150/150	60 / -	1	-40	≤-40	≤-40	Flowmeter	Pc Survey	35620
3*	220/220	60 / -	1	-40	≤40	≤40	Flowmeter	Mars Simulation	35621
4	250/250	60 / -	1	-40	≤-40	≤-40	Flowmeter	Pc Survey	35622
5	300/300	60 / -	1	-40	≤-40	≤-40	Flowmeter	Pc Survey	35623
6	100/100	30 / -	1	-20	≤-20	≤-20	Flowmeter	Pc Survey	36639
7	150/150	30 / -	1	-20	≤-20	≤-20	Flowmeter	Pc Survey	35640
8	220/220	60 / -	1	-20	≤-20	≤-20	Flowmeter	Pc Survey	35641
9	250/250	30 / -	1	-20	≤-20	≤-20	Flowmeter	Pc Survey	35642
10	300/300	30 / -	1	-20	≤-20	≤-20	Flowmeter	Pc Survey	35643
11	100/100	30 / -	1	0	≤0	≤0	Flowmeter	Pc Survey	35634
12	150/150	30 / -	1	0	≤0	≤0	Flowmeter	Pc Survey	35635
13	220/220	60 / -	1	0	≤0	≤0	Flowmeter	Pc Survey	35636
14	250/250	30 / -	1	0	≤0	≤0	Flowmeter	Pc Survey	35363
15	300/300	30 / -	1	0	≤0	≤0	Flowmeter	Pc Survey	35638
16	100/100	30 / -	1	30	≤30	≤30	Flowmeter	Pc Survey	35629
17	150/150	30 / -	1	30	≤30	≤30	Flowmeter	Pc Survey	35630
18	220/220	60 / -	1	30	≤30	≤30	Flowmeter	Pc Survey	35630
19	250/250	30 / -	1	30	≤30	≤30	Flowmeter	Pc Survey	35632
20	300/300	30 / -	1	30	≤30	≤30	Flowmeter	Pc Survey	35633

Table 4.
MON-25/MMH Test Matrix at –40C

Test No.	FFP/OFP (psia)	Run Duration		Temperatures (°F)			Flow Path	Comments	ARC Test Number
		On/Off (sec)	No. of Pulses	Propellant	Start				
					Valve	Inj.			
1	220/220	1200 / -	1	-40	≤-40	≤-40	Flowmeter	Duration Test	35625
2	220/220	1200 / -	1	-40	≤-40	≤-40	Flowmeter	Duration Test	35626
3	220/220	1200 / -	1	-40	≤-40	≤-40	Flowmeter	Duration Test	35627
4	220/220	600 / -	1	-40	≤-40	≤-40	Flowmeter	Duration Test	35624
5	220/220	600 / -	1	-40	≤-40	≤-40	Flowmeter	Duration Test	35628
6	220/220	600 / -	1	-40	≤-40	≤-40	Flowmeter	Duration Test	
7	220/220	300 / -	1	-40	≤-40	≤-40	Flowmeter	Duration Test	35618
8	220/220	300 / -	1	-40	≤-40	≤-40	Flowmeter	Duration Test	
9	220/220	300 / -	1	-40	≤-40	≤-40	Flowmeter	Duration Test	
10	220/250	60 / -	1	-40	≤-40	≤-40	Flowmeter	MR Survey	35647
11	220/190	60 / -	1	-40	≤-40	≤-40	Flowmeter	MR Survey	35648
12	190 / 220	60 / -	1	-40	≤-40	≤-40	Flowmeter	MR Survey	35649
13	220/220	0.1/0.1	20	-40	≤-40	≤-40	Bellows	Pulse Test	35644
14	220/220	0.2/0.2	20	-40	≤-40	≤-40	Bellows	Pulse Test	35645
15	220/220	0.5/0.5	20	-40	≤-40	≤-40	Bellows	Pulse Test	35646

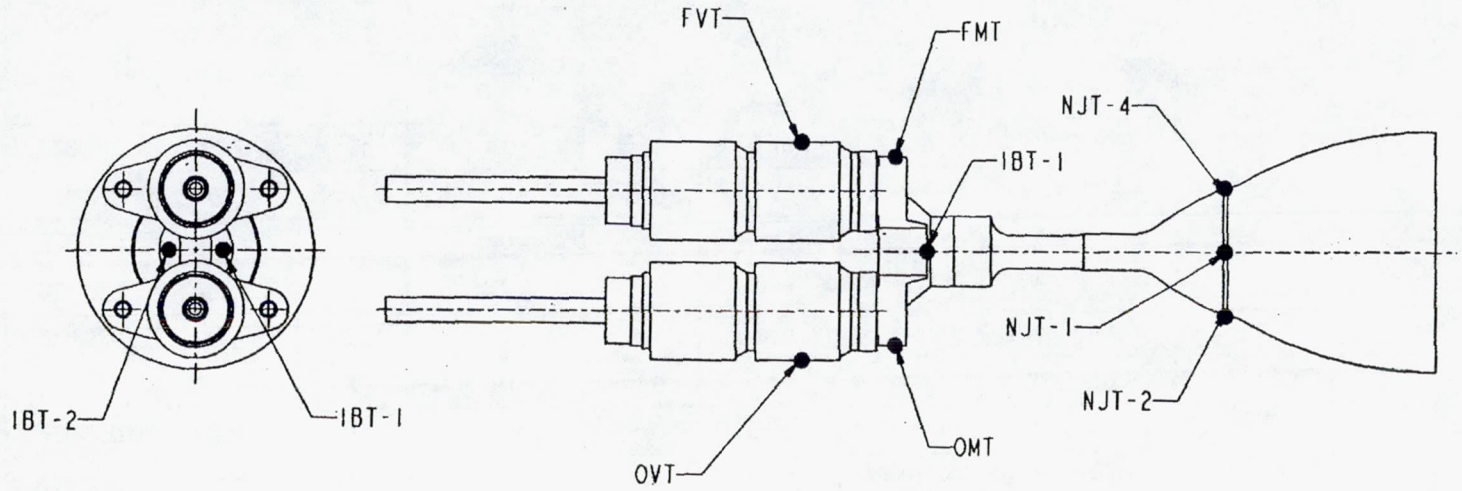

Figure 14. Thermocouple Locations

6.0 TEST RESULTS

Table 5 provides a summary of all the tests conducted during this program. The detailed test data is given in Volume 2. Most of the tests were of 30s or 60s duration and for these tests, the results shown in Table 5 are at the end of the run. For the long duration 600s and 1200s runs, a data slice at 60s and at the end of the run are given in Table 5. Given in Table 5 are results for thrust, Isp, mixture ratio(MR), propellant flowrates(total, fuel, oxidizer), propellant temperatures and valve and injector temperatures before the start of the test. Also shown is a value for Pc which is calculated from the measured thrust, assuming a value for the thrust coefficient(Cf) of 1.770. C* is calculated from this estimated value for Pc. The maximum chamber temperature measured during the test using the Agema infrared camera is also given in Table 5.

Test 35607 was a 30s test which was terminated at 28s when an excessive amount of fuel was observed coming from the nozzle. This test was successfully rerun as Test 35610. It was suspected that there was gas in the oxidizer line during Test 35607 which caused poor combustion. This thruster has a high fraction of the fuel in the barrier so the chamber runs relatively cold, however, a consequence of this is that it is difficult to burn all the fuel, particularly when the feed pressure is low and the propellant is cold. Typically, at the low feed pressure conditions fuel was observed collecting around and vaporizing from the rim of the nozzle.

Test 35464 was a pulse test with a 0.500/0.500s duty cycle. This test was terminated before completion when fuel was observed coming from the nozzle and the strip chart data showed no evidence that combustion was occurring in the chamber. The previous two pulse tests with duty cycle of 0.100/0.100s and 0.200/0.200s ran successfully.

Test 35649 was terminated early since the MON-25 oxidizer was exhausted early in the test. During the test, fuel was observed running out of the nozzle. The test data shows the mixture ratio decreasing during the test, indicating the oxidizer was being exhausted.

No.	Test No.	Date	Feed Pres. OFP/FFP bar	Run Time On/Off sec	Pulses	Data Slice sec	Thrust N	Isp sec	Pc bar	Cstar m/s	MR	Propellant Flowrates Total gm/s	Fuel gm/s	Ox gm/s	Max Cham Temp C	Injector Temp C	Propellant Temperatures Ox C	Fuel C	Pre-test Hardware T Ox Valve C	Fuel Valve C	Injector C	COMMENTS
1	35606	28 Oct	15.2/15.2	60	1	60	10.15	277.6	7.12	1504	1.616	3.726	1.424	2.301	note 4	51	25	25	22	22	23	
2	35607	"	6.9/6.9	28	1																	Test terminated
3	35608	29 Oct	13.8/13.8	60	1	60	8.77	254.8	6.17	1384	1.585	3.507	1.357	2.150		48	21	21	25	23	26	
4	35609	"	10.3/10.3	60	1	60	7.03	249.8	4.94	1355	1.546	2.869	1.127	1.742		48	21	22	25	24	34	
5	35610	"	6.9/6.9	60	1	60	4.54	216.7	3.18	1171	1.254	2.135	0.947	1.188		48	21	21	24	23	31	
6	35611	"	17.2/17.2	60	1	60	11.04	280.5	7.77	1522	1.604	4.010	1.540	2.470		49	21	22	21	19	28	
7	35612	"	20.7/20.7	60	1	60	12.68	285.1	8.93	1549	1.624	4.534	1.728	2.806		50	21	21	19	19	31	
8	35613	"	15.2/17.2	60	1	60	10.28	266.1	7.21	1440	1.801	3.938	1.406	2.532		50	21	21	24	24	30	
9	35614	"	15.2/13.1	60	1	60	9.12	264.6	6.41	1435	1.396	3.514	1.467	2.048		46	21	21	22	20	33	
10	35615	"	13.1/15.2	60	1	60	8.77	244.0	6.17	1324	1.837	3.662	1.291	2.371		48	21	21	19	17	29	
11	35616	"	15.2/15.2	.10/.10	20	na	0.85	201.1			1.622	0.433	0.165	0.268		26	18	19	20	19	22	
12	35617	"	15.2/15.2	60	1	60	10.59	288.3	7.43	1561	1.600	3.745	1.440	2.304		47	20	21	16	16	18	Test cell pressure = 0.20 psia
13	35618	4 Nov	15.2/15.2	300	1	60	9.48	264.9	6.67	1438	1.865	3.647	1.273	2.374	623	19	-38	-39	-38	-43	-40	
	"	"	"	"		300	9.43	268.0	6.65	1457	1.794	3.588	1.284	2.304		18	-39	-39				
14	35619	"	6.9/6.9	60	1	60	3.20	130.7	2.26		1.798	2.499	0.893	1.606		3	-38	-39	-39	-43	-41	
15	35620	5 Nov	10.3/10.3	60	1	60	6.72	231.4	4.74	1259	1.920	2.960	1.014	1.946	293	11	-40	-41	-43	-51	-38	
16	35621	"	15.2/15.2	60	1	60	10.28	288.4	7.23	1564	1.900	3.633	1.253	2.380	359	17	-41	-41	-53	-58	-52	Test cell pressure = 0.20 psia
17	35622	"	17.2/17.2	60	1	60	10.24	265.5	7.20	1441	1.931	3.929	1.341	2.589	591	17	-41	-41	-53	-60	-43	
18	35623	10 Nov	20.7/20.7	60	1	60	11.97	278.5	8.43	1514	1.858	4.381	1.533	2.848	888	23	-40	-41	-51	-46	-40	
19	35624	"	15.2/15.2	600	1	60	8.05	225.0	5.65	1217	1.963	3.649	1.232	2.417	662		-41	-41	-62	-51	-29	
	"	"	"	"		600	9.57	268.6	6.73	1458	1.840	3.631	1.278	2.352		18	-39	-39				
20	35625	11 Nov	15.2/15.2	1200	1	60	9.52	266.7	6.68	1444	1.882	3.640	1.263	2.377	673		-40	-41	-43	-46	-41	
	"	"	"	"		1200	9.61	269.5	6.77	1463	1.852	3.636	1.275	2.361		20	-41	-39				
21	35626	"	15.2/15.2	1200	1	60	8.90	249.8	6.27	1357	1.948	3.632	1.232	2.400	678		-40	-42	-47	-49	-43	
	"	"	"	"		1200	9.66	269.8	6.79	1464	1.848	3.648	1.281	2.367		19	-41	-39				
22	35627	"	15.2/15.2	1200	1	60	9.35	266.6	6.57	1446	1.942	3.573	1.214	2.359	893		-42	-42	-44	-46	-39	
	"	"	"	"		1200	9.52	266.2	6.69	1442	1.801	3.647	1.302	2.345		18	-39	-38				
23	35628	"	15.2/15.2	600	1	60	9.70	273.0	6.82	1481	1.865	3.622	1.264	2.358	679		-37	-39	-44	-46	-51	
	"	"	"	"		600	9.61	271.8	6.76	1474	1.802	3.605	1.286	2.318		18	-40	-38				
24	35629	12 Nov	6.9/6.9	30	1	30	4.72	197.2	3.31	1067	1.663	2.438	0.916	1.523		26			-3	-5	-2	
25	35630	"	10.3/10.3	30	1	30	6.94	235.8	4.90	1283	1.664	3.001	1.126	1.874	262	28	-2	-2	-4	-7	-8	
26	35631	"	15.2/15.2	60	1	60	9.83	268.7	6.91	1456	1.650	3.731	1.408	2.323	629	32	-2	-3	-9	-12	-1	
27	35632	"	17.2/17.2	30	1	30	10.90	275.2	7.66	1492	1.644	4.038	1.527	2.511	712	32	-1	-2	-11	-12	-4	
28	35633	"	20.7/20.7	30	1	30	12.42	280.1	8.74	1522	1.644	4.518	1.709	2.809	878	34	-1	-1	-10	-12	-3	
29	35634	"	6.9/6.9	30	1	30	4.98	212.6	3.51	1155	1.787	2.390	0.857	1.532		17	-17	-17	-22	-23	-22	
30	35635	"	10.3/10.3	30	1	30	7.30	245.9	5.12	1330	1.806	3.025	1.078	1.947	268	19	-18	-19	-23	-24	-22	
31	35636	"	15.2/15.2	60	1	60	10.01	272.9	7.04	1480	1.764	3.740	1.353	2.387	679	24	-19	-19	-26	-28	-19	
32	35637	"	17.2/17.2	30	1	30	10.90	278.4	7.66	1509	1.690	3.992	1.484	2.508	732	24	-18	-19	-22	-25	-21	
33	35638	"	20.7/20.7	30	1	30	12.50	283.2	8.81	1539	1.713	4.501	1.659	2.842	912	26	-18	-19	-30	-32	-21	
34	35639	"	6.9/6.9	30	1	30	4.76	201.9	3.35	1096	1.839	2.404	0.847	1.557		11	-29	-29	-29	-32	-33	
35	35640	"	10.3/10.3	30	1	30	7.12	247.4	5.01	1344	1.793	2.934	1.050	1.883	264	14	-29	-30	-31	-33	-30	
36	35641	"	15.2/15.2	60	1	60	9.88	272.6	6.94	1477	1.782	3.694	1.328	2.366	665	19	-31	-31	-35	-38	-29	
37	35642	"	17.2/17.2	30	1	30	10.86	277.3	7.64	1505	1.787	3.991	1.432	2.559	734	21	-29	-30	-34	-36	-31	
38	35643	"	20.7/20.7	30	1	30	12.28	281.7	8.63	1528	1.801	4.444	1.587	2.858	891	23	-30	-31	-37	-38	-28	
39	35644	"	15.2/15.2	.10/.10	20	na	0.81	208.4			1.915	0.397	0.136	0.261		-34	-38	-39	-43	-44	-43	
40	35645	"	15.2/15.2	.20/.20	20	na	1.62	224.1			2.159	0.737	0.233	0.503		-22	-39	-40	-48	-49	-43	
41	35646	"	15.2/15.2	.50/.50	11	na										-42						Terminated, no combustion
42	35647	"	15.2/17.2	60	1		9.83	258.3	6.93	1404	2.127	3.881	1.241	2.640	615	18	-39	-40	-45	-47	-42	
43	35648	"	15.2/13.1	60	1		8.94	265.9	6.28	1441	1.712	3.429	1.264	2.165	482	15	-40	-41	-46	-47	-41	
44	35649	"	13.1/15.2	10	1											-29						Stopped: ox depleted during ru

TEST NOTES

1. Pc calculated from thrust assuming Cf = 1.77
2. Throat area for C* calculation is:
3. For pulse runs, values in thrust colum 0.07865 cm2
4. The chamber temperature data for Tests 35606-35617 has been lost due to an instrumentation error.

Table 5. Mars Flyer Program Test Data Summary

Figure 15 shows the time history for the propellant, fuel valve, oxidizer valve and injector temperatures for Test 35625, which was a 1200s test at the nominal 15.2 bar (220 psia) feed pressure and with –40C propellant. Figure 15 shows that the injector and valve temperatures were below –40C at the start of the run. Pre-test hardware temperatures for each test are given in Table 5. The results in Figure 15 show the valve and injector temperatures rise smoothly during the run with steady-state valve temperatures being reached after 500s and the injector temperature after about 300s.

Figure 16 shows the time history of thrust, specific impulse and mixture ratio for Test 35625. Thrust and Isp are relatively constant except for two bumps which appear to be correlated with the dips in the propellant temperatures shown in Figure 12. Figure 17 shows a higher resolution chart of the mixture ratio time history. As the injector temperature increases, the mixture ratio shifts downward reaching a steady-state value of about 1.84. The nominal mixture ratio for the thruster with 21C propellants is 1.65; the changes in propellant viscosity caused by operation with –40C propellants cause the mixture ratio to shift from a nominal 1.65 to 1.84.

Figure 18 shows the time history of the propellant flowrates for Test 35625. The flows are quite steady throughout the run. The oxidizer flow shows two small oscillations associated with the pump cycling off and being restarted. The fuel flow shows a small increase during the start transient as the injector temperature increases as this is responsible for the decrease in mixture ratio during the start transient.

Figure 19 shows the effect of propellant temperature on thruster mixture ratio for tests at the nominal 15.2 bar (220 psia) feed pressure. The data covers the propellant temperature range of 25C to –42C (77F to –44F). The data trend shows that as propellant temperature decreases, the mixture ratio increases. As discussed in Section 2, this is caused by the large increase in the fuel viscosity as the propellant temperature decreases. This thruster was designed for a nominal mixture ratio of 1.65 with 21C (70F) propellants and as the results show, the mixture ratio shift is

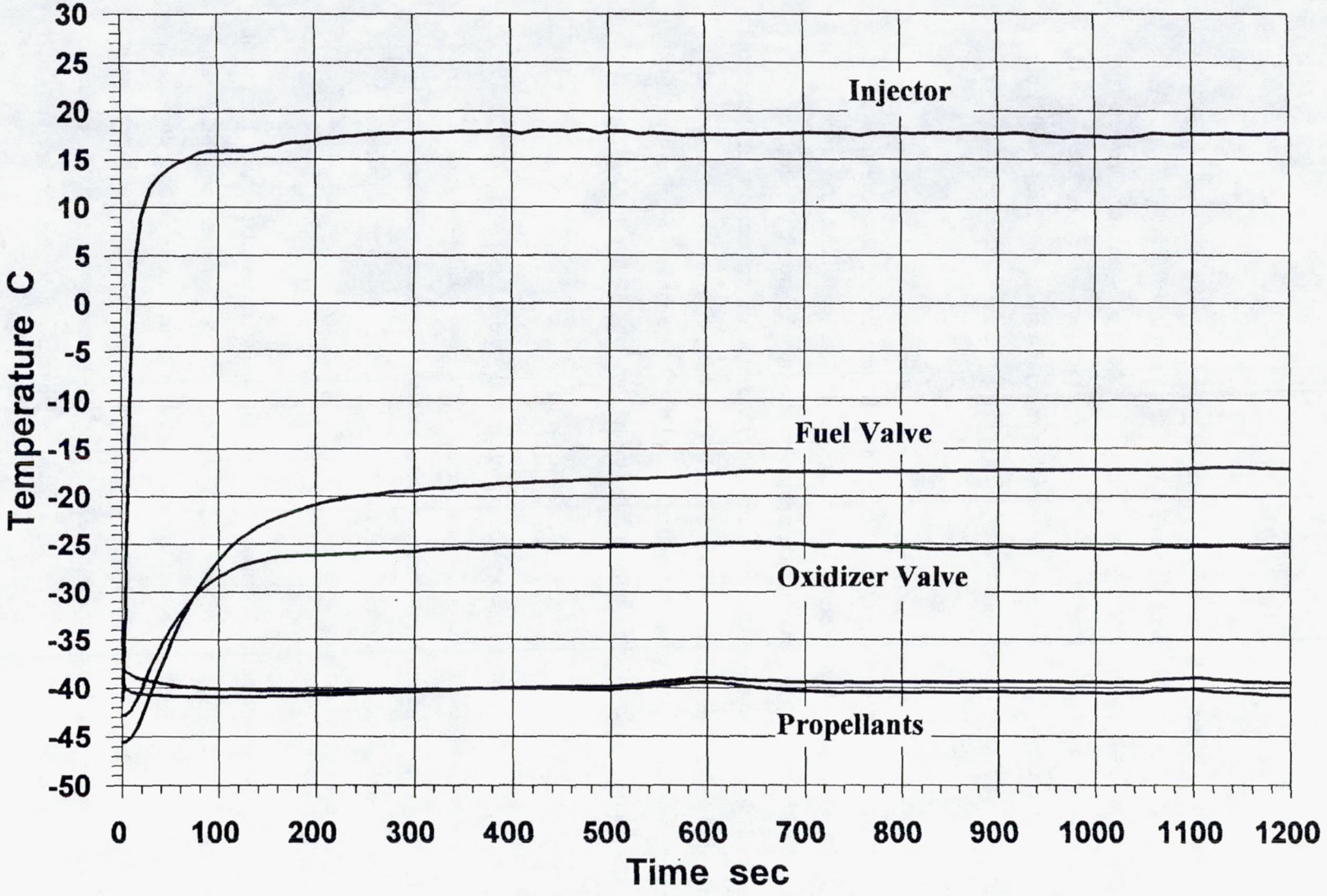

Figure 15. Temperature Time History, Test 35625

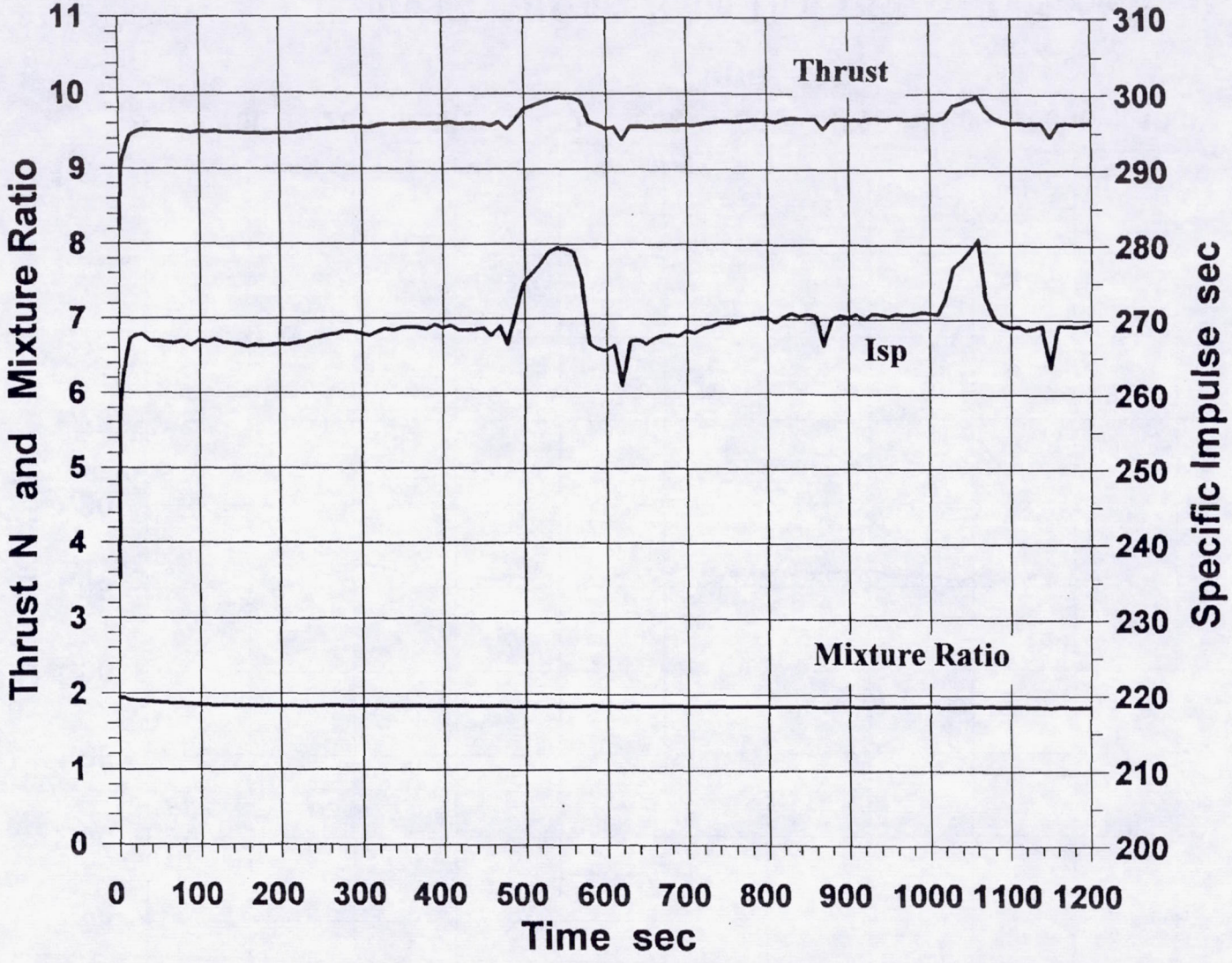

Figure 16. Thrust, Isp and MR History, Test 35625

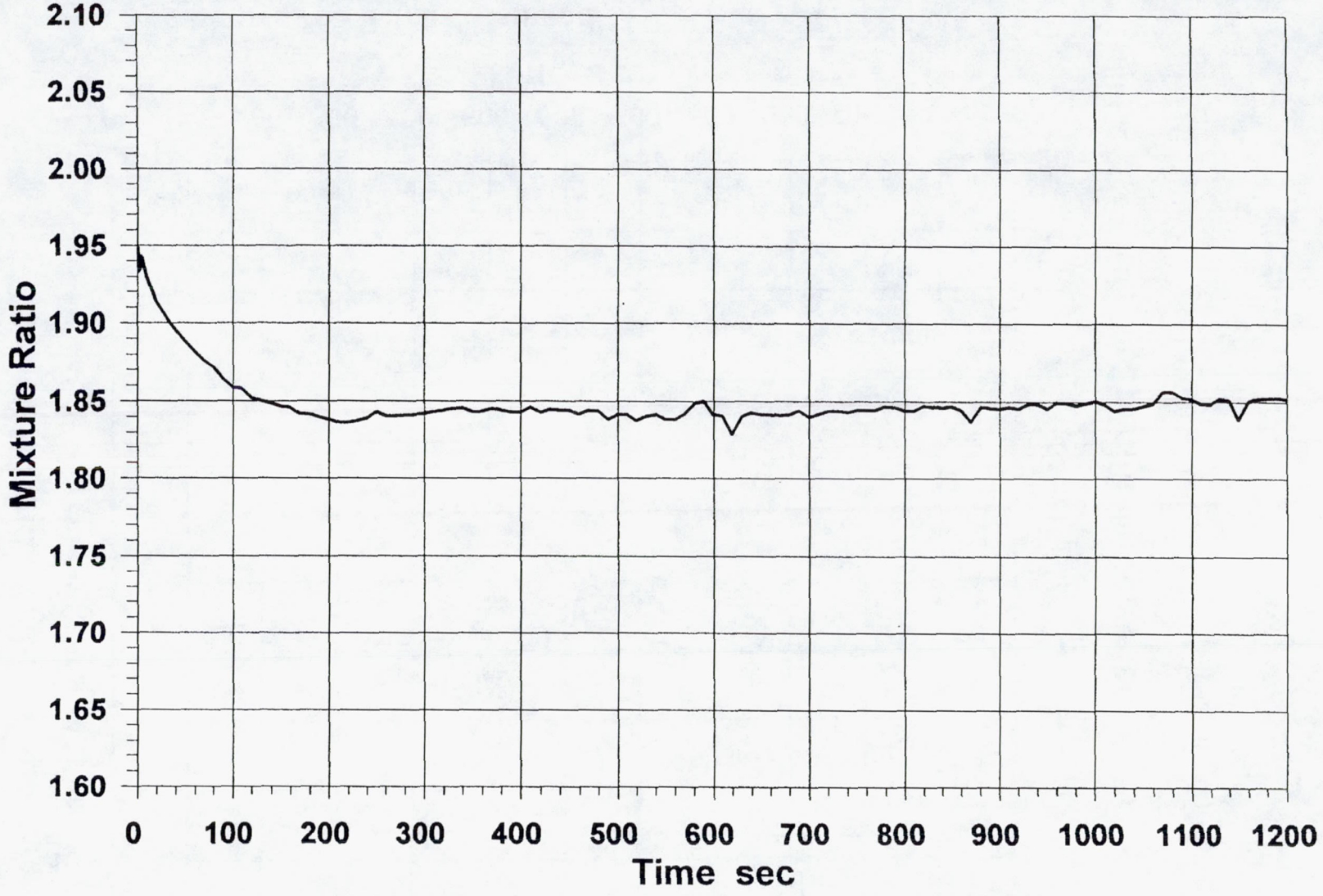

Figure 17. Mixture Ratio Time History, Test 35625

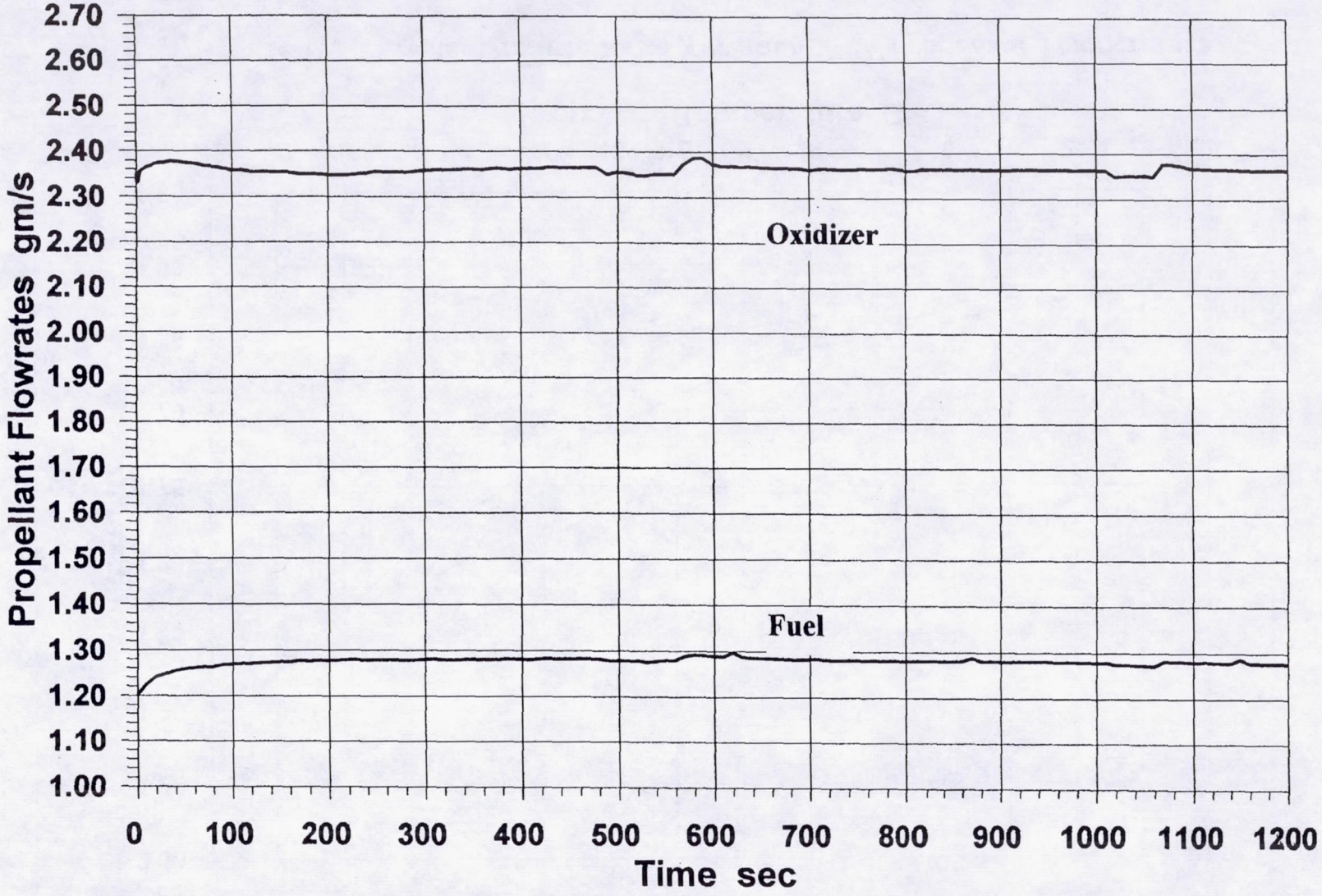

Figure 18. Propellant Flowrate Time History, Test 35625

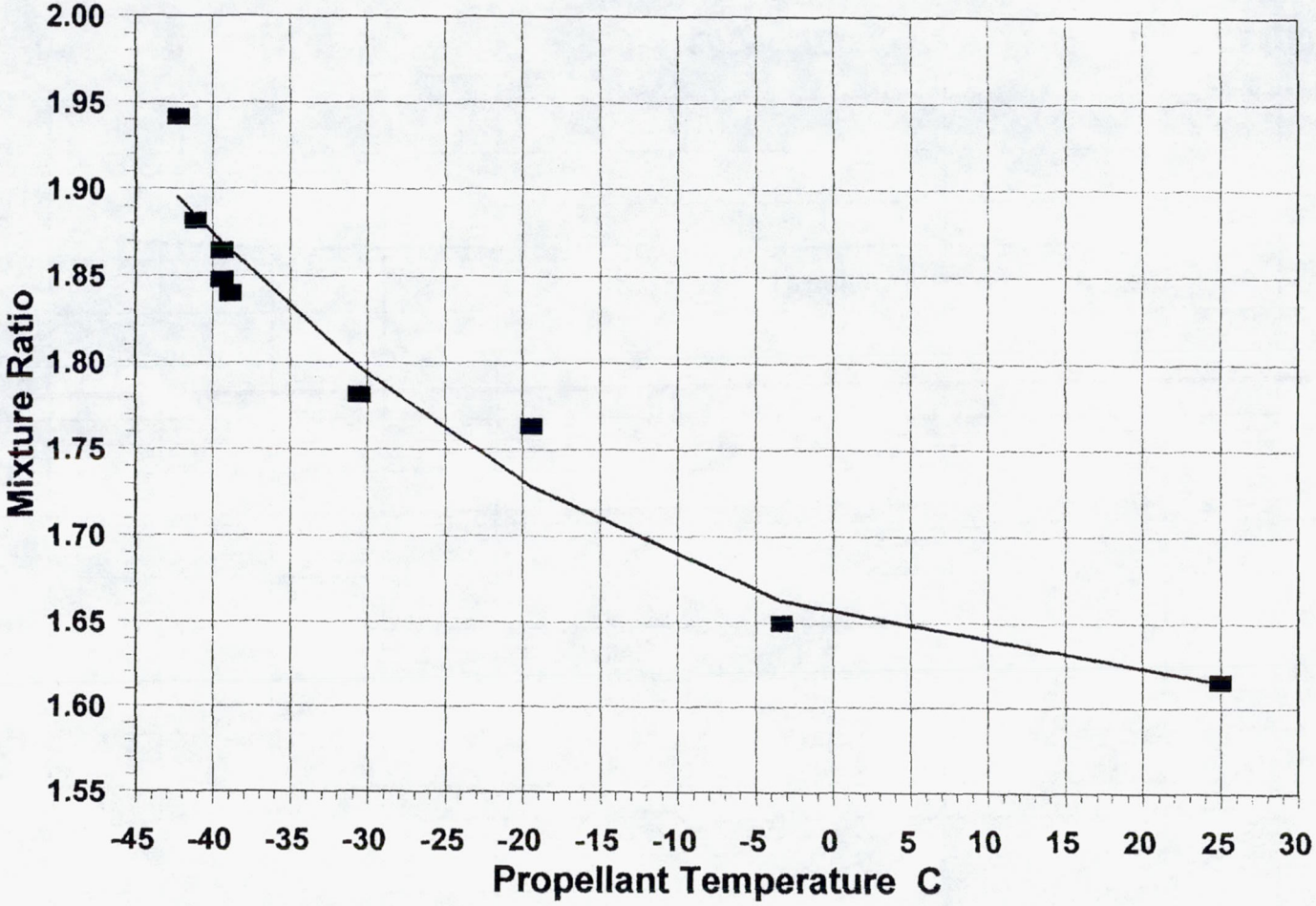

Figure 19. Thruster Mixture Ratio Variation With Propellant Temperature

modest for temperatures above about –4C (25F), but increases rapidly for temperature below this level. It should be noted that it would be relatively easy to redesign the thruster by modifying the orifices and flow passages to provide a mixture ratio of 1.65 with –40C (-40F) propellants such that optimum performance could be obtained for the Mars environment.

Figure 20 shows how thruster specific impulse is affected by propellant temperature. The effect is quite modest with Isp decreasing by about 10s as the propellant temperature is decreased from 25C (77F) to –42C (-44F). Figure 4 shows how Isp varies with MR for 21C (10F) propellants and these results show that as MR increases from 1.65 to 1.85 for the 16 bar tests, Isp decreases by about 5s. This suggests that the decrease in Isp due to operation with cold propellants is caused about equally by the induced shift in mixture ratio and by the propellant temperature, itself.

Figure 21 shows the effect of both feed pressure and propellant temperature on the thruster mixture ratio. The results show that at all propellant temperatures, except the 21C (70F) case, mixture ratio is relatively insensitive to feed pressure. With 21C (70F) propellants, the mixture ratio decreases as feed pressure decreases and falls sharply for feed pressures below about 10.3 bar (150 psia). This occurs because at low feed pressures, the oxidizer tends to boil in the injector causing a decrease in the oxidizer flowrate and a downward shift in mixture ratio. This does not occur with cold propellants since they can absorb the injector heating without reaching the saturation temperature of the oxidizer.

Figure 22 shows how thruster specific impulse varies with feed pressure and propellant temperatures. The results show that Isp decreases as feed pressure and propellant temperatures decrease. The effect of propellant temperature has been discussed. The decrease with feed pressure is typical for a thruster of this type and is due to a lower combustion efficiency as mass flowrate and chamber pressure decrease.

ARC's 2 lbf thruster uses a high level of fuel barrier cooling to maintain low chamber and injector temperatures when the thruster is firing. The chamber temperatures are measured

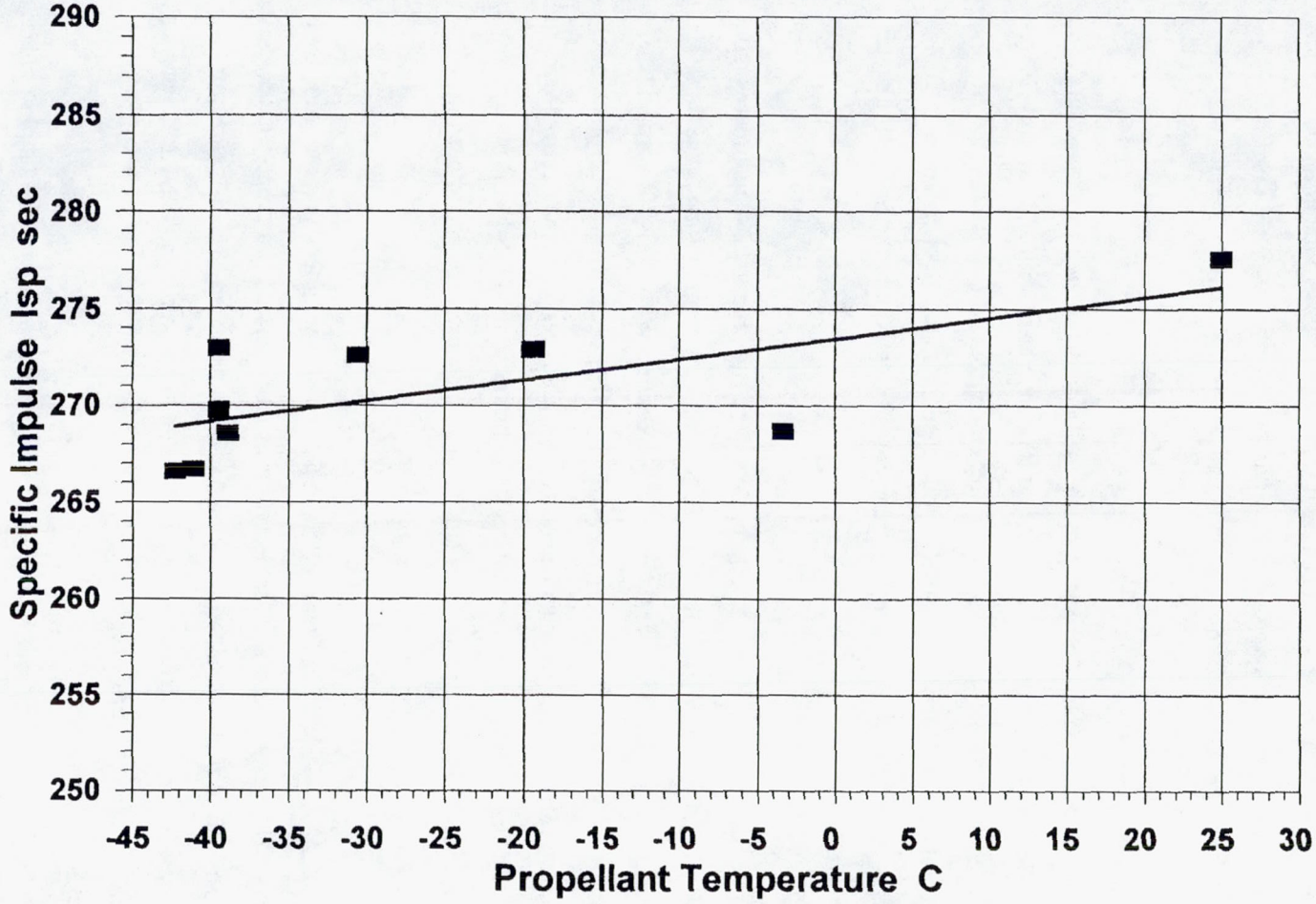

Figure 20. Specific Impulse Variation With Propellant Temperature

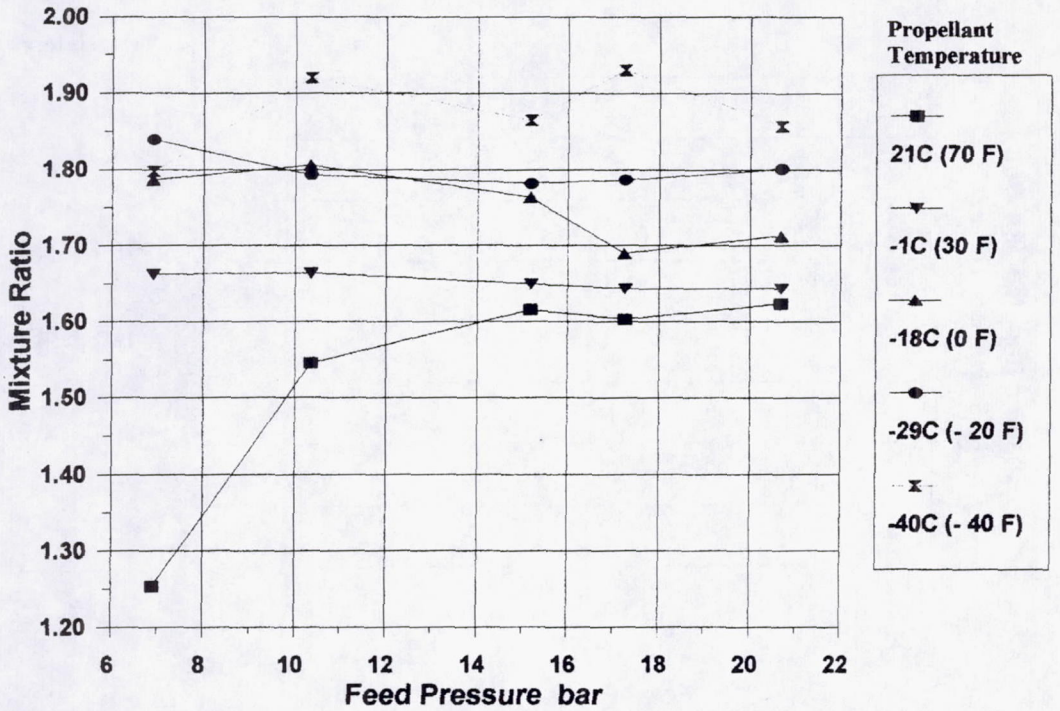

Figure 21. Effect of Propellant Feed Pressure and Temperature on Mixture Ratio

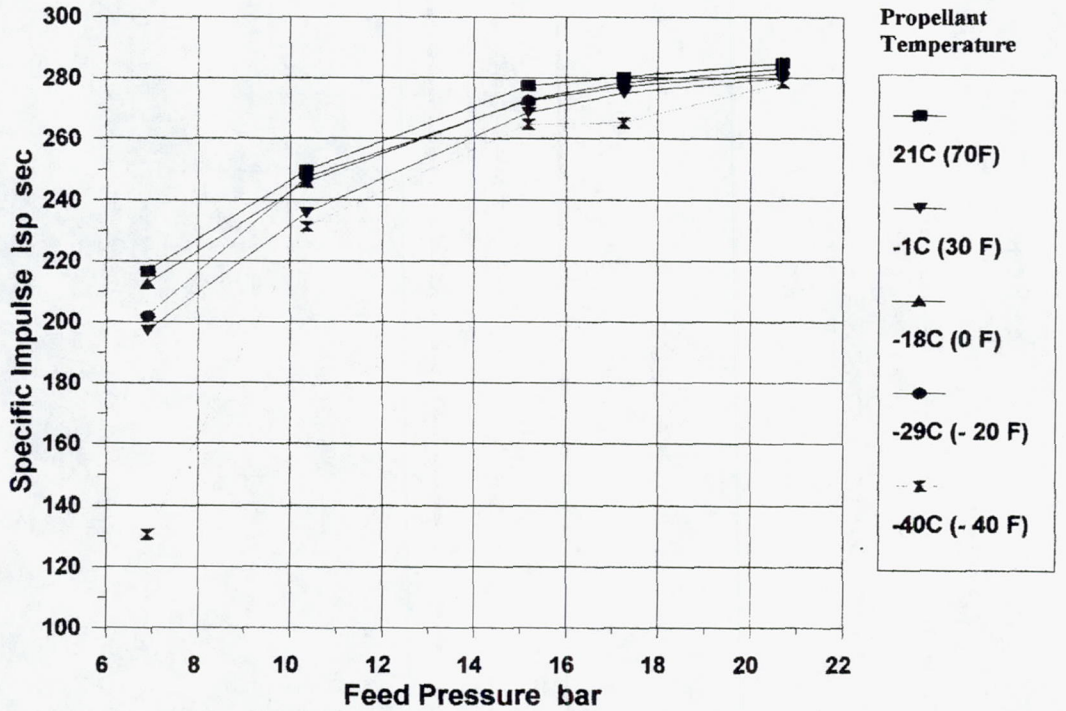

Figure 22. Effect of Propellant Feed Pressure and Temperature On Specific Impulse

using an Agema infrared camera and the data in Table 5 that chamber temperatures are below about 870C (1700F) at all conditions. At the lower feed pressures, chamber temperatures were below the infrared scanner measurement threshold of 260C (500F).

Figure 23 shows how the injector temperatures are affected by the propellant feed pressure and temperature. Due to the high level of barrier cooling in this thruster, the injector temperatures are quite low. At the normal operating condition with 21C (70F) propellant, the injector temperature is about 49C (120F) over the entire range of feed pressures. As shown in Figure 23, the injector temperature decreases as the propellant temperature is reduced. As propellant temperature is reduced, the injector temperatures show a greater sensitivity to feed pressure. The strong influence of propellant temperature on the injector temperature is expected since the propellant provides the primary cooling for the injector.

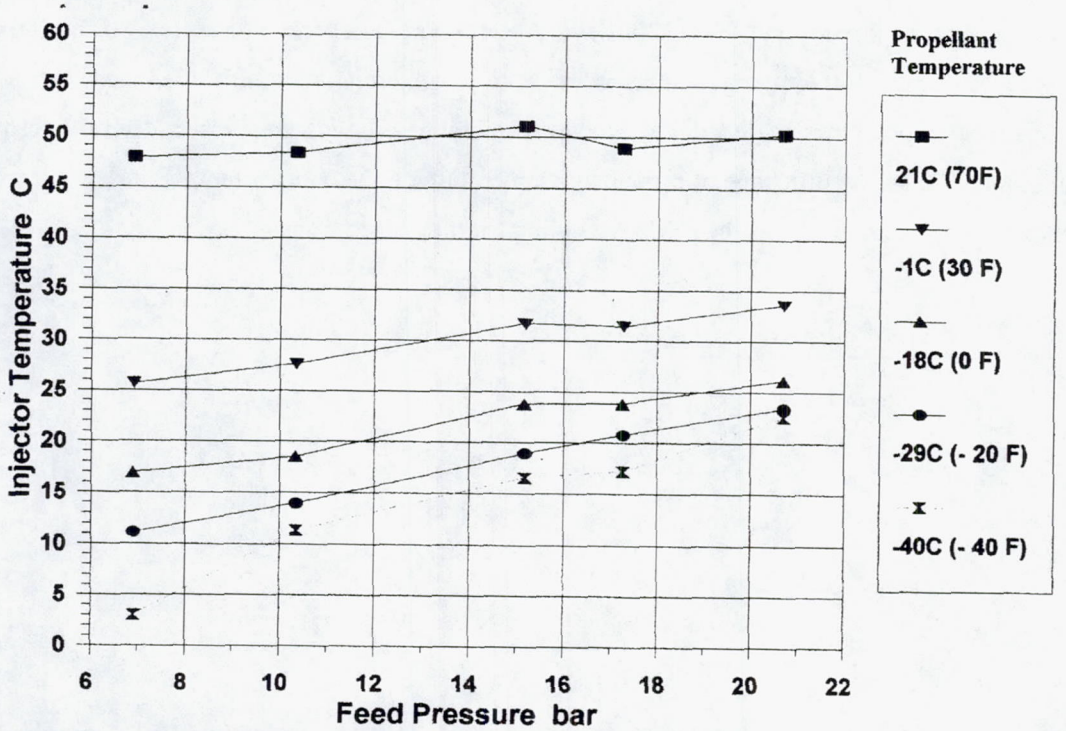

Figure 23. Effect of Propellant Feed Pressure and Temperature On Injector Temperature

7.0 CONCLUSIONS

ARC's 10N thruster was successfully tested with propellant cooled to –40C and the thruster and valves cooled below this level. The thruster was operated successfully over the entire propellant temperature range of 21C to –40C (70F to –40F) and feed pressure range of 6.9 – 20.7 bar (100-300 psia) required by the NASA-approved test matrix. While the thruster was not designed to operate at these conditions, it did demonstrate the capability to operate successfully at the temperature conditions expected to be encountered in the Mars environment.

When operating with –40C propellants, the thruster experienced a shift in mixture ratio from the nominal value of 1.65 with 21C propellants to about 1.85. This shift is caused by the increase in the MMH viscosity as propellant temperatures are reduced with a consequent reduction in the MMH flowrate and increase in mixture ratio. The increase in mixture ratio and the lower energy content of the –40C propellants cause a slight reduction of specific impulse of about 10s compared to the baseline value with 21C propellants.

During this program, ARC successfully demonstrated the ability to manufacture MON-25 as required to conduct these tests. The procedures are now in place to make this propellant for any future activities. Further, ARC developed and demonstrated propellant conditioning systems for the fuel and oxidizer with the capability to deliver propellants to the thruster at –40C with a tolerance of ±1C for tests of any duration. This ability to make propellants and to precisely control propellant temperatures provides NASA the demonstrated capability to conduct such Mars environment tests in the future.

The testing conducted on this program was exploratory in nature. The purpose was to use an existing thruster design to determine if there were any unexpected problems which would be encountered when operating a thruster with MON-25/MMH propellants at –40C. The conclusion to be derived from these tests is that no such problems were uncovered and that a properly designed thruster should have no difficulty operating in the Mars environment.

8.0 RECOMMENDATIONS

Propellant Properties

There is a lack of data on the properties of MON-25, particularly at the low temperature conditions of interest for the Mars environment. Data on the thermodynamic and transport properties of this propellant over the 100C to –50C range is needed to support thruster design and performance evaluation activities. It is recommended that NASA compile a database of MON-25 properties, identify deficiencies in the database, and initiate a program to obtain the required data.

Thruster Design

The results in this report show that a thruster designed for 21C propellants will operate somewhat differently when tested with –40C propellants. The reasons for the mixture ratio shift and specific impulse decrease observed herein are understood. The mixture ratio shift can be corrected by either modifying the injection orifices in the thruster or possibly, by using a different set of trim orifices upstream of the valve. Modifying the design will allow one to recover the Isp lost to the mixture ratio shift. It is recommended that in any future activity to examine propulsion for the Mars environment, NASA provide a set of design objectives for the thruster and consider modifying an existing design to meet these requirements before initiating a test evaluation.

REPORT DOCUMENTATION PAGE

Form Approved
OMB No. 0704-0188

1. AGENCY USE ONLY (Leave blank)	2. REPORT DATE	3. REPORT TYPE AND DATES COVERED
	April 2001	Final Contractor Report

4. TITLE AND SUBTITLE

Mars Flyer Rocket Propulsion Risk Assessment
ARC Testing

5. FUNDING NUMBERS

WU–755–B4–01–00
NAS3–99197

6. AUTHOR(S)

Atlantic Research Corporation

7. PERFORMING ORGANIZATION NAME(S) AND ADDRESS(ES)

Atlantic Research Corporation
6686 Walmore Road
Niagara Falls, New York 14304–1697

8. PERFORMING ORGANIZATION REPORT NUMBER

E–12642

9. SPONSORING/MONITORING AGENCY NAME(S) AND ADDRESS(ES)

National Aeronautics and Space Administration
Washington, DC 20546–0001

10. SPONSORING/MONITORING AGENCY REPORT NUMBER

NASA CR—2001-210709

11. SUPPLEMENTARY NOTES

Project Managers, Brian Reed, 216–977–7489, and James Biaglow, 216–977–7480, Power and On-Board Propulsion Technology Division, NASA Glenn Research Center, organization code 5430.

12a. DISTRIBUTION/AVAILABILITY STATEMENT

Unclassified - Unlimited
Subject Category: 20 Distribution: Nonstandard

Available electronically at http://gltrs.grc.nasa.gov/GLTRS

This publication is available from the NASA Center for AeroSpace Information, 301–621–0390.

12b. DISTRIBUTION CODE

13. ABSTRACT ***(Maximum 200 words)***

This report describes the investigation of a 10-N, bipropellant thruster, operating at –40 °C, with monomethylhydrazine (MMH) and 25% nitric oxide in nitrogen tetroxide (MON-25). The thruster testing was conducted as part of a risk reduction activity for the Mars Flyer, a proposed mission to fly a miniature airplane in the Martian atmosphere. Testing was conducted using an existing thruster, designed for MMH and MON-3 propellants. MON-25 oxidizer was successfully manufactured from MON-3 by the addition of nitric oxide. The thruster was operated successfully over a range of propellant temperatures (–40 to 21 °C) and feed pressures (6.9 to 20.7 kPa). The thruster hardware was always equal or lower than the propellant temperature. Most tests were 30- and 60-second durations, with 600- and 1200-second duration and pulse testing also conducted. When operating at –40 °C, the mixture ratio of the thruster shifted from the nominal value of 1.65 to about 1.85, probably caused by an increase in MMH viscosity, with a corresponding reduction in MMH flowrate. Specific impulse at –40 °C (at nominal feed pressures) was 267 sec, while performance was 277 sec at 21 °C. This difference in performance was due, in part, to the mixture ratio shift.

14. SUBJECT TERMS

Liquid rocket propellants; Rocket testing; Mixed oxides of nitrogen; Mars flyer

15. NUMBER OF PAGES

54

16. PRICE CODE

A04

17. SECURITY CLASSIFICATION OF REPORT	18. SECURITY CLASSIFICATION OF THIS PAGE	19. SECURITY CLASSIFICATION OF ABSTRACT	20. LIMITATION OF ABSTRACT
Unclassified	Unclassified	Unclassified	

APPENDIX B: MARS FLYER ROCKET PROPULSION RISK ASSESSMENT
Kaiser Marquardt Final Report

This report is being reprinted in its entirety as originally printed in April 2001. The reader should note that the original page numbers have been retained.

NASA/CR—2001-210710

Mars Flyer Rocket Propulsion Risk Assessment
Kaiser Marquardt Testing

Kaiser Marquardt
Van Nuys, California

Prepared under Contract NAS3–99198

National Aeronautics and
Space Administration

Glenn Research Center

April 2001

Trade names or manufacturers' names are used in this report for identification only. This usage does not constitute an official endorsement, either expressed or implied, by the National Aeronautics and Space Administration.

Available from

NASA Center for Aerospace Information
7121 Standard Drive
Hanover, MD 21076
Price Code: A03

National Technical Information Service
5285 Port Royal Road
Springfield, VA 22100
Price Code: A03

Available electronically at http://gltrs.grc.nasa.gov/GLTRS

TABLE OF CONTENTS

LIST OF FIGURES

LIST OF TABLES

LIST OF NOMENCLATURE

Symbols

C^*	characteristic velocity
δ	ignition delay
F, FT	thrust (vacuum, unless otherwise specified)
η_{C^*}	C* efficiency
I_{sp}, ISP	specific impulse (vacuum, unless otherwise specified)
N_2O_4	dinitrogen tetroxide
NO	nitric oxide
O/F	oxidizer-to-fuel mixture ratio
p_{cell}, PCELL	test cell pressure
p_{mf}, PMF	fuel inlet manifold pressure
p_{mo}, PMO	oxidizer inlet manifold pressure
t	time
T_{c1}, TC1	injector-chamber interface temperature #1
T_{c2}, TC2	injector-chamber interface temperature #2
T_{ch}, TCH	chamber temperature
T_{mf}, TMF	fuel inlet manifold temperature
T_{mo}, TMO	oxidizer inlet manifold temperature
t_{off}	valve time off
t_{on}	valve time on
T_{f1}, TF1	oxidizer-side valve flange temperature
T_{f2}, TF2	fuel-side valve flange temperature
T_{vf}, TVF	fuel-side valve temperature
T_{vo}, TVO	oxidizer-side valve temperature
I_V, VI	valve current
V_V, VV	valve voltage
w_{fu}, WFU	fuel flow rate
w_{ox}, WOX	oxidizer flow rate

Acronyms

ACC1	accelerometer #1
C-103	columbium-metal alloy
CD-ROM	compact disc read-only memory
GN2	gaseous nitrogen
LN2	liquid nitrogen
MMH	monomethylhydrazine
MON-25	mixed oxides of nitrogen, 75% N2O4 / 25% NO by weight
MON-3	mixed oxides of nitrogen, 97% N2O4 / 3% NO by weight
NASA	National Aeronautics and Space Administration
RAM	random-access memory
SCXI	National Instruments signal conditioning system

1 INTRODUCTION

The Mars Flyer mission proposed by the National Aeronautics and Space Administration will fly a miniature airplane in the Martian atmosphere on the centennial anniversary of the Wright brother's first powered flight. At the time of proposal, both, an electric motor-driven propeller and a chemical rocket engine were under consideration for the Mars Flyer propulsion system. As part of a risk reduction investigation, Kaiser Marquardt was contracted to validate, by test demonstration, the use of a chemical thruster utilizing mixed oxides of nitrogen and monomethylhydrazine. The objective was to provide NASA with as much data as possible for the flight system decision.

Preliminary studies performed by NASA showed that a thrust level of 8.9 N would be appropriate for a rocket-powered Mars Flyer. The Mars Flyer will be power-limited and volume-limited, therefore, the rocket propulsion system will have to employ storable propellants and be capable of operating in the Martian environment without thermal management. Without thermal management, the entire propulsion system, including propellants, will be subjected to extremely low temperatures as the average diurnal temperature of the surface-level Martian atmosphere is –40 degrees Celsius.

An experimental investigation was conducted to assess the performance of an 8.9-N, bipropellant thruster operating at –40 °C with monomethylhydrazine (MMH) and mixed oxides of nitrogen (MON). To facilitate engine operation at low temperatures, dinitrogen tetroxide, N_2O_4, was saturated with nitric oxide, NO, to lower the freezing point. The freezing point of the industry-standard, 3% nitric oxide in dinitrogen tetroxide (MON-3) is -15 °C. By increasing the nitric oxide content to 25% (MON-25), the freezing point was lowered to –55 °C, thus enabling safe operation of the thruster at –40 °C with sufficient margin for error. The thruster was tested in a near-vacuum environment and conditioned, along with the propellants, to –40 °C prior to hot firing. Thruster operating parameters included oxidizer-to-fuel mixture ratios of 1.6 to 2.7 and inlet pressure ranging from 689 to 2070 kPa. The test matrix consisted of many 10-second firings and several 60, 300, 600, and 1200-second firings. Measurements included thrust, propellant flow rates, propellant inlet pressures and temperatures, engine temperatures, system vibrations, and valve control-signal characteristics. Data obtained from testing were analyzed to determine engine performance characteristics such as ignition delay, specific impulse, I_{sp}, versus oxidizer-to-mixture ratio, O/F, I_{sp} versus thrust, F, and the vibration frequency spectrum. Preliminary results indicate that the additional nitric oxide not only permits lower propellant temperatures, but also compensates for the loss of performance associated with the lower propellant temperatures by introducing additional chemical energy to the combustion process. Results exhibited comparable, if not superior, performance as compared to those obtained with the same thruster fired at normal operating temperatures (~22 °C) using MON-3 and MMH.

2 TEST PROGRAM

2.1 Test Article

The test article used in this investigation was the Kaiser Marquardt Model R-53 8.9-N bipropellant thruster shown in Figure 1. The thruster consists of three primary components, the control valve, the propellant injector, and the chamber-nozzle assembly. The engine control valve is a Moog torque-motor bipropellant type designed to simultaneously control the flow of both oxidizer and fuel. The injector consists of a single unlike-doublet with two separate injection ports for fuel-film cooling of the combustion chamber wall. The portion of fuel used for fuel-film cooling was, by design, to be 30% of the total flow. As a result of manufacturing difficulties, however, the cooling fuel was only

20% of the total flow, which resulted in significantly higher chamber temperatures during hot firing. The single unlike-doublet is a pair of injection ports designed to impinge a stream of oxidizer with a stream of fuel inside the combustion chamber and very near the external face of the injector (see schematic shown in Figure 2). The chamber-nozzle assembly consists of a single piece of forged C-103 columbium (niobium) alloy with a silicide coating to prevent oxidation. In these tests, the chamber was operated at temperatures of up to 1500 °C for a total of nearly 10,000 seconds.

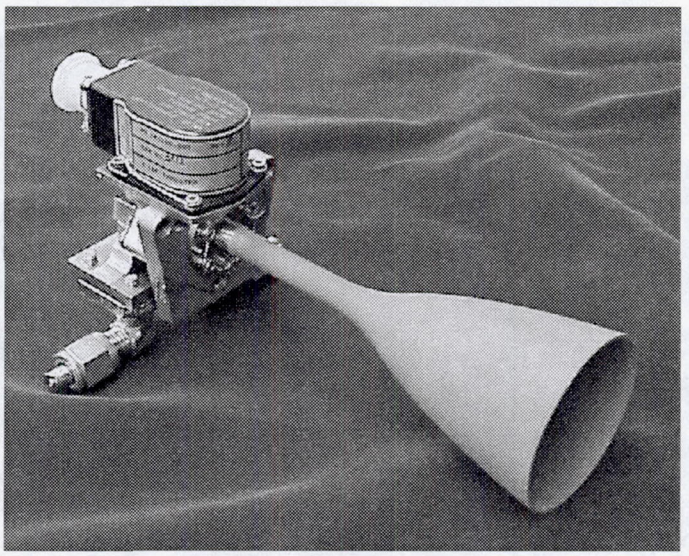

Figure 1 Kaiser Marquardt Model R-53 8.9-N bipropellant thruster

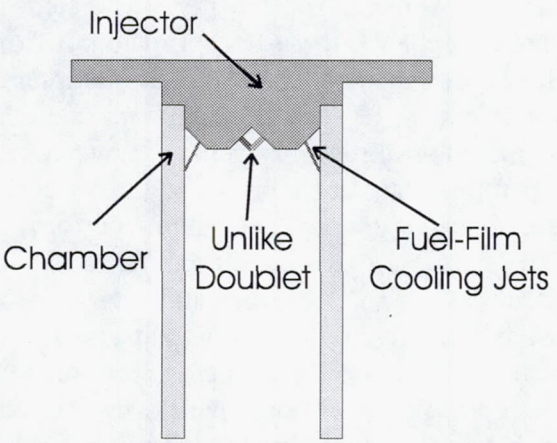

Figure 2 R-53 propellant injection and fuel-film cooling scheme.

2.2 Test Facilities

All testing was conducted in Cell 9 of the Kaiser Marquardt Rocket Test Facility located in Van Nuys, California and shown in Figure 3. The Cell 9 Rocket Test Facility includes a small thrust stand (see Figure 4) located within a very large vacuum sphere (see Figure 3). The vacuum sphere may be evacuated using a large steam ejection system or a series of Stokes pumps and Roots blowers shown in Figure 5. The facility is fully automated and operated from a remote data acquisition and control center shown in Figure 6. Data acquisition was performed using a National Instruments SCXI signal conditioning system controlled by an Intel Pentium II 500 MHz computer having 1 gigabyte of RAM,

an 18 gigabyte hard drive, a 53-cm monitor, and a CD-ROM writer. The MON-25 propellant was produced on-site and analyzed in the Kaiser Marquardt chemistry lab.

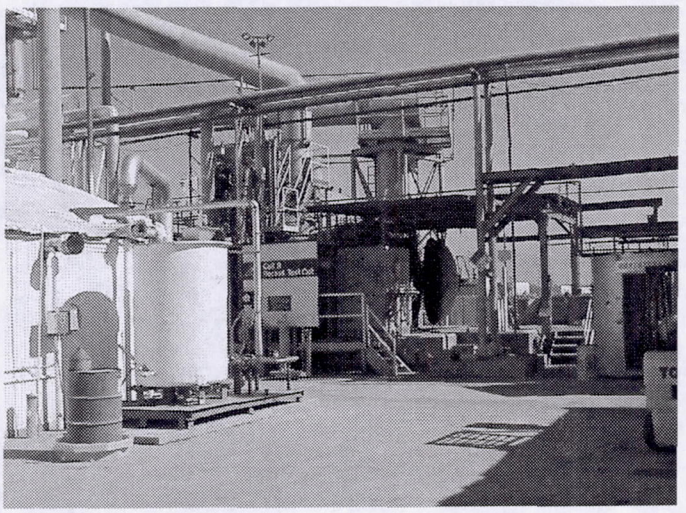

Figure 3 Kaiser Marquardt Cell 9 rocket test facility.

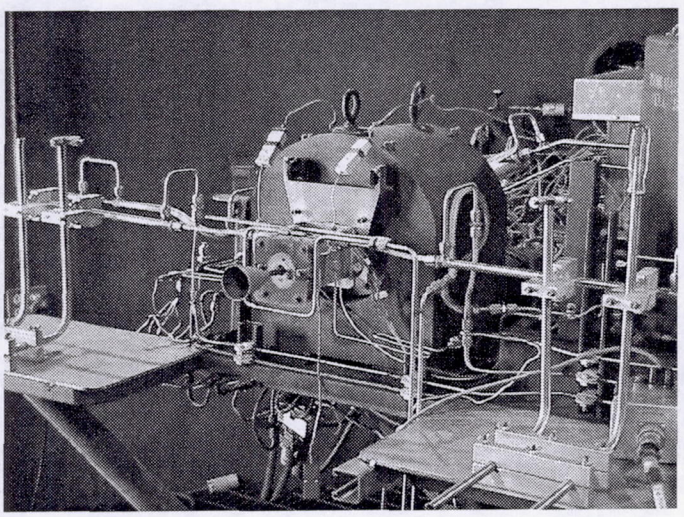

Figure 4 R-53 thruster mounted on Cell 9 small rocket thrust stand.

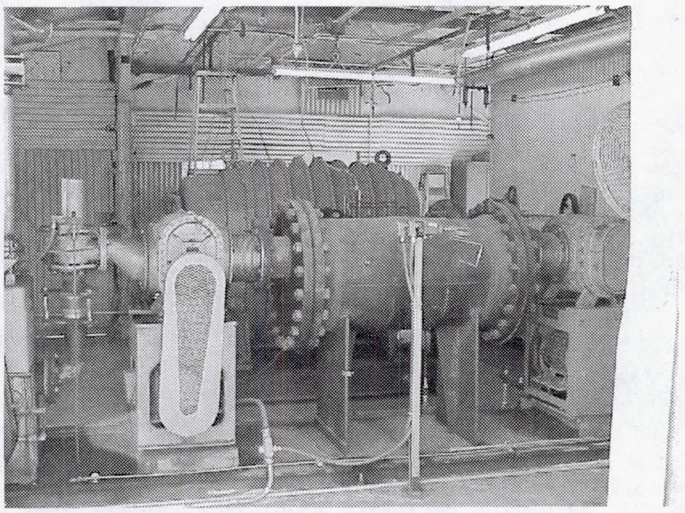

Figure 5 Roots blowers and Stokes pumps for cell evacuation.

Figure 6 Cell 9 data acquisition and facility control center.

2.3 Facility Modifications

To accommodate testing of the Model R-53 8.9-N thruster at –40 °C, it was necessary to modify the existing propellant conditioning system and to make provisions for thermal conditioning of the thruster hardware. Normally, propellants are conditioned using an Environmental Industries (EI) Model ME2110 refrigeration system. This system, however, is only capable of conditioning propellants to –7 °C. Therefore, a Government-supplied thermal conditioning system consisting of two FTS Model RC10B0, shown in Figure 7, was used in conjunction with the existing system. This combination system enabled conditioning of the propellants to temperatures below –46 °C.

Conditioning of the propellants was achieved using a system of co-annular plumbing, where the propellants were passed through an interior passage encased in an outer tube of flowing refrigerant. This system of co-annular plumbing began at the main propellant run tanks, extended to the engine valve inlets, and was interrupted only by those transition joints and valves where the system could not be practically implemented. Conditioning was divided into two stages. The first stage utilized the

normal EI refrigeration system with ethylene glycol as the refrigerant and the second stage utilized the FTS refrigeration system with a silicon-based refrigerant. The first stage conditioned the propellants in the storage tanks and in the lines up to the cell vacuum sphere. The second stage conditioned the propellants from just inside the cell wall up to the engine inlets. The first stage temperature was controlled at –7 °C, while the second stage temperature was set at the desired run temperature of down to –40 °C.

To provide a stable propellant temperature throughout the duration of hot firings, lasting up to 20 minutes, one-gallon, chilled accumulator tanks were installed serially in-line with the propellant supply lines. These tanks were located inside the cell vacuum sphere and controlled with the second-stage thermal conditioning system. This arrangement provided a buffer between the propellant chilled to the desired run temperature and the higher-temperature propellant entering from outside the cell vacuum sphere.

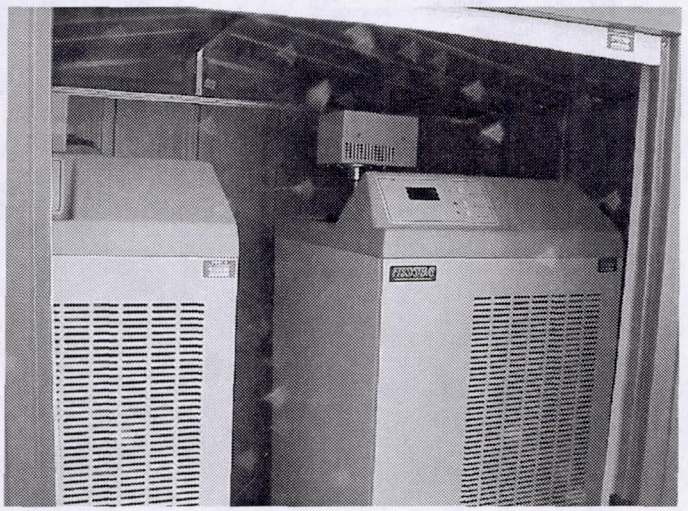

Figure 7 FTS Model RC10B0 refrigeration units in protective shed.

The engine hardware was conditioned to –40 °C on the thrust stand through the use of a nitrogen gas purge. Liquid nitrogen was circulated through a reservoir, which contained a helical heat exchanger tube through which gaseous nitrogen was passed. The cold gaseous nitrogen was introduced to the engine hardware through a system of normal impingement jets shown in Figure 8. A ring containing several jet orifices cooled the engine valve, injector, and chamber. A bar, also containing several jet orifices, cooled the engine inlets and the short sections of unconditioned, flexible propellant lines. Figure 9 shows a schematic of the entire setup including the propellant and engine hardware conditioning systems.

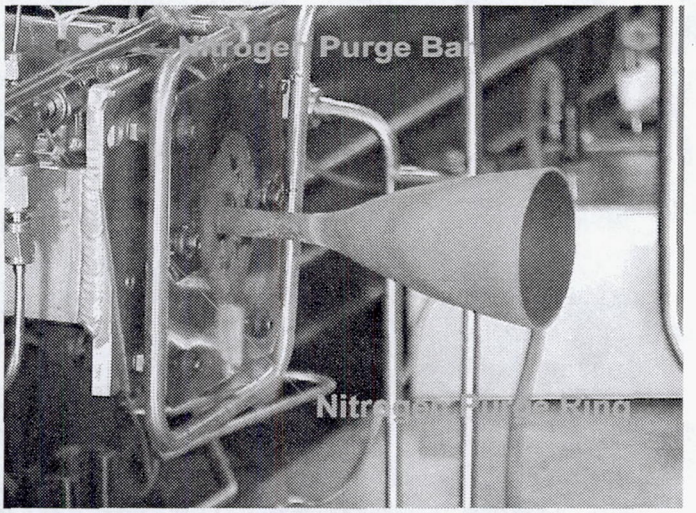

Figure 8 Nitrogen purges for engine thermal conditioning.

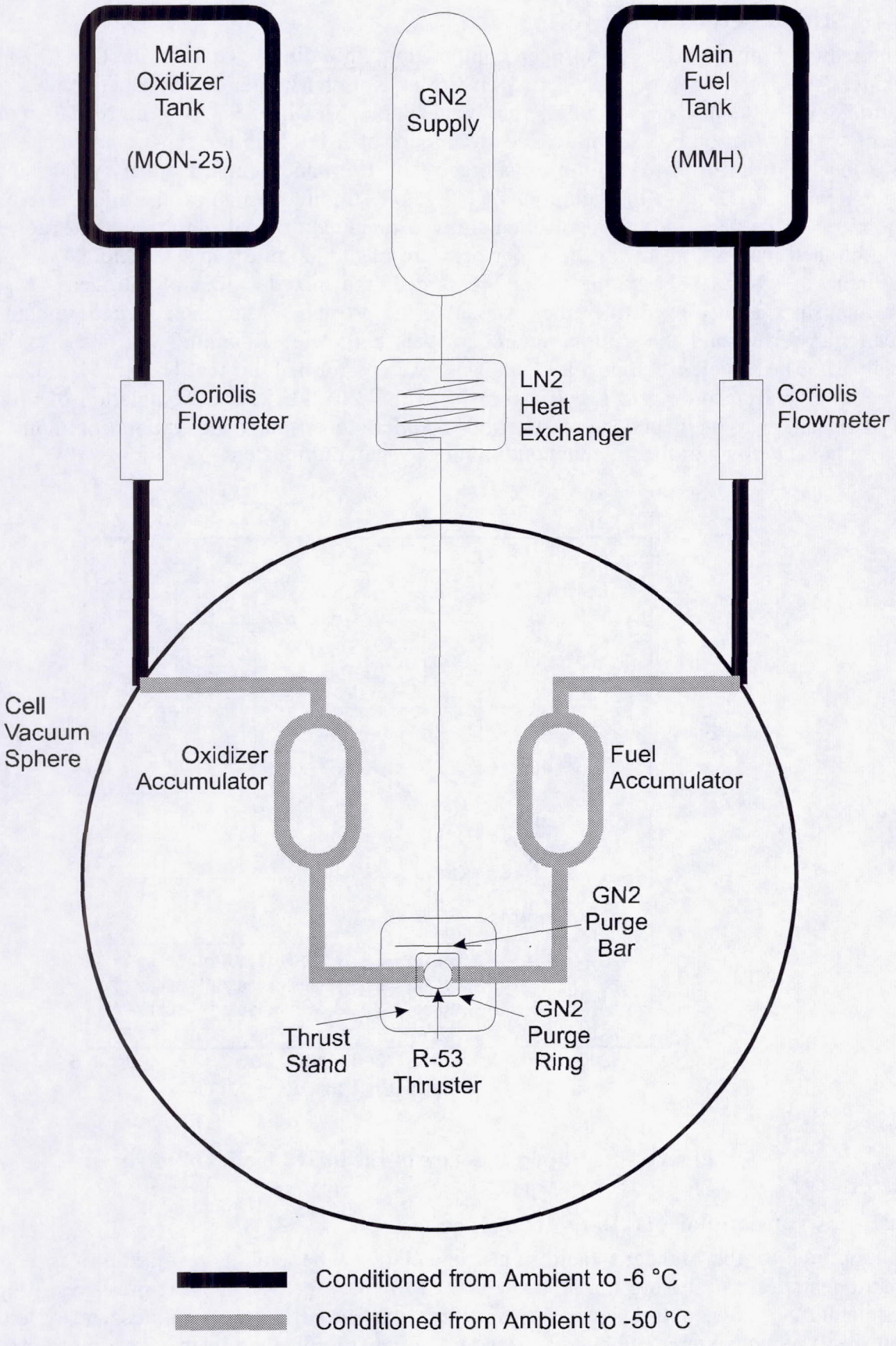

Figure 9 Facility Flow Schematic for Mars Flyer Testing

2.4 MON-25 Production

The required mixed oxides of nitrogen composition, 75% dinitrogen tetroxide (N_2O_4) and 25% nitric oxide (NO) by weight, was produced on-site at Kaiser Marquardt. Production was achieved by introducing gaseous NO to commercially available MON-3 (3% NO in N_2O_4) in a controlled reaction. Production began with a known amount of MON-3 in the run-storage tank. Nitric oxide was then allowed to flow into the run-storage tank from an external storage cylinder mounted on a weight balance. Because the saturation of NO into N_2O_4 involves an exothermic reaction, the flow of the nitric oxide was carefully controlled so as to preclude thermal run-away. The storage tank was conditioned to –7 °C to lower the vapor pressure of the mixture and to accelerate the process. For reference, Figure 10 shows the vapor pressure of the mixed oxides of nitrogen. A tank stirring mechanism was also used to further accelerate the process. After the required amount of NO had been transferred and the saturation process was complete, a sample was taken for composition analysis. The species composition analysis was performed in the Kaiser Marquardt chemistry laboratory and according to specification MIL-PRF-26539E. After completion of production, the storage tank was held under pressure (> 700 kPa) to ensure composition continuity. This also permitted shutdown of the thermal conditioning system during storage.

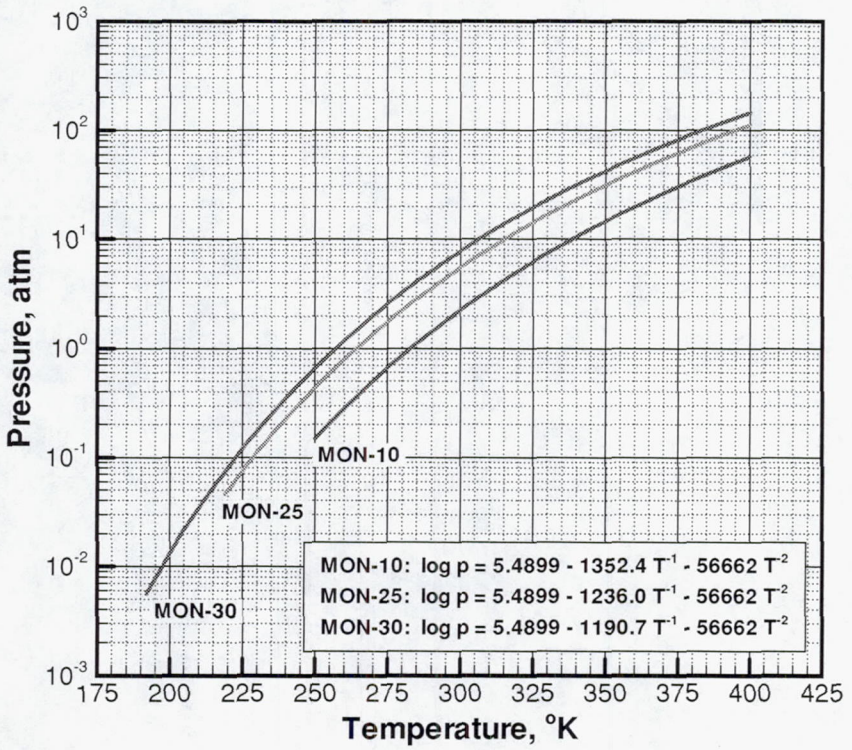

Figure 10 Vapor pressure of the mixed oxides of nitrogen.

2.5 Instrumentation and Data Acquisition

In addition to the standard facility instrumentation, the engine test setup was equipped with instrumentation to measure thrust, propellant flow rates, propellant inlet pressures, propellant inlet temperatures, valve control signal characteristics, various engine temperatures, and system vibrations. All measurements were calibrated in standard (English) units and later converted to metric (System International) units. Table 1 shows a summary of the engine test setup-specific instrumentation along

with the ranges of interest. Figure 11 shows the locations of all engine thermocouples. Data acquisition was performed using a National Instruments SCXI signal conditioning system controlled by an Intel Pentium II 500 MHz computer having 1 gigabyte of RAM, an 18 gigabyte hard drive, a 53-cm monitor, and a CD-ROM writer.

Table 1 Engine Test Setup-Specific Instrumentation

MEASUREMENT	ACRONYM	UNITS	MIN	MAX	CUT
Fuel Flow Rate	WFU	lbm/sec	0.002	0.01	
Oxidizer Flow Rate	WOX	lbm/sec	0.002	0.01	
Thrust	FT	lbf	0	5	
Fuel Inlet Manifold Pressure	PMF	psia	0	300	
Oxidizer Inlet Manifold Pressure	PMO	psia	0	300	
Cell Pressure	PCELL	psia	0	1.0	
Valve Voltage	VV	volts	0	50	
Valve Current	VI	amps	0	1	
Fuel Inlet Manifold Temperature	TMF	°F	-60	120	
Oxidizer Inlet Manifold Temperature	TMO	°F	-60	120	
Chamber Temperature	TCH	°F	1500	3000	2800 max
Injector/Chamber Temperature	TC1	°F	-60	1000	800 max
Injector/Chamber Temperature	TC2	°F	-60	1000	800 max
Valve Temperature - Fuel Side	TVF	°F	-60	500	250 max
Valve Temperature - Oxidizer Side	TVO	°F	-60	500	250 max
Flange Temperature	TF1	°F	-60	1000	250 max
Flange Temperature	TF2	°F	-60	1000	250 max
Accelerometer	ACC1	g	-100	+100	

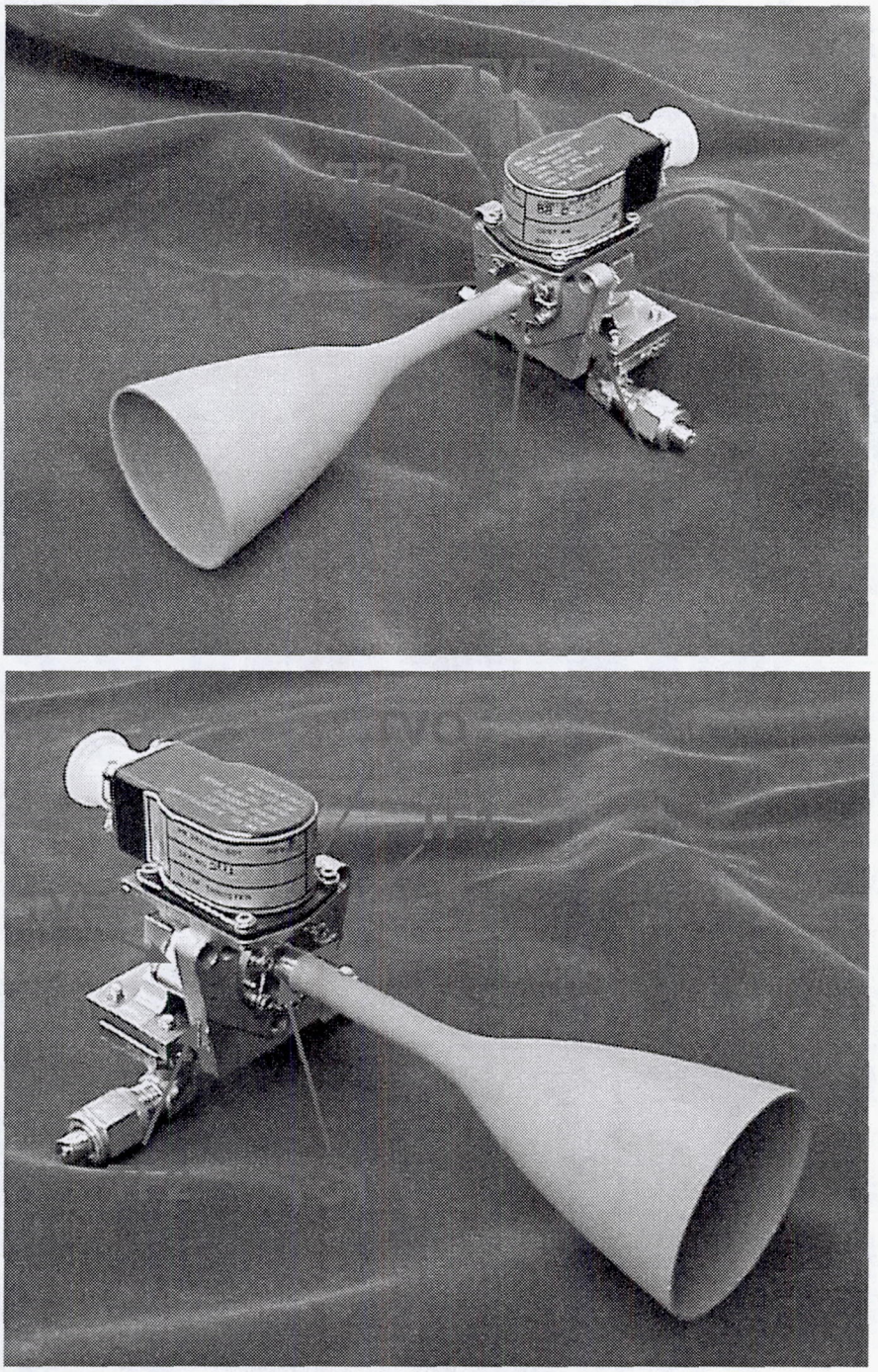

Figure 11 Engine thermocouple locations.

3 RESULTS AND DISCUSSION

The thruster was tested with propellant inlet pressures ranging from 723 to 2315 kPa, yielding vacuum thrust levels of 4.5 to 10.6 N with mixture ratios from 1.6 to 2.7. Table 2 shows a summary of the tests performed.

Table 2 Actual Test Matrix Performed

RUN	p_{mo}	p_{mf}	t_{ON}	t_{OFF}	PULSES	t_{prop}	p_{cell}
	kPa	kPa	sec	sec		°C	kPa
688	1571	1565	10	---	1	-40	< 0.15
689	1570	1555	10	---	1	-40	< 0.15
690	1567	1586	10	---	1	-40	< 0.15
691	1566	1658	10	---	1	-40	< 0.15
692	1564	1795	10	---	1	-40	< 0.15
693	1543	1836	10	---	1	-40	< 0.15
694	1549	1828	10	---	1	-40	< 0.15
695	1550	1904	10	---	1	-40	< 0.15
696	1576	2022	10	---	1	-40	< 0.15
697	1522	2076	10	---	1	-40	< 0.15
698	1479	2108	10	---	1	-40	< 0.15
699	1447	2134	10	---	1	-40	< 0.15
700	1449	2177	10	---	1	-40	< 0.15
701	1621	1766	10	---	1	-40	< 0.15
702	1657	1729	10	---	1	-40	< 0.15
703	1657	1693	10	---	1	-40	< 0.15
704	1657	1624	10	---	1	-40	< 0.15
705	1695	1559	10	---	1	-40	< 0.15
706	1727	1591	10	---	1	-40	< 0.15
707	1824	1629	10	---	1	-40	< 0.15
708	1553	1835	10	---	1	-40	< 0.15
709	1696	1971	10	---	1	-40	< 0.15
710	1861	2108	10	---	1	-40	< 0.15
711	1967	2248	10	---	1	-40	< 0.15
713	2028	2315	10	---	1	-40	< 0.15
714	1407	1697	10	---	1	-40	< 0.15
715	1306	1555	10	---	1	-40	< 0.15
716	1202	1416	10	---	1	-40	< 0.15
717	1072	1278	10	---	1	-40	< 0.15
718	929	1105	10	---	1	-40	< 0.15
719	792	963	10	---	1	-40	< 0.15
720	723	848	10	---	1	-40	< 0.15
721	1551	1831	10	---	1	-40	< 0.15
722	1544	1828	300	---	1	-40	< 0.15
726	1564	1839	10	---	1	-7	< 0.15
727	1555	1831	10	---	1	-7	< 0.15
728	1607	1758	10	---	1	-7	< 0.15
729	1556	1836	10	---	1	-18	< 0.15
730	1553	1827	10	---	1	-18	< 0.15
733	1566	1838	10	---	1	-18	< 0.15
735	1552	1835	0.1	0.1	20	-40	< 0.15
736	1551	1828	0.1	0.1	20	-40	< 0.15
737	1551	1825	0.1	0.1	20	-40	< 0.15
739	1551	1827	1200	---	1	-40	< 0.15
740	1551	1827	1200	---	1	-40	< 0.15
741	1547	1826	60	---	1	-40	1.5
742	1551	1827	1200	---	1	-40	< 0.15
743	1519	1853	1200	---	1	-40	< 0.15
744	1528	1827	600	---	1	-40	< 0.15
745	1520	1819	600	---	1	-40	< 0.15
746	1533	1820	600	---	1	-40	< 0.15
747	1536	1820	300	---	1	-40	< 0.15
748	1540	1826	300	---	1	-40	< 0.15
749	1530	1828	300	---	1	-40	< 0.15
750	1551	1827	300	---	1	-40	< 0.15

Initial tests were performed to ascertain the propellant inlet pressure producing a vacuum thrust level, F_{vac}, of 8.9 N and an oxidizer-to-fuel mixture ratio, O/F, of 2.1. The engine was designed to produce these nominal values for equal inlet pressures of 1517 kPa. Improper propellant-flow trim orifices, however, required oxidizer and fuel inlet pressures of 1551 and 1827 kPa, respectively, to produce the nominal performance.

Measurements included thrust, propellant flow rates, propellant inlet pressures and temperatures, engine temperatures, system vibrations, and valve control-signal characteristics. Data obtained from testing were analyzed to determine engine performance characteristics such as ignition delay, specific impulse, I_{sp}, versus oxidizer-to-mixture ratio, O/F, I_{sp} versus thrust, F, and the vibration frequency spectrum. In each firing, 1 second of pre-fire data was taken to obtain an accurate pre-run thrust tare and to ensure that all instrumentation was operating properly prior to firing. In each case, 10 seconds of data was taken after the hot firing to obtain a post-run thrust tare and to observe thermal soak back trends.

The total firing time for the matrix described in Table 2 is nearly 8600 seconds. Although the amount of fuel-film cooling was much less than the design value, resulting in very high chamber temperatures, the engine did survive the entire test matrix. In fact, an additional 2400 seconds of firing time were put on the engine to dispose of the excess propellants. Record of these final runs was not possible, because the remaining propellant was downstream of the flow meters.

3.1 Ignition Characteristics

Ignition delay was measured as the time between control signal "ON" and the first instance of measurable thrust minus the valve response time. Figure 12 shows the ignition delay plotted versus vacuum thrust level for a constant mixture ratio of 2.1±0.05. As the thrust level was decreased from approximately 10.6 N to 4.5 N, the ignition delay increased from 7.5 ms to 11.5 ms. Ignition delay versus mixture ratio, on the other hand, displayed no significant trend. Overall, ignition delay is very similar to that exhibited by the same thruster fired at normal operating temperatures (~22 °C) using MON-3 and MMH.

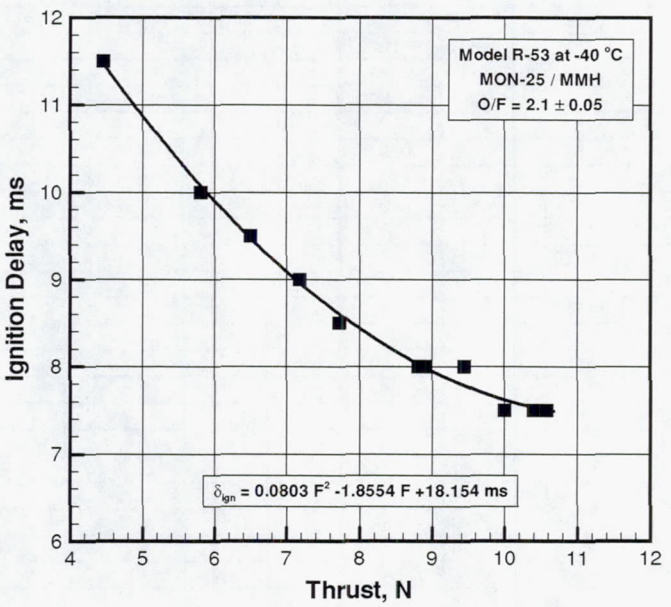

Figure 12 Ignition delay versus thrust.

At low thrust levels, roughly less than 6 N, the startup process exhibited a two-stage behavior. Immediately after ignition, the engine produced very little thrust, less than 1 N, for about 10 ms after which, the thrust abruptly reached its full steady state value. This delay in full combustion results in an accumulation of propellants followed by a detonation and a momentary spike in chamber pressure and thrust. The engine, however, was not damaged as a result of this phenomena.

3.2 Performance Mapping

Thirty-three 10-second hot firings were made at various thrust levels and mixture ratios to map the domain of performance for a range of inlet pressure with the engine and propellants conditioned to –40 °C. Initially, several trim runs were made to identify the nominal inlet pressures yielding an oxidizer-to-fuel mixture ratio, O/F, of 2.1 at a vacuum thrust level, F_{vac}, of 8.9 N. The nominal inlet pressures, p_{mo} and p_{mf}, were determined to be 1550 and 1830 kPa, respectively. Excursions from the nominal inlet pressures were such that, either the thrust was held constant at nominal while varying the mixture ratio or, *vice versa*. Performance data shown in the following plots and listed in Table 4 of the Appendix are averaged over the next-to-last second of each run.

Figure 13 shows a typical thrust trace for a 10-second hot firing. The thrust trace shown in Figure 13 was passed through a digital band-reject filter designed to eliminate both 60-Hz noise and thrust-stand ringing which would otherwise obfuscate the true engine thrust response. Figure 14 shows the power spectral density of the raw, unfiltered thrust signal, clearly identifying the 160-Hz natural frequency of the thrust-stand load cell and the 60-Hz line interference.

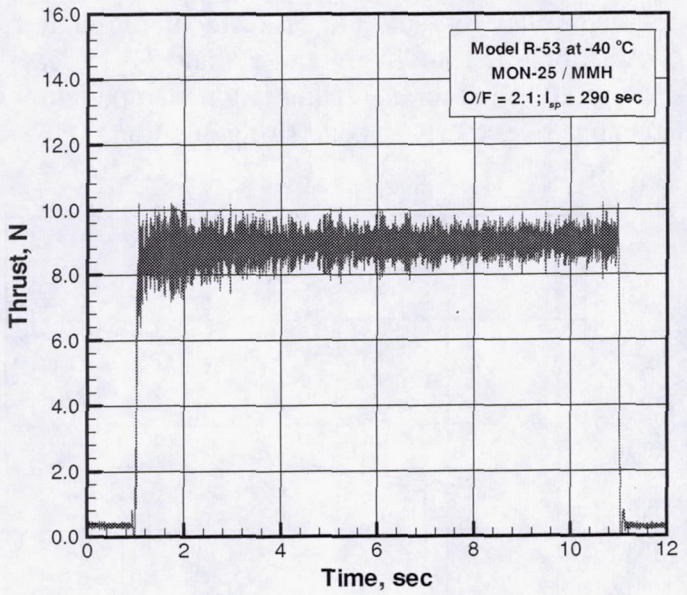

Figure 13 Typical filtered thrust trace for a 10-second run (Run #693).

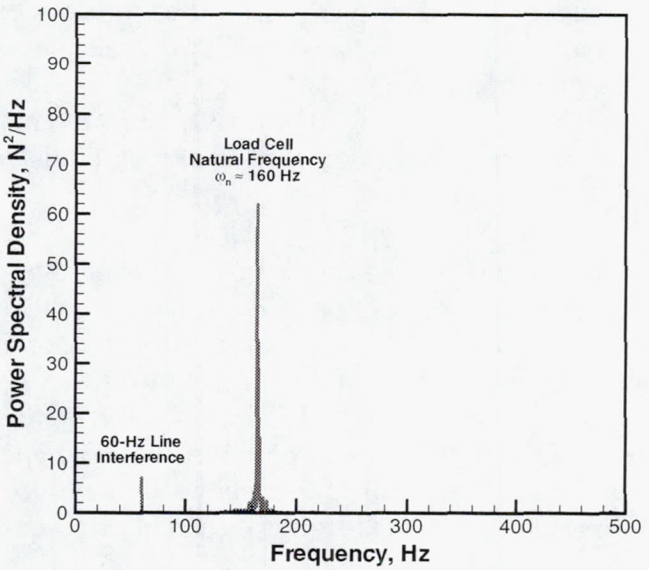

Figure 14 Typical power spectral density versus frequency of a raw thrust signal.

Figure 15 shows traces of the chamber and the injector-chamber interface temperatures, T_{ch}, and T_{c1} and T_{c2}, respectively. During hot fire, the chamber temperature increases monotonically and reaches a maximum of 1360 °C. Immediately after engine shutdown, T_{ch} decreases exponentially. Chamber temperatures below 900 °C could not be ascertained using the optical pyrometer and are, therefore, not plotted. Both injector-chamber interface temperatures increase very quickly over the first two seconds of hot firing then roll over and increase slowly throughout the entire run, reaching a maximum of 160 °C. After engine shutdown, both T_{c1} and T_{c2} increase and reach a maximum soak-back temperature of 290 °C after 7 seconds. Other engine temperature were not plotted because they showed no significant change over the 10-second firing duration.

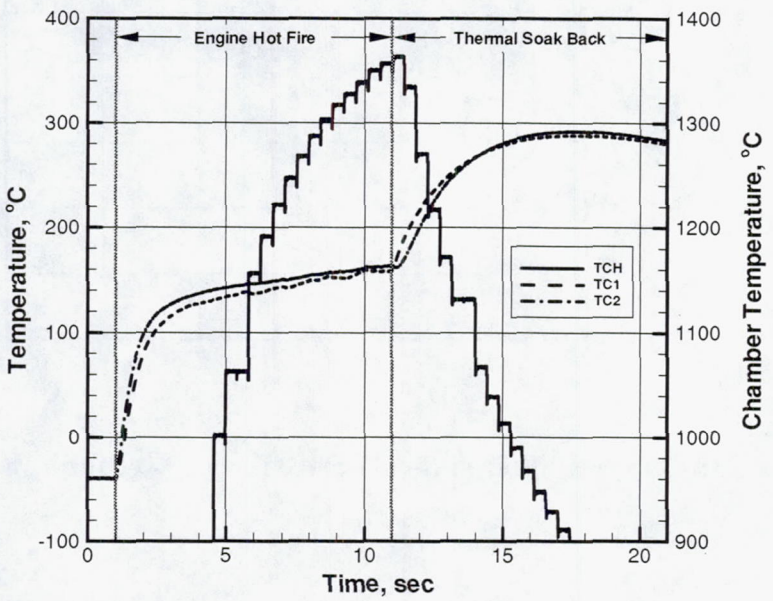

Figure 15 Typical thermal characteristics of a 10-sec hot fire; F = 8.9N, O/F = 2.2.

Figure 16 shows a plot of C^* efficiency versus vacuum thrust level for a constant mixture ratio of 2.1±0.05. The C^* efficiency is defined as the ratio of actual-to-theoretical characteristic velocities.

$$\eta_{C^*} = \frac{C^*_{actual}}{C^*_{theoretical}} \tag{1}$$

The C^* efficiency increased with thrust from 80.5% at 4.23 N to 93.0% at 10.2 N. For thrust levels above 8.5 N, the C^* efficiency appears to be relatively constant, however, it drops off sharply for thrust levels of less the 7 N. The empirical data was used to develop the following analytical curve fit for η_{C^*} as a function of thrust at an O/F of 2.1:

$$\eta_{C^*} = 0.0007630F^3 - 0.02205F^2 + 0.2150F + 0.2187; \quad 4.2\,\text{N} < F < 10.2\,\text{N}; \quad O/F = 2.1 \tag{2}$$

A chemical equilibrium computer code was used to determine the theoretical C^* values. The actual C^* values were calculated based on measured vacuum specific impulse, $I_{sp,vac}$, calculated thrust coefficient, and an assumed nozzle efficiency of 97%. The thrust coefficient along with the corresponding chamber pressure was determined iteratively using a chemical equilibrium and nozzle expansion code.

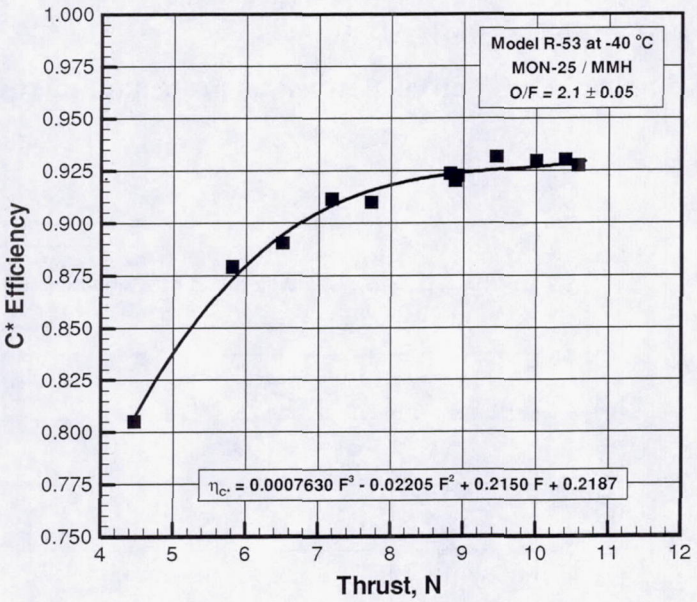

Figure 16 C* efficiency versus thrust.

Figure 17 shows C* efficiency as a function of the oxidizer-to-fuel mixture ratio, O/F, for a constant vacuum thrust level of 8.9±0.22 N. As the mixture ratio is increased, the C* efficiency initially increases from 92.6% at 1.61 to a maximum recorded value of 93.3% at 1.99 after which it decreases to 87.1% at 2.75. The experimental data was used to construct the following analytical curve fit for a thrust level of 8.9 N:

$$\eta_{C^*} = -0.0755(O/F)^2 + 0.2827(O/F) + 0.6629; \quad 1.61 < O/F < 2.75; \quad F = 8.9\text{N} \tag{3}$$

Using Eq. 3, the optimal mixture ratio is 1.87 producing an η_{C^*} of 92.8%, however, additional data is necessary to validate these values of regression analysis since the actual data show a maximum closer to 2.0.

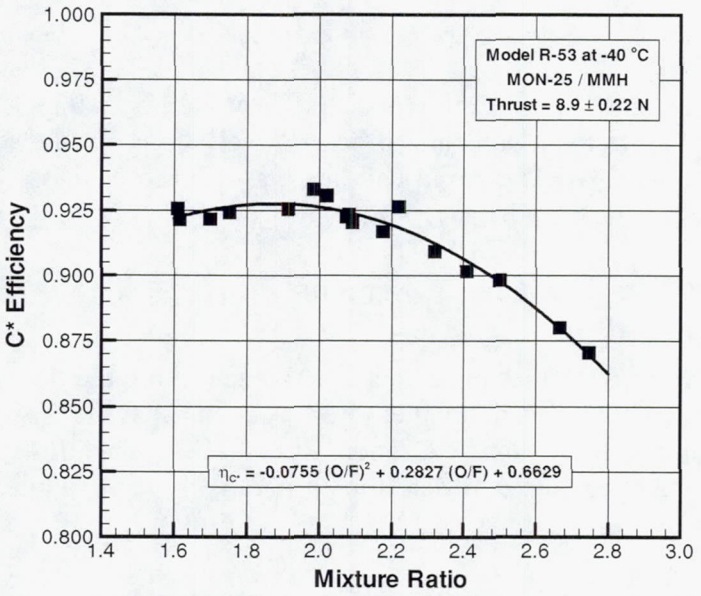

Figure 17 C* efficiency versus propellant mixture ratio.

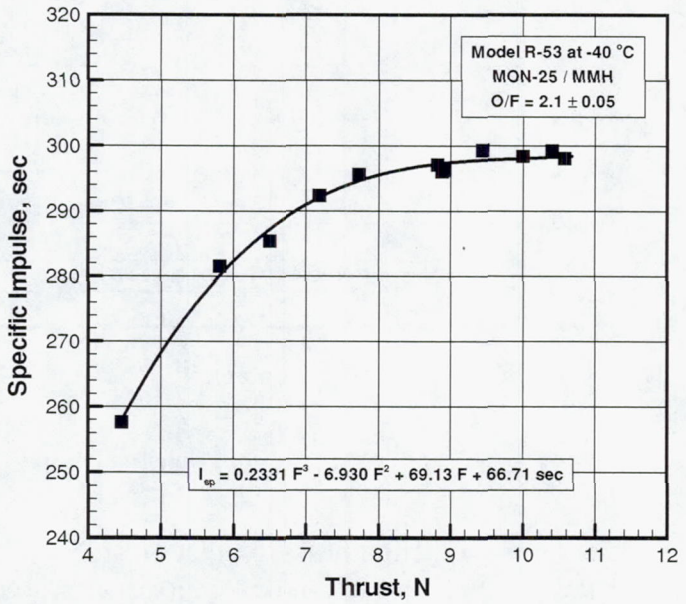

Figure 18 Specific impulse versus thrust.

Figure 18 shows a plot of vacuum specific impulse versus vacuum thrust for a constant mixture ratio of 2.1±0.05. Because the thrust coefficient is nearly constant at 1.84, the specific impulse is directly

proportional to the C^* efficiency and therefore shows the same trends. That is, as thrust increases, specific impulse also increases over the range tested. At 4.46 N of vacuum thrust, the measured I_{sp} was 257.6 sec, while at 10.58 N the I_{sp} was 298.1 sec. For thrust levels above 8.5 N, the specific impulse appears to be relatively constant, however, it drops off sharply for thrust levels of less the 7 N. The empirical data was used to construct the following analytical curve fit for an O/F of 2.1:

$$I_{sp} = 0.2331F^3 - 6.930F^2 + 69.13F + 66.71\,(\text{sec}); \quad 4.2\,\text{N} < F < 10.2\,\text{N}; \quad O/F = 2.1 \qquad (4)$$

Figure 19 shows a plot of vacuum specific impulse as a function of the oxidizer-to-fuel mixture ratio, O/F, for a constant vacuum thrust level of 8.9±0.22 N. Again, because the thrust coefficient is nearly constant at 1.84, the specific impulse is directly proportional to the C^* efficiency and therefore shows the same trends. As the mixture ratio is increased, $I_{sp,vac}$ initially increases from 294.1 sec at 1.61 to a maximum recorded value of 300.7 sec at 1.99 after which it decreases to 271.1 sec at 2.75. The experimental data was used to construct the following analytical curve fit for a thrust level of 8.9 N:

$$I_{sp} = -41.559(O/F)^2 + 160.58(O/F) + 142.84\,(\text{sec}); \quad 1.61 < O/F < 2.75; \quad F = 8.9\text{N} \qquad (5)$$

Using Eq. 3, the optimal mixture ratio is 1.93 producing an I_{sp} of 298.0, however, additional data is necessary to validate these values of regression analysis since the actual data show a maximum closer to 2.0.

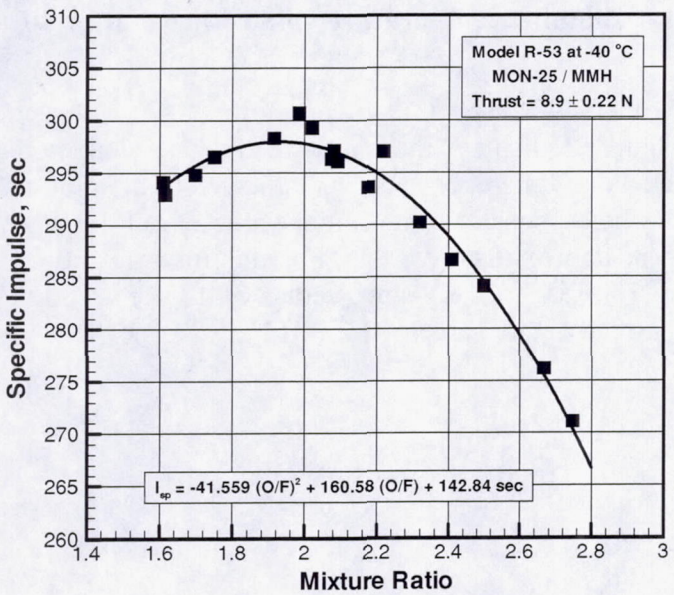

Figure 19 Specific impulse versus propellant mixture ratio.

Figure 20 shows as plot of chamber temperature averaged over the next-to-last second of each ten-second run versus vacuum thrust for a constant mixture ratio of 2.1±0.05. As thrust was increased from 4.46 N to 10.58 N, the chamber temperature increased from 993 °C to 1751 °C. This was to be expected as both the combustion efficiency and amount of total energy increase with thrust over the range of inlet pressures tested. The empirical data was used to construct the following analytical curve fit for an O/F of 2.1:

$$T_{ch} = -11.545F^2 + 297.7F - 105.7\ (\mathrm{K}); \quad 4.2\ \mathrm{N} < F < 10.2\ \mathrm{N};\ O/F = 2.1 \tag{4}$$

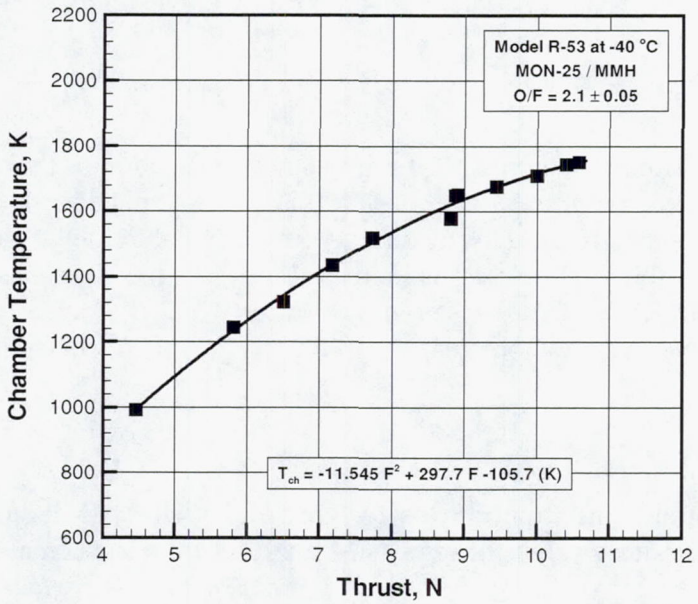

Figure 20 Chamber temperature versus thrust after 10 seconds of hot fire.

3.3 Steady-State Characteristics

The plot shown in Figure 21 displays the quasi-steady-state characteristics of the Model R-53. The term quasi-steady-state is used here, because, as indicated in the plot, the mixture ratio decreases with time and could not be held constant at its initial value of 2.1. The *O/F* does eventually, however, reach a steady value of approximately 1.82. For this mixture ratio, the injector-chamber interface temperatures, T_{c1} and T_{c2}, reach steady-state values of 145 and 180 °C, respectively. The chamber temperature reaches a steady-state value of 1420 °C.

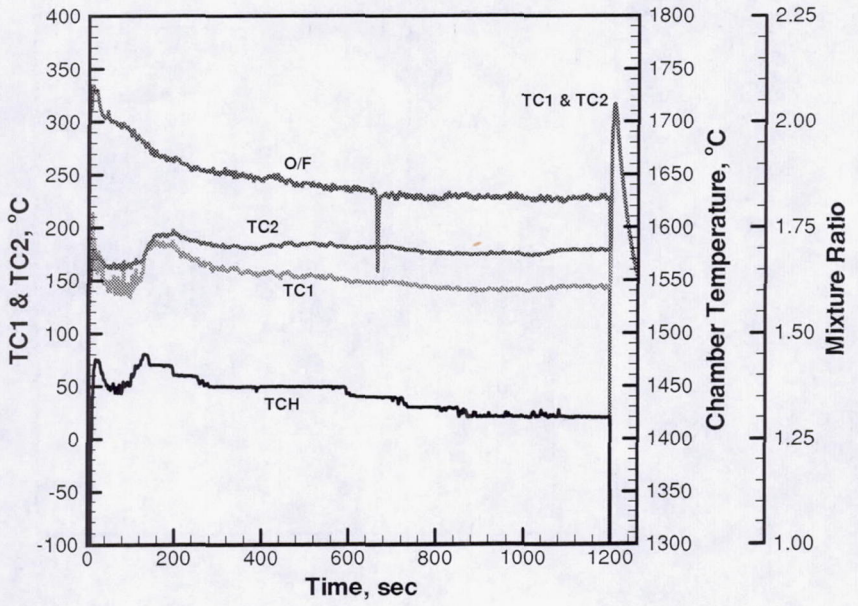

Figure 21 Quasi-steady-state thermal characteristics for a long-duration burn.

Figure 22 shows various temperature traces of the engine control valve and propellants for the same 1200-second burn shown in Figure 21. Note that the engine valve temperatures do not achieve steady state even after a 1200-sec burn. After 1200 seconds, the valve flange temperatures, T_{f1} and T_{f2}, are approximately 0 °C and the valve body temperatures, T_{vo} and T_{vf}, are approximately –12 °C. The propellant manifold temperatures, T_{mo} and T_{mf}, are shown for reference. It was not possible to maintain T_{mo} and T_{mf} at –40 °C for the entire duration of the run.

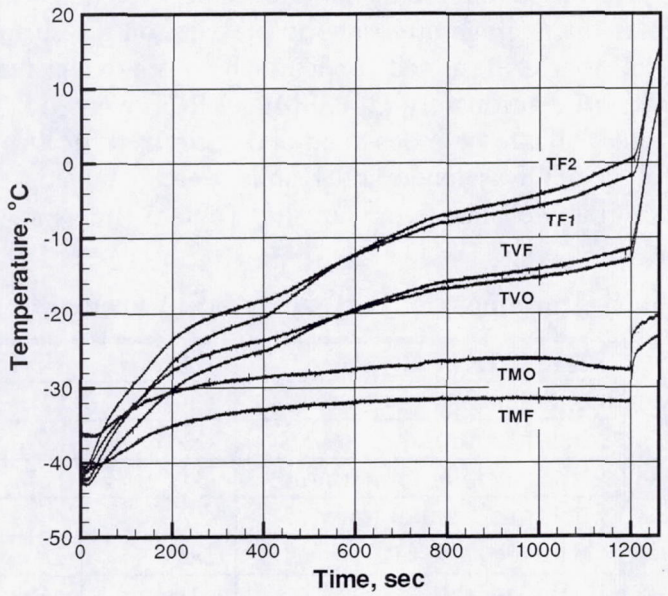

Figure 22 Engine control valve and manifold temperatures for a long-duration burn.

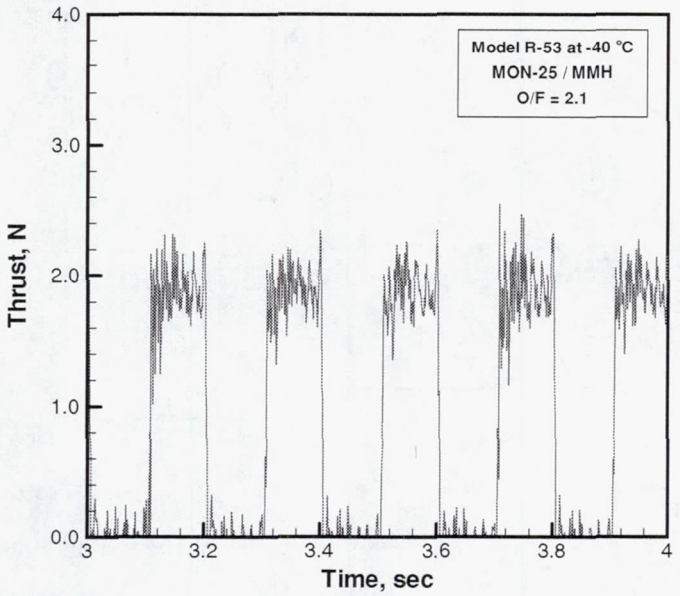

Figure 23 Several pulses from series of 20 with 50% duty cycle and a 0.2-sec period

3.4 Pulsing Performance

Figure 23 shows several typical pulses from a series of 20 with a 50% duty cycle and a 200-ms period (t_{on}/t_{off} = 0.1/0.1 seconds). After 20 pulses, the vacuum impulse bit reaches an average value of 0.22 N-s.

3.5 Performance at 1.4-kPa Cell Pressure

Although the engine was designed to operate in a vacuum environment, a single run was made to ascertain the performance of the engine at nominal inlet pressures with a cell pressure of 1.4 kPa. The idea was to simulate the average atmospheric pressure on the surface of Mars. It was expected that the flow inside the nozzle, designed for a much lower exhaust pressure, would separate and performance would drop off significantly. If the Model R-53 were to be flown within the atmosphere of Mars, the nozzle would have to be redesigned and optimized for the 1.5-kPa ambient pressure. In any event, a sixty-second run was made and results were obtained. Video recordings did indeed show nozzle flow separation well inside the nozzle. Table 3 shows a summary of the averages over the last second of the run.

Table 3 Summary of Performance at Elevated Cell Pressure

PARAMETER	VALUE	UNITS
Oxidizer inlet pressure	1547	kPa
Fuel inlet pressure	1826	kPa
Oxidizer inlet temperature	-31	°C
Fuel inlet temperature	-37	°C
Oxidizer flow rate	2.07	g/sec
Fuel flow rate	1.085	g/sec
Mixture ratio	1.9	
Thrust	7.7	N

Specific impulse	249.0	sec
Cell pressure	1.5	kPa
Chamber temperature	1443	°C

3.6 Vibration Characteristics

An accelerometer was attached to the back of the engine control valve to ascertain the system vibration characteristics. Figure 24 shows a typical accelerometer trace for the first 20.48 ms of a nominal 10-sec hot firing. The accelerometer had an accurate response range of up to 50,000 Hz with a resonant frequency of nearly 90,000 Hz. The data was sampled at 200,000 Hz using an IOTech high-speed data acquisition system. The highest-amplitude vibrations were experienced during the first 2 ms of startup after which the vibration was significantly reduced. There are momentary increases in the vibration amplitude, but they rarely exceed ±10 g.

Figure 25 shows the power spectral density versus frequency obtained from the accelerometer response trace shown in Figure 24.

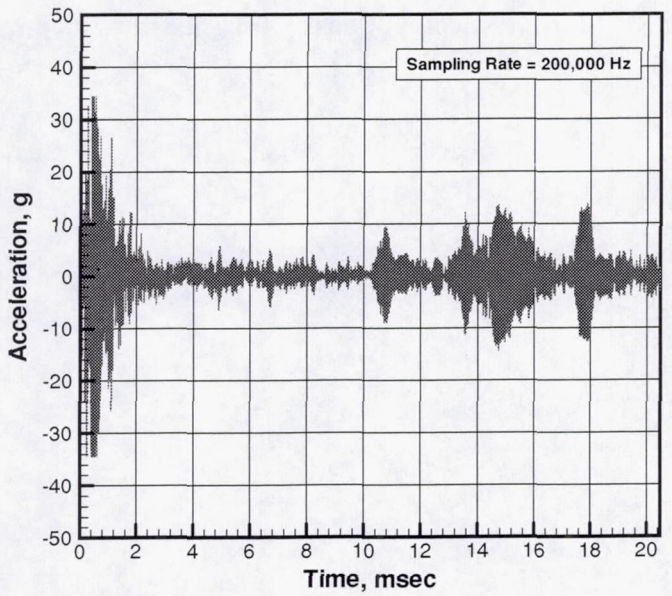

Figure 24 Accelerometer trace during first 20.48 ms of hot fire.

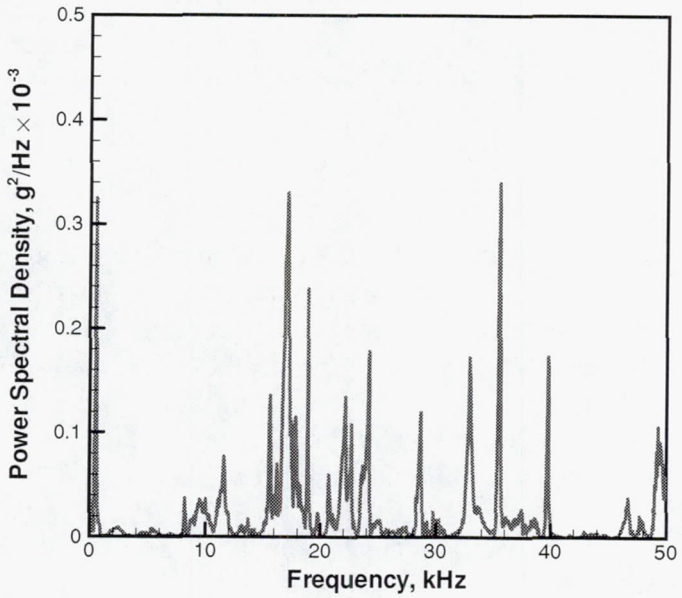

Figure 25 Power spectral density for the first 20.48 msec of hot fire.

4 NEW TECHNOLOGY

While no new technologies were developed within the scope of this effort, the technology demonstrated may be applied to other missions besides the Mars Flyer program. Test results show great promise for any power-limited space application where thermal management of the propulsion system may be restricted or even eliminated. Such missions include interplanetary travel, planetary descent and ascent, and intra-atmospheric planetary navigation.

5 SUMMARY AND CONCLUSIONS

An experimental investigation was conducted to assess the performance of an 8.9-N, bipropellant thruster operating at –40 °C with monomethylhydrazine (MMH) and mixed oxides of nitrogen (MON). To facilitate engine operation at low temperatures, dinitrogen tetroxide, N_2O_4, was saturated with nitric oxide, NO, to lower the freezing point. The freezing point of the industry-standard, 3% nitric oxide in dinitrogen tetroxide (MON-3) is -15 °C. By increasing the nitric oxide content to 25% (MON-25), the freezing point was lowered to –55 °C, thus enabling safe operation of the thruster at –40 °C with sufficient margin for error. The thruster was tested in a near-vacuum environment and conditioned, along with the propellants, to –40 °C prior to hot firing. Thruster operating parameters included oxidizer-to-fuel mixture ratios of 1.6 to 2.7 and inlet pressure ranging from 689 to 2070 kPa. The test matrix consisted of many 10-second firings and several 60, 300, 600, and 1200-second firings. Measurements included thrust, propellant flow rates, propellant inlet pressures and temperatures, engine temperatures, system vibrations, and valve control-signal characteristics. Data obtained from testing were analyzed to determine engine performance characteristics such as ignition delay, specific impulse, I_{sp}, versus oxidizer-to-mixture ratio, O/F, I_{sp} versus thrust, F, and the vibration frequency spectrum.

Although more data will be necessary to fully characterize the performance of the Model R-53 at –40 °C fired with MMH and MON-25, the following general statements can be made.

- The engine was successfully operated at a thrust level of 8.9-N and –40 °C when fired with MMH and MON-25.
- Performance is comparable to operation at normal temperatures (22 °C) with MMH and MON-3.
- At nominal inlet pressures, the ignition delay is approximately 8 ms, which is comparable to operation at normal temperatures with MMH and MON-3.
- Based on regression analyses, optimal performance for the 8.9-N thruster will be obtained at an O/F of 1.93 with an anticipated average specific impulse of 298 sec.
- The thruster accumulated nearly 10,000 seconds of operation without failure.
- For a duty cycle of 50% with a 200-ms period, the average vacuum impulse bit was 0.22 N-sec
- The thruster was successfully operated in an atmosphere of 1.5 kPa.
- The thruster exhibits no detrimental vibrations during hot firing.

APPENDIX

Summary Data Listings

Table 4 Performance Summary Data for 10-second Hot Firings.

RUN	P_{mo}	P_{mf}	T_{mo}	T_{mf}	w_o	w_f	O/F	F	P_{cell}	F_{vac}	$I_{sp,vac}$	T_{ch}	C*	C_f	P_c	δ
	kPa	kPa	°C	°C	g/sec	g/sec		N	Pa	N	sec	°C	m/sec		kPa	ms
688	1571	1565	-35.7	-41.3	2.196	0.855	2.57	8.36	73.1	8.50	284.0	1377	1500	1.857	595.9	8.0
689	1570	1555	-36.1	-41.3	2.223	0.840	2.65	8.14	88.0	8.30	276.4	1279	1459	1.858	581.9	8.0
690	1567	1586	-37.9	-44.2	2.218	0.856	2.59	8.12	104.7	8.32	276.0	1308	1458	1.857	583.7	8.0
691	1566	1658	-37.9	-46.7	2.163	0.878	2.46	8.27	111.7	8.48	284.5	1324	1505	1.854	596.0	8.0
692	1564	1795	-38.0	-37.2	2.125	0.977	2.18	8.79	76.5	8.93	293.6	1385	1558	1.847	629.6	8.0
693	1543	1836	-38.6	-39.3	2.071	0.998	2.07	8.73	100.9	8.92	296.3	1379	1576	1.844	630.0	8.0
694	1549	1828	-37.8	-39.3	2.070	0.989	2.09	8.74	77.6	8.88	296.1	1377	1575	1.844	627.4	8.0
695	1550	1904	-38.4	-39.9	2.035	1.025	1.99	8.82	109.8	9.02	300.7	1375	1603	1.839	639.1	8.0
696	1576	2022	-39.0	-39.9	2.048	1.070	1.92	8.99	69.6	9.12	298.3	1379	1594	1.835	647.3	8.0
697	1522	2076	-37.0	-38.9	1.977	1.129	1.75	8.79	125.1	9.03	296.5	1343	1595	1.823	645.2	8.0
698	1479	2108	-38.7	-39.6	1.928	1.134	1.70	8.69	85.8	8.85	294.8	1313	1590	1.818	634.2	8.0
699	1447	2134	-37.8	-38.6	1.868	1.160	1.61	8.51	116.9	8.73	294.1	1279	1594	1.809	629.0	8.0
700	1449	2177	-38.1	-39.5	1.889	1.169	1.62	8.51	145.8	8.78	292.9	1273	1587	1.810	632.3	8.0
701	1621	1766	-38.2	-40.1	2.125	0.957	2.22	8.79	97.1	8.98	297.0	1352	1576	1.849	632.5	8.0
702	1657	1729	-37.3	-39.6	2.202	0.949	2.32	8.74	121.5	8.97	290.2	1341	1538	1.851	631.0	8.0
703	1657	1693	-37.3	-39.7	2.226	0.924	2.41	8.69	87.5	8.85	286.6	1332	1517	1.853	622.3	8.0
704	1657	1622	-37.3	-39.7	2.232	0.893	2.50	8.46	129.6	8.71	284.1	1306	1502	1.855	611.3	8.0
705	1695	1559	-38.2	-40.5	2.301	0.863	2.67	8.31	107.5	8.51	274.4	1311	1447	1.859	596.4	8.0
706	1727	1591	-38.6	-41.2	2.325	0.872	2.67	8.40	138.9	8.66	276.2	1318	1457	1.859	606.7	8.0
707	1824	1629	-39.1	-40.7	2.425	0.883	2.75	8.57	116.9	8.79	271.1	1320	1434	1.854	617.7	8.0
708	1553	1835	-39.1	-40.2	2.028	1.003	2.02	8.71	99.1	8.90	299.3	1360	1596	1.840	629.9	8.0
709	1696	1971	-39.3	-39.8	2.171	1.046	2.07	9.17	147.1	9.45	299.3	1403	1593	1.842	667.9	8.0
710	1861	2108	-39.8	-40.5	2.331	1.086	2.15	9.73	140.7	10.00	298.4	1436	1585	1.846	705.3	7.5
711	1967	2248	-40.2	-40.6	2.411	1.134	2.13	10.20	108.9	10.40	299.2	1471	1590	1.846	734.0	7.5
713	2028	2315	-40.4	-40.8	2.468	1.150	2.15	10.41	88.4	10.58	298.1	1478	1584	1.846	746.3	7.5
714	1407	1697	-40.4	-41.1	1.868	0.920	2.03	8.03	84.0	8.19	299.4	1299	1594	1.842	579.1	8.5
715	1306	1555	-40.2	-41.7	1.803	0.863	2.09	7.52	111.1	7.73	295.6	1246	1572	1.844	545.8	8.5
716	1202	1416	-41.3	-42.2	1.705	0.801	2.13	6.92	138.0	7.18	292.3	1162	1553	1.846	506.8	9.0
717	1072	1278	-41.1	-42.3	1.580	0.744	2.12	6.28	121.6	6.51	285.5	1050	1517	1.846	459.2	9.5
718	929	1105	-39.8	-40.7	1.427	0.677	2.11	5.64	87.3	5.81	281.5	971	1496	1.845	410.1	10.0
719	792	963	-38.8	-40.2	1.270	0.632	2.01	4.87	122.4	5.10	273.4	727	1457	1.841	360.7	11.0
720	723	848	-38.8	-40.2	1.191	0.575	2.07	4.23	125.2	4.46	257.6	721	1370	1.844	315.3	11.5
721	1551	1831	-39.8	-39.6	2.044	0.982	2.08	8.64	92.7	8.82	297.1	1304	1580	1.844	622.9	8.0

REPORT DOCUMENTATION PAGE

Form Approved
OMB No. 0704-0188

1. AGENCY USE ONLY (*Leave blank*)	2. REPORT DATE	3. REPORT TYPE AND DATES COVERED
	April 2001	Final Contractor Report

4. TITLE AND SUBTITLE

Mars Flyer Rocket Propulsion Risk Assessment
Kaiser Marquardt Testing

5. FUNDING NUMBERS

WU–755–B4–01–00
NAS3–99198

6. AUTHOR(S)

Kaiser Marquardt

7. PERFORMING ORGANIZATION NAME(S) AND ADDRESS(ES)

Kaiser Marquardt
Rocket Propulsion Systems
16555 Saticoy Street
Van Nuys, California 91406–1739

8. PERFORMING ORGANIZATION REPORT NUMBER

E–12643

9. SPONSORING/MONITORING AGENCY NAME(S) AND ADDRESS(ES)

National Aeronautics and Space Administration
Washington, DC 20546–0001

10. SPONSORING/MONITORING AGENCY REPORT NUMBER

NASA CR—2001-210710

11. SUPPLEMENTARY NOTES

Kaiser Marquardt has been acquired by General Dynamics, Ordinance and Tactical Systems, Aerospace Operations, 11441 Willows Road N.E., P.O. Box 97009, Redmond, WA 98073-9709. Project Managers, Brian Reed, 216–977–7489, and James Biaglow, 216–977–7480, Power and On-Board Propulsion Technology Division, NASA Glenn Research Center, organization code 5430.

12a. DISTRIBUTION/AVAILABILITY STATEMENT

Unclassified - Unlimited
Subject Category: 20 Distribution: Nonstandard

Available electronically at http://gltrs.grc.nasa.gov/GLTRS

This publication is available from the NASA Center for AeroSpace Information, 301–621–0390.

12b. DISTRIBUTION CODE

13. ABSTRACT ***(Maximum 200 words)***

This report describes the investigation of a 10-N, bipropellant thruster, operating at –40 °C, with monomethylhydrazine (MMH) and 25% nitric oxide in nitrogen tetroxide (MON-25). The thruster testing was conducted as part of a risk reduction activity for the Mars Flyer, a proposed mission to fly a miniature airplane in the Martian atmosphere. Testing was conducted using an existing thruster, designed for MMH and MON-3 propellants. The nitric oxide content of MON-3 was increased to 25%, to lower its freezing point to –55 °C. The thruster was conditioned, along with the propellants, to temperature prior to hot firing. Thruster operating parameters included oxidizer-to-fuel mixture ratios of 1.6 to 2.7 and inlet pressure ranging from 689 to 2070 kPa. The test matrix consisted of many 10-second firings and several 60-, 300-, 600-, and 1200-second firings, as well as pulse testing. The thruster successfully accumulated nearly 10,000 seconds of operation without failure, at temperatures ranging from –40 °C to 22 °C. At nominal inlet pressures, the ignition delay was comparable to MMH/MON-3 operation. The optimal performance for the 8.9-N thruster was determined to be at a mixture ratio of 1.93 with an average specific impulse of 298 sec.

14. SUBJECT TERMS

Liquid rocket propellants; Rocket testing; Mixed oxides of nitrogen; Mars flyer

15. NUMBER OF PAGES
35

16. PRICE CODE
A03

17. SECURITY CLASSIFICATION OF REPORT	18. SECURITY CLASSIFICATION OF THIS PAGE	19. SECURITY CLASSIFICATION OF ABSTRACT	20. LIMITATION OF ABSTRACT
Unclassified	Unclassified	Unclassified	

REPORT DOCUMENTATION PAGE

Form Approved
OMB No. 0704-0188

1. AGENCY USE ONLY (*Leave blank*)	2. REPORT DATE	3. REPORT TYPE AND DATES COVERED
	August 2001	Technical Memorandum

4. TITLE AND SUBTITLE

Overview of Propulsion Systems for a Mars Aircraft

5. FUNDING NUMBERS

WU–710–70–23–00

6. AUTHOR(S)

Anthony J. Colozza, Christopher J. Miller, Brian D. Reed,
Lisa L. Kohout, and Patricia L. Loyselle

7. PERFORMING ORGANIZATION NAME(S) AND ADDRESS(ES)

National Aeronautics and Space Administration
John H. Glenn Research Center at Lewis Field
Cleveland, Ohio 44135–3191

8. PERFORMING ORGANIZATION REPORT NUMBER

E–12541

9. SPONSORING/MONITORING AGENCY NAME(S) AND ADDRESS(ES)

National Aeronautics and Space Administration
Washington, DC 20546–0001

10. SPONSORING/MONITORING AGENCY REPORT NUMBER

NASA TM—2001-210575

11. SUPPLEMENTARY NOTES

This report includes NASA CR—2001-210709 and NASA CR—2001-210710 in appendixes. Anthony J. Colozza, Dynacs Engineering Company, Inc., 2001 Aerospace Parkway, Brook Park, Ohio 44142; and Christopher J. Miller, Brian D. Reed, Lisa L. Kohout, and Patricia L. Loyselle, NASA Glenn Research Center. Responsible person, Lisa Kohout, organization code 5440, 216–433–8004.

12a. DISTRIBUTION/AVAILABILITY STATEMENT

Unclassified - Unlimited
Subject Category: 07 Distribution: Nonstandard

Available electronically at http://gltrs.grc.nasa.gov/GLTRS

This publication is available from the NASA Center for AeroSpace Information, 301–621–0390.

12b. DISTRIBUTION CODE

13. ABSTRACT ***(Maximum 200 words)***

The capabilities and performance of an aircraft depends greatly on the ability of the propulsion system to provide thrust. Since the beginning of powered flight, performance has increased in step with advancements in aircraft propulsion systems. These advances in technology from combustion engines to jets and rockets have enabled aircraft to exploit our atmospheric environment and fly at altitudes near the Earth's surface to near orbit at speeds ranging from hovering to several times the speed of sound. One of the main advantages of our atmosphere for these propulsion systems is the availability of oxygen. Getting oxygen basically "free" from the atmosphere dramatically increases the performance and capabilities of an aircraft. This is one of the reasons our present-day aircraft can perform such a wide range of tasks. But this advantage is limited to Earth; if we want to fly an aircraft on another planetary body, such as Mars, we will either have to carry our own source of oxygen or use a propulsion system that does not require it. The Mars atmosphere, composed mainly of carbon dioxide, is very thin. Because of this low atmospheric density, an aircraft flying on Mars will most likely be operating, in aerodynamical terms, within a very low Reynolds number regime. Also, the speed of sound within the Martian environment is approximately 20 percent less than it is on Earth. The reduction in the speed of sound plays an important role in the aerodynamic performance of both the aircraft itself and the components of the propulsion system, such as the propeller. This low Reynolds number-high Mach number flight regime is a unique flight environment that is very rarely encountered here on Earth.

14. SUBJECT TERMS	15. NUMBER OF PAGES
Planetary exploration; Propulsion and power; Aircraft	121
	16. PRICE CODE

17. SECURITY CLASSIFICATION OF REPORT	18. SECURITY CLASSIFICATION OF THIS PAGE	19. SECURITY CLASSIFICATION OF ABSTRACT	20. LIMITATION OF ABSTRACT
Unclassified	Unclassified	Unclassified	